Furin-mediated proteolytic activation of *Drosophila* FGF homologue Branchless

Von der Fakultät für Lebenswissenschaften

der Technischen Universität Carolo-Wilhelmina

zu Braunschweig

zur Erlangung des Grades einer

Doktorin der Naturwissenschaften

(Dr. rer. nat.)

genehmigte

D i s s e r t a t i o n

von Tatyana Koledachkina
aus Vyazniky, Russische Föderation

1. Referent: Professor Dr. Hans-Henning Arnold
2. Referent: apl. Professor Dr. Reinhard Schuh
eingerichtet am: 06.10.2010
mündliche Prüfung (Disputation) am: 21.12.2010

Druckjahr 2011

TABLE OF CONTENTS

ABBREVIATIONS

FGF	Fibroblast Growth Factor
FGFR	Fibroblast Growth Factor Receptor
Bnl	Branchless
Btl	Breathless
Pyr	Pyramus
Ths	Thisbe
Htl	Heatless
HSPG	Heparan Sulphate Proteoglycan
SPP	Signal peptide peptidase
SPC	Subtilisin-like proprotein convertase
PC	Prohormone convertase
NGF	Nerve growth factor
TGF-β	Transforming growth factor-β
APP	β -amyloid precursor protein
Dpp	Decapentaplegic
Wg	Wingless
AKH	Adipokinetic hormone
MAPK	Mitogen activated protein kinase
RTK	Receptor tyrosine kinase
Shh	Sonic hedgehog
GTPase	Guanidine triphosphatase

GFP	Green Fluorescent Protein
Ser	Serine
Arg	Arginine
Gln	Glutamin
Asn	Asparagine
Asp	Aspartic acid
Lys	Lysine
Thr	Threonine
Leu	Leucine
Ile	Isoleucine
Val	Valine
His	Histidine
UAS	Upstream Activating Sequence
N-	Amino-
C-	Carboxy-
NLS	Nuclear localization signal
ER	Endoplasmic reticulum
TGN	*trans*-Golgi network
μg	microgram
μl	microlitre
Ab'	Primary antibody
BSA	Bovine Serum Albumin
CNS	Central Nervous System

DNA	Deoxyribonucleic acid
RNA	Ribonucleic acid
dsRNA	Double-stranded RNA
E.coli	*Escherichia coli*
UV	ultraviolet
nm	nanometer
kDa	kilo Dalton
bp	base pair
LB	Luria Bertani
PBS	Phosphate Buffered Saline
PBT	PBS with 0,01% Tween-20
PCR	Polymerase Chain Reaction
rpm	revolutions per minute
SDS	Sodium Dodecyl Sulphate
PAGE	Polyacrylamide Gel Electrophoresis
DAPI	4',6-Diamidin-2'-phenylindoldihydrochlorid
MWCO	Molecular weight cut off
EGTA	Ethylene glycol tetraacetic acid
HRP	Horse radish peroxydase

ABSTRACT

Fibroblast growth factors (FGFs) are secreted signaling proteins that are highly conserved from nematodes to humans. They are essential both for embryonic development as well as for various biological and pathological processes during adulthood. *Drosophila* FGF Branchless (Bnl) demonstrates high similarity to mammalian FGFs and is involved in the development of fly tracheal system. However, Bnl contains extended N- and C-terminal domains with unknown function, which make the protein approximately 3 times longer than mammalian FGF homologues.

This thesis reports about proteolytic processing of the Bnl protein that removes its N- and C-terminal regions and liberates the central FGF domain. According to the obtained results, this cleavage is required for Bnl activation and is essential for correct development of embryonic tracheal system. *Drosophila* Furin1 protease was identified as an enzyme responsible for Bnl processing. Four conserved furin recognition motives were found in the Bnl protein, however, only three of them contribute to Bnl cleavage in *Drosophila* cell culture. Interestingly, a similar furin recognition motif was identified in FGF10, the vertebrate homologue of Bnl. Moreover, this motif is conserved in vertebrate FGF10 homologues and is processed by a Furin-related protease in *Drosophila* cell culture.

Taking together, the results of this study suggest a novel furin-mediated mechanism of post-translational regulation of FGF activity during tracheal development in *Drosophila*. Moreover, the obtained data raise the possibility that the observed regulatory mechanism is evolutionary conserved and the biological function of vertebrate homologues of Bnl is modulated in a similar fashion.

1 INTRODUCTION

Embryonic development is a complex process that involves formation, growth, specification and shaping of various tissues and organs of a body. It relies on numerous cell to cell signaling events, which orchestrate and coordinate the whole morphogenetic process according to a certain developmental program. Therefore, precise temporal and spatial regulation of expression and function of signaling proteins is essential for proper embryonic development (Gilbert, 2006). This regulation occurs at several levels including modulation of gene expression as well as post-translational proteolytic processing of already synthesized signaling molecules. Such protelytic maturation is performed by members of the subtilisin-like proprotein convertase (SPC) family of endoproteases. These enzymes are responsible for proteolytic modification of different proteins in eukaryotes, including peptide hormones and growth factors (Steiner, 1998). Fibroblast growth factors (FGFs) are highly conserved signaling molecules, implicated in various aspects of embryonic development in vertebrates and invertebrates, including mesoderm induction, formation of organs and branching morphogenesis (Böttcher and Niehrs, 2005; Kadam et al., 2009). However, post-translational regulation of their biological activity is poorly studied. The present thesis provides the information about post-translational proteolytic activation of *Drosophila* FGF homologue Branchless (Bnl), which is performed by a subtilisin-like proprotein convertase and is essential for Bnl function during development of embryonic tracheal system.

1.1 Proteolytic processing of proteins in eukaryotic cells

Many eukaryotic proteins are synthesized in cells as large precursor molecules that are subsequently subjected to limited proteolysis. Intracellular protein processing represents a specific regulatory mechanism that serves various biological purposes (reviewed in Turk, 2006).

Proteins that possess an amino-terminal (N-terminal) signal sequence are co-translationally transferred into the lumen of the endoplasmic reticulum (ER). This translocation is regulated by proteolytic cleavage of the signal sequence by a specific enzyme called signal peptide peptidase (SPP). Therefore, proteolytic processing is essential for the liberation of the newly produced polypeptide into the ER lumen and eventually for its direction to the destination place (Martoglio and Dobberstein, 1998; Emanuelsson et al., 2007; Alberts et al., 2002).

Futhermore, proteolytic processing also serves as a mechanism of regulation of intercellular communication, since many prohormones, neuropeptides, extracellular receptors and growth factors require post-translational proteolytic activation (Rockwell et al., 2002; Holyoak et al., 2004). The proteolysis preferentially occurs at specific amino acid residues (protease recognition sites) and represents a protein modification step rather than its degradation into separate amino acids. Such proteolytic precursor modification is very common among eukaryotes and frequently occurs at repetitive basic amino acid residues (Steiner, 1998; Rockwell et al., 2002).

1.1.1 Subtilisin-like proprotein convertases (SPCs)

The specialized family of calcium-dependent serine proteases called subtilisin-like proprotein convertases is known to be responsible for the proteolytic activation of many secreted proproteins. The first member of this group, Kex2 protease (kexin, E.C. 3.4.21.61), was identified in *Saccharomyces cerevisiae*. This enzyme was implicated in proteolytic maturation of an α-mating factor in MATα haploid yeast cells (Leibowitz and Wickner, 1976; Achstetter and Wolf, 1985).

There are several kexin homologues identified in mammalian cells. They include furin, prohormone convertase (PC) 1/3, PC2, PC4, PC5/6, PC7 and PACE4. These proteins contain a conserved catalytic domain, also present in Kex2, and an additional Homo B domain (or P domain) required for their proteolytic activity. Some of the SPC family members also carry cystein-rich and serine/threonine-rich domains of unknown function (Figure 1). Moreover, all these enzymes are initially synthesized as zymogens and undergo subsequent autoproteolytic activation (Rockwell et al., 2002; Thomas, 2002).

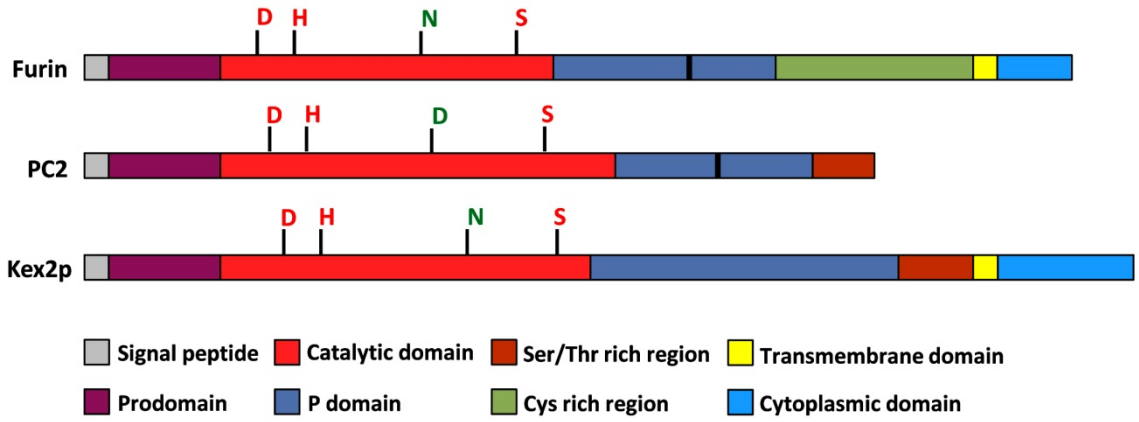

Figure 1: Comparison of subtilisine-like proprotein convertases (adapted from Thomas, 2002). Schematic representation of furin, PC2 and kexin. The active site residues are in red. The oxyanion-hole amino acids are marked in green.

Mammalian SPCs are subdivided into two classes by the presence or absence of a transmembrane domain. PC1/3, PC2 and PC4 do not carry the transmembrane domain, they are expressed in a tissue-specific manner and localize to the regulated secretory pathway (Rockwell et al., 2002). These enzymes are sorted into specific cellular compartments such as secretory granules that are enriched with protein precursors for several hours. Conversely, Kex2, Furin, PC7 and PACE4 are ubiquitously expressed transmembrane proteins that localize to the constitutive secretory pathway where they cycle between several cellular compartments (Mains et al., 1997; Rockwell et al., 2002). These proteases are transiently exposed to specific targets in the presence of a large amount of non-substrate proteins. Thus, the two subgroups of SPCs demonstrate different expression profiles, time of action and specificity towards protein precursors (Rockwell et al., 2002).

Members of the SPC family as well as the non specific digestive enzymes utilize the same mechanism of peptide bond cleavage characteristic for serine proteases. They catalyze the reaction of acyl transfer mediated by a group of catalytic amino acids (serine, histidine and aspartate) in the reactive center of the molecule (Perona and Craik, 1995; Holyoak et al., 2004). However, subtilisin-like proteases possess an additional catalytic residue called oxyanion hole Asn that also contributes to their proteolytic activity. (Holyoak et al., 2004; Rockwell et al., 2002) (Figure 1).

Proprotein convertases preferentially recognize and cleave their target proteins C-terminally at dibasic residues –K–R↓– or –R–R↓– (arrow shows the cleavage site; K – Lys; R – Arg). However, upstream basic amino acids may also contribute to the consensus recognition (Rockwell et al., 2002).

1.1.2 Furin

Human furin, which encodes a Kex2 homolog (Bresnahan et al., 1990), is the best studied member of the mammalian SPC family. It was shown to be involved in the processing of diverse protein precursors including growth factors, neuropeptides, extracellular matrix components and other proteases (Molloy et al., 1994; reviewed in Thomas, 2002). Human furin is a relatively big (794 amino acids) single-span transmembrane protein, whose homologues are ubiquitously expressed among vertebrate species. The protein carries a N-terminal signal peptide that directs the protease precursor to the ER lumen. Like other member of the SPC family, furin possesses the amino-terminal pro-peptide, which is removed in two steps by autocatalytic processing. This event was reported to be essential for furin folding, translocation and activation of its proteolytic activity (Anderson et al., 1997). The

catalytic domain of furin shows homology to subtilisin-like domains of the other proprotein convertases and contains the conserved Asp, His and Ser residues that constitute the catalytic triad found in all serine proteases (Thomas, 2002; Holyoak et al., 2004). In addition, furin contains a specific P-domain identified in subtilisin-like proprotein convertases but absent in bacterial subtilisin. The precise function of this domain remains elusive, however, it was proposed to be essential for modulation of pH and calcium requirements of the protease (Zhou et al., 1999; Thomas et al., 2002).

In contrast to the kexin protease, which cleaves proproteins at dibasic residues, the consensus motif recognized by furin is –R–X–K/R–R↓– (where X is any amino acid and the arrow identifies the cleavage position) and requires additional basic amino acid residues upstream of the cleavage point. Additionally, furin proteases effectively process a so-called minimal furin site, which includes two arginines separated by any two amino acids (–R–X–X–R↓–) (Krysan et al., 1999; Thomas, 2002; Rockwell et al., 2002).

The localization of furin protease within the cell is very dynamic and is described as a rapid cycling between *trans*-Golgi network (TGN), endosomic compartments and the cellular surface (Molloy et al., 1994; Molloy et al., 1999) (Figure 2).

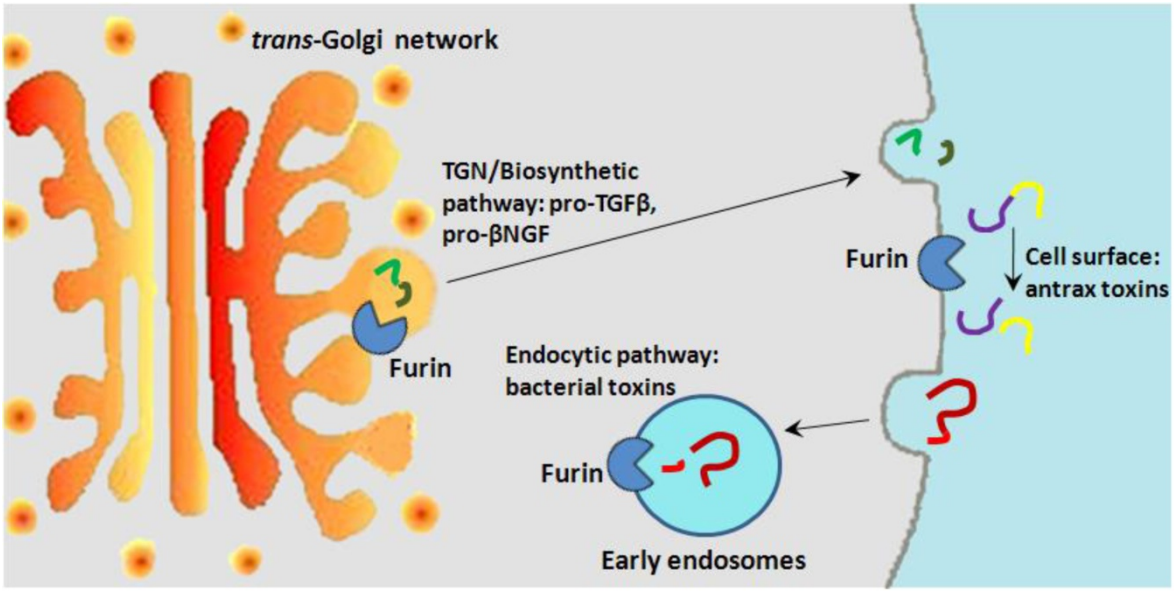

Figure 2: Furin subcellular localization. Furin (shown in blue) dynamically cycles between several cellular compartments. In TGN it cleaves different signaling propeptides and proreceptors. Cell-surface furin was shown to process the anthrax toxin. In early endosomes furin activates bacterial toxins, including diphtheria toxin and *Pseudomonas* exotoxin A.

Such complex enzyme trafficking contributes to the diversity of the intra- and extracellular substrates processed by furin and completely depends on the cytoplasmic domain of furin (Anderson et al., 1997; Molloy et al., 1999). The mechanism of furin intracellular trafficking is not completely understood. However, previous studies supposed that furin anterograde and retrograde transport is clathrin-mediated (Teuchert et al., 1999; Crump et al., 2001). Moreover, cell-surface furin can be internalized by endocytosis, which requires a specific interaction of the cytoplasmic tail of the enzyme with adaptor proteins (Liu et al., 1997).

Furin plays an essential role in cellular communication during embryogenesis, homeostasis maintenance and disease. It was shown to regulate neuronal survival by proteolytic activation of pro-β-nerve growth factor (pro-β-NGF) (Lee et al., 2001b). Also, furin activity is required for Notch and Transforming growth factor-β (TGF-β) signaling (Bush et al., 2001; Cui et al., 2001). Furthermore, furin participates in proteolytic modification of the β-amyloid precursor protein (APP), thus being involved in the pathogenesis of Alzheimer's disease (Walter et al., 2001; Isacson et al., 2002). Furin proteolytic activity was implicated in tumor metastasis and its expression is upregulated in many cancers (Bassi et al., 2001; Mbikay et al., 1997). Moreover, cell-surface furin is able to activate bacterial toxins (Molloy et al., 1992; Klimpel et al., 1992) and cause maturation of viral particles (including avian influenza virus, HIV-1 and measles virus) (Molloy et al., 1999; Thomas, 2002) (Figure 2).

Thus, furin represents a specific proprotein convertase with highly dynamic intracellular trafficking, whose proteolytic activity is involved in various biological and pathological aspects of cellular life and intercellular communication.

1.1.3 *Drosophila* SPCs

Three members of the SPC family were identified in *Drosophila*: Dfurin1 (Dfur1), Dfurin2 (Dfur2) and Amontillado (Amon). Dfur1 and Dfur2 proteases were characterized *in vitro* and demonstrate a close relation to mammalian furin (Roebroeck et al., 1991; Roebroeck et al., 1992; Roebroeck et al., 1993), whereas Amon shows homology with PC2 convertase (Siekhaus and Fuller, 1999).

As their mammalian homologues, both *Drosophila* furins are transmembrane proteins that carry a N-terminal signal sequence and are preferentially localized in the late Golgi. The enzymes contain a subtilisin-like catalytic domain and a prodomain that is removed during protease maturation by autocatalytic cleavage (De Bie et al., 1995). Unlike human furin that has only one known isoform, Dfur1 exists in several different

isoforms (dfurin1, dfurin1-CRR and dfurin1-X) that differ in their subcellular localization (Roebroeck et al., 1993; Molloy et al., 1994; De Bie et al., 1995) (Figure 3).

Drosophila furins show similar proteolytic activity *in vitro*, however, they demonstrate non-overlapping zygotic expression during embryogenesis (Roebroeck et al., 1993; De Bie et al., 1995). Both Dfur1 and Dfur2 transcripts are maternally supplied and demonstrate ubiquitous localization in early embryos. Later in development Dfur1 expression can be detected in various organs including the central nervous system (CNS), hindgut and lateral clusters of epithelial cells (Hayflick et al., 1992; Roebroeck et al., 1993; De Bie et al., 1995). Dfur2 transcripts are revealed in the embryonic nervous system and in the developing trachea at late embryonic stages (Roebroeck et al., 1995).

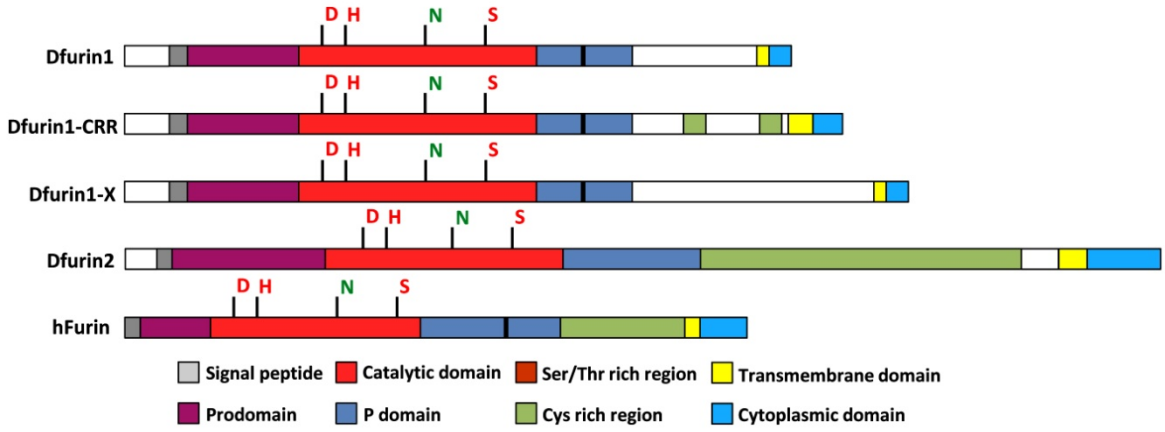

Figure 3: *Drosophila* furins (adapted from De Bie et al., 1995). Schematic drawing of the alternatively spliced *Drosophila* Furin1 isoforms (Dfurin1, Dfurin1-CRR and Dfurin1-X), *Drosophila* Furin2 (Dfurin2) and human furin (hFurin). The active site residues are in red. The oxyanion-hole amino acids are marked in green.

Drosophila Amon is a PC2 homolog and was implicated in the development of the embryonic nervous system. Embryos deficient for the *amon* gene demonstrate partial embryonic lethality and have an impaired hatching behavior and larval growth, however, no morphological defects can be observed in these mutants (Siekhaus and Fuller, 1999; Rayburn et al., 2003).

Although substrates for *Drosophila* SPCs were unknown for some time, it was recently shown that a fly homolog of TGF-β, Decapentaplegic (Dpp), undergoes multistep proteolytic maturation catalyzed by both *Drosophila* furins (Künnapuu et al., 2009). Moreover, Dfur1 and Dfur2 demonstrate differential specificity towards the three Dpp cleavage sites that represents a mechanism of ligand activity modulation

(Künnapuu et al., 2009). In contrast to the conservation of furin function for TGFβ/Dpp processing, furin-mediated cleavage is not essential for *Drosophila* Notch pathway, since the major pool of fly Notch can be detected as a full-length protein (Kidd and Lieber, 2002). Moreover, *Drosophila* adipokinetic hormone (AKH), the fly analog of glucagon, represents a substrate for Amon (Rhea et al., 2010).

In present work, one of the *Drosophila* fibroblast growth factors Branchless (Bnl) is identified as a novel target for the Dfur1 protease and this processing is essential for Bnl biological function.

1.2 Fibroblast growth factors

Fibroblast growth factors (FGFs) constitute a large family of highly conserved signaling molecules found in eukaryotes from nematodes to humans. These factors are involved in a broad spectrum of biological processes in living organisms, including angiogenesis, wound healing, limb formation, branching morphogenesis of epithelial tubes and cancerogenesis (reviewed in Ornitz and Itoh, 2001; Affolter and Caussinus, 2008; Korc and Friesel, 2009). Despite the given name, these cytokines regulate not only fibroblast proliferation, but also known as potential mitogens for endothelial cells, smooth muscle cells, chondrocytes and other cell types. Moreover, these factors are required for cellular differentiation, survival and migration (Ornitz and Itoh, 2001).

1.2.1 Members of vertebrate FGF family of proteins

Mammalian FGF family consists of 23 members identified up to date. The first member of this family – basic fibroblast growth factor (FGF2) was identified in 1975 as a potent inducer of cell proliferation from bovine pituitary gland (Gospodarowicz, 1975; Ribatti et al., 2007). FGF3-FGF9 were discovered in mammalian cell culture or identified as oncogenes (Coulier et al., 1991; Tanaka et al., 1992; Itoh and Ornitz, 2008). Other FGFs were identified on the basis of their sequence homology (Ribatti et al., 2007).

Vertebrate FGFs are relatively small proteins whose molecular mass varies from 17 to 34 kDa. The FGF core domain contains 28 highly conserved and six identical amino acids (Ornitz, 2000; Plotnikov et al., 2000). Moreover, structural analysis of FGF1 and FGF2 revealed a specific FGF domain structure, containing 12 antiparallel β strands, which was shown to be critical for FGF receptor binding (Figure 4) (Eriksson et al., 1990; Zhu et al., 1990).

Most FGF family members contain classical N-terminal signal sequence and are effectively secreted from the producing cells. However, some vertebrate FGFs (FGF1, FGF2, FGF9, FGF16 and FGF20) possess no signal peptide, but are nevertheless found in the extracellular space. Among those, FGF1 and FGF2 are released from cells upon cellular damage. Also, a special exocytic secretory mechanism was proposed for these FGFs. Other FGF proteins lacking classical N-terminal signal peptides contain an internal hydrophobic sequence, which was demonstrated to be responsible for their secretion (Mignatti et al., 1992; Ornitz and Itoh, 2001; Itoh and Ornitz, 2004).

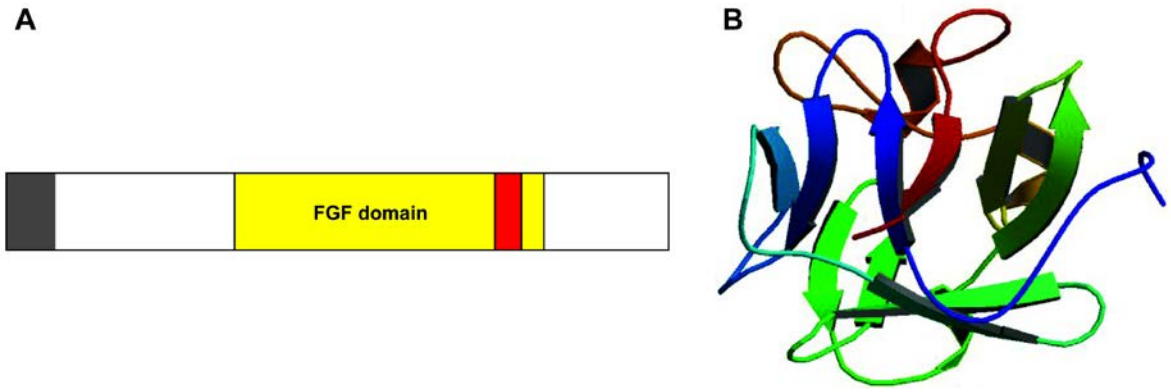

Figure 4: FGF protein structure. (A) Schematic representation of a typical FGF protein (adapted from Ornitz and Itoh, 2001). The N-terminal signal peptide is shown in grey. The heparin-binding domain is in red. **(B)** 3D structure of the human FGF1 as a prototypic FGF ligand (from Protein Data Bank online resource).

Fibroblast growth factors as well as many other extracellular signaling peptides carry varying degrees of N- and O-linked glycosylation. FGF3, FGF4, FGF9, FGF16, FGF17 and FGF18 contain a single N-glycosylation motif, which is required for their secretion from the cells (Kiefer et al., 1993; Miyakawa and Imamura, 2003). Moreover, N-linked glycosylation was also implicated in FGF4 stability, since the unglycosylated protein undergoes proteolytic cleavage outside the cell (Bellosta et al., 1993). FGF5, FGF6, FGF7 and FGF10 demonstrate both N- and O-glycosylation (Bates et al., 1991; Asada et al., 1999; Hsu et al., 1998; Park et al., 1998), whereas FGF23 carries only an O-linked sugar modification, which is required for its secretion (Fukumoto, 2005; Bergwitz et al., 2009).

Members of the FGF family were also shown to interact with heparin and heparan sulfate proteoglycans (HSPGs). This is a group of glycoproteins found on the cell surface or in the extracellular matrix (ECM). These proteins carry linear heparin sulfate glycosaminoglycan (HSGAG) sugar chains attached to specific amino acid residues. HSPGs were implicated in a number of signal transduction pathways, including FGF signaling (Häcker et al., 2005; Dreyfuss et al., 2009;

Gutierrez et al., 2010). Moreover, structural studies have identified HSPGs as essential components of the FGF-FGFR signaling complex and shown that a highly variable tissue-specific modification pattern of linked glycosaminoglycans modulates the specificity of receptor-ligand interaction (Ornitz, 2000; Pellegrini, 2001; Sugaya et al., 2008).

1.2.2 *Drosophila* FGFs: Pyramus and Thisbe

Drosophila melanogaster possesses three genes encoding FGF homologues: *thisbe* (*ths*, also known as *fgf8-like1*), *pyramus* (*pyr*, *fgf8-like2*) and *branchless* (*bnl*) (Sutherland et al., 1996; Gryzik and Müller, 2004; Stathopoulos et al., 2004). Ths and Pyr contain 748 and 766 amino acid residues and show high homology to human FGF8 (32-35% amino acid identity in the FGF core domain) (Gryzik and Müller, 2004; Stathopoulos et al., 2004). Both proteins carry N-teminal signal peptides and are secreted from the cells (Stathopoulos et al., 2004; Gryzik and Müller, 2004). Interestingly, neither Pyr nor Ths possess a heparin binding domain found in other FGF proteins and probably do not interact with extracellular HSPGs or this interaction is not specific (Stathopoulos et al., 2004).

The expression of both FGFs is identical at the early stages of *Drosophila* embryogenesis and is localized in the lateral neurogenic ectoderm, suggesting the redundancy of their biological function. However, later in development the expression pattern of Pyr and Ths becomes distinct from each other and can be revealed in different subsets of the embryonic neuroectoderm (Gryzik and Müller, 2004; Stathopoulos et al., 2004). Moreover, investigation of *Drosophila* embryos lacking *pyr* and/or *ths* expression suggests that the ligands have overlapping as well as individual biological functions during embryonic development (Introduction 1.4.1; Kadam et al., 2009; Klingseisen et al., 2009).

1.2.3 *Drosophila* FGFs: Bnl

Drosophila FGF Bnl is a 770 amino acid protein, with a molecular mass of 84 kDa (Sutherland et al., 1996) (Figure 5). Among vertebrate FGFs Bnl shows the highest homology to FGF10, which is essential for vertebrate lung development (Min et al., 1999). Bnl carries a N-terminal signaling sequence and is secreted (Sutherland et al., 1996). Moreover, similar to other members of the FGF family, the Bnl ligand possesses the heparin binding domain that enables its interaction

with extracellular HSPGs. Despite the high similarity to known FGFs, Bnl (as well as the other *Drosophila* FGFs Pyr and Ths) is unusually large compared to vertebrate FGFs, whose maximal molecular weight does not exceed 37 kDa (Ornitz and Itoh, 2001; Sutherland et al., 1996). The conserved FGF domain of Bnl is flanked by the extensive N- and C-terminal regions that are not present in vertebrate homologues (Figure 5). These regions demonstrate no similarity to any known proteins and contain repetitive stretches of Ser or Gln residues of unknown purpose (Sutherland et al., 1996).

Figure 5: *Drosophila* Bnl protein and its relation to human FGFs. (**A)** Schematic representation of the Bnl protein compared to human FGFs (adapted from Sutherland et al., 1996). The N-terminal signal peptides are marked in black, the FGF homology domains are shown in yellow. Numbers show percent of homology in the core domain. **(B)** Relation of Bnl to the human FGF members based on their amino acid homology.

Bnl demonstrates a highly dynamic expression pattern during *Drosophila* embryonic development. Its expression starts at stage 5 of fly embryogenesis around the cephalic furrow and at the posterior transversal furrow. At stage 11, Bnl can be detected in multiple epidermal clusters near invaginating tracheal cells and continues later at the places of subsequent migration of the growing tracheal branches. During later stages, Bnl epidermal expression fades and the protein is detected in the embryonic gut (Sutherland et al., 1996). Bnl is the only ligand for the receptor tyrosine kinase Breathless (Btl) (Sutherland et al., 1996) and their interaction was shown to be essential for tracheal development in *Drosophila* (Klämbt et al., 1992; Reichman-Fried et al., 1994).

1.3 FGF signaling

FGF signaling is initiated by specific interaction of the extracellular FGF ligand with the cell-surface FGF receptor (FGFR). This interaction leads to the receptor activation and induces specific intracellular signaling cascade, depending on FGF-FGFR combination and cell context (Eswarakumar et al., 2005). FGF signaling may result in various cellular responses including expression of target

genes, rearrangement of actin cytoskeleton, cell proliferation and survival (Ornitz and Itoh, 2001).

1.3.1 FGF signaling in vertebrates

There are four *Fgfr* genes (*Fgfr1-4*) described in humans and mice. They encode receptor tyrosine kinase (RTK), transmembrane proteins that carry an extracellular domain containing three immunoglobulin-like (Ig-like) domains, one of which is responsible for ligand binding. An intracellular portion of these receptors contains a tyrosine kinase domain, which enables protein phosphorylation (Mohammadi et al., 2005).

The knowledge about the mechanism of FGF signaling is based on studies of mammalian FGFR1 and other vertebrate RTKs. Extracellular FGF-FGFR interaction results in conformational changes in two neighboring FGFR molecules and promotes their dimerization. This dimerization enables intracellular tyrosine-kinase domains to cross-phosphorylate each other at different tyrosine residues. This phosphorylation activates downstream signal transduction (Mohammadi et al., 2005). The activated FGF receptor induces phosphorylation and recruitment of various docking and adaptor molecules and protein kinases, hence propagating the signal and transforming the extracellular stimuli into the intracellular signaling cascade (Turner and Grose, 2010) (Figure 6). Phosphorylated tyrosine residues of FGFR serve as binding sites for the adaptor protein FRS2 (Fibroblast growth factor receptor substrate 2) (Lin et al., 1998).

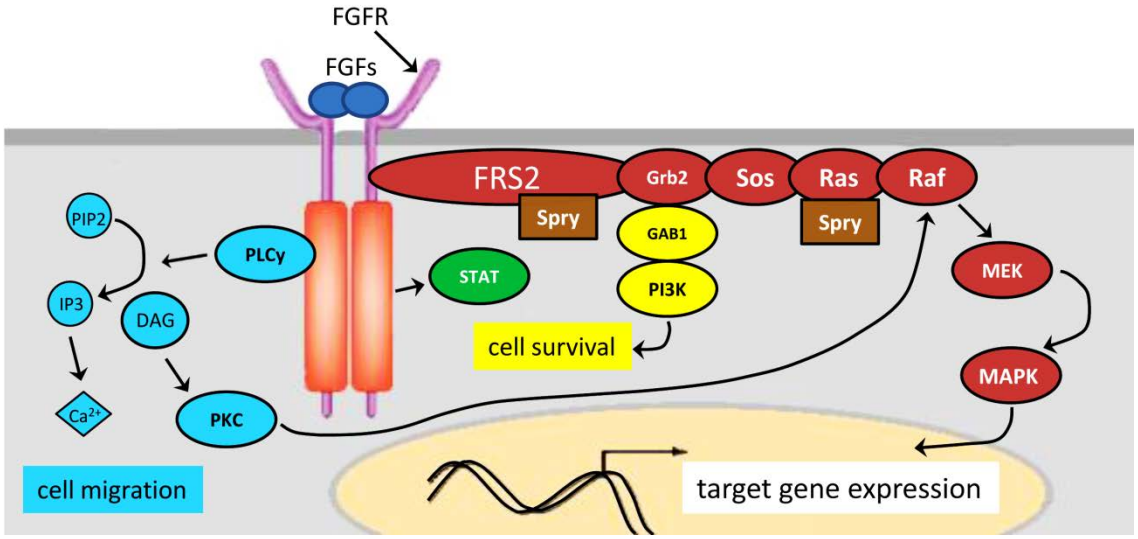

Figure 6: FGF signaling pathway (adapted from Turner and Grose, 2010). Schematic representation of the signaling network mediated by activated FGFR with the four basic pathways: Ras/MAPK (red), PI 3-kinase (yellow), PLCγ (blue) and STAT (green). The negative regulator of the FGF signaling, Sprouty, is shown in brown.

It contains a phosphotyrosine-binding (PTB) domain and was shown to constitutively interact with the juxtamembrane region of the FGFR even without receptor activation. This interaction enables FRS2 phosphorylation and recruits another adaptor protein, Growth factor receptor-bound 2 (GRB2) and the guanidine nucleotide exchange factor (GEF) Son of sevenless (SOS) (Kouhara et al., 1997; Eswarakumar et al., 2005). These proteins in turn activate the membrane-bound GTPase Ras and facilitate the GTP-GDP exchange. This results in recruitment of an intracellular serin/threonin protein kinase cascade (MAPKKK/RAF; MAPKK/MEK and MAPK/ERK1/2) and leads to the activation of nuclear transcription factors (c-myc, AP1 or proteins of the E-twenty-six (ETS) family) and eventually to changes in gene expression (Böttcher and Niehrs, 2005; Turner and Grose, 2010).

Moreover, a separate branch of FGF signaling involves GRB2-accociated binding protein 1 (GAB1), which recruits PI 3-kinase cascade and activates the cell survival pathway (Kouhara et al., 1997) (Figure 6). Another direction of the FGF pathway represents an FRS2-independent signaling cascade and involves phopholipase Cγ (PLCγ) (Figure 6). This signaling pathway was shown to be required for the rearrangement of actin cytoskeleton and cell migration (Böttcher and Niehrs, 2005; Turner and Grose, 2010). Depending on certain cellular context, the extracellular activation of FGFR may result in several other downstream pathways involving the P38 kinase, Jun N-terminal kinase and Signal transducer and activator of transcription (STAT) signaling (Boilly et al., 2000; Hart et al., 2000). The time required for the cell to respond to FGFR activation varies from several minutes, when the signaling results in rearrangement of actin cytoskeleton, to hours if it involves regulation of gene expression and requires protein biosynthesis (Alberts et al., 2002).

1.3.2 Regulation of the FGF signaling

FGF signaling is thoroughly regulated at several levels by extracellular and intracellular modulators. The extracellular regulation of FGF signaling is mediated by heparan sulfate proteoglycans (HSPGs). As already mentioned above, the extracellular carbohydrate chains of HSPGs interact with FGF ligands and stabilize their interaction with receptors, thus facilitating the signal transduction within the tissue. Several *in vivo* studies report about the biological relevance of HSPGs for FGF mediated signaling in vertebrates as well as in *Drosophila* (Garcia-Garcia and Anderson, 2003; Lin et al., 1999; Raman and Kuberan, 2010).

One of the specific intracellular antagonists of FGF-mediated signaling is Sprouty (Spry). This protein was first identified in *Drosophila* as a negative regulator of FGF signaling during tracheal development (Hacohen et al., 1998) and later was found to be conserved and play a similar role in mammals (Tefft et al., 1999). Spry carries a highly conserved cysteine-rich domain on the C-terminus, which is essential for the protein recruitment to the plasma membrane and defines the inhibitory function (Lim et al., 2002). Spry expression is activated by FGF signaling, thus representing a negative feedback loop (de Maximy et al., 1999). The negative regulation of FGF signaling by Spry was shown to occur at the level of Grb2 and Ras (reviewed in Christofori et al., 2003) (Figure 6).

1.3.3 FGF signaling in *Drosophila* melanogaster

There are two FGF receptors in *Drosophila*, Breathless (Btl) and Heartless (Htl), showing similar composition as the vertebrate FGFRs Btl receptor is expressed mainly in the tracheal cells and is responsible for the morphogenesis of tracheal branches during development of the embryonic tracheal system (Introduction 1.4.2; Glazer and Shilo, 1991; Reichman-Fried et al., 1994). Htl (Shishido et al., 1997; Gisselbrecht et al., 1996) is required for mesodermal cell migration during gastrulation and for the differentiation of mesodermal derivatives such as cardial and pericardial cells, somatic muscle founder cells, hemolymph and fat body cells (Mandal et al., 2004; Wilson et al., 2005). Bnl represents the only ligand for the Btl receptor (Sutherland et al., 1996), whereas Pyr and Ths were both shown to bind Htl (Stathopoulos et al., 2004; Gryzik and Müller, 2004). Similar to vertebrates, HSPGs were implicated in FGF signaling in *Drosophila* (Lin et al., 1999; Yan and Lin, 2007; Lindner et al., 2007).

Surprisingly, the *Drosophila* homologues of vertebrate adaptor proteins do not fulfill similar functions during Htl- and Btl-mediated FGF signaling. Instead, other components required for the intracellular propagation of the signaling were identified. One of them – downstream of FGFR (Dof) (also named Stumps (Sms) and Heartbroken (Hbr) (Michelson et al., 1998; Vincent et al., 1998; Imam et al., 1999), was shown to participate in all biological processes that require FGF signaling and, similar to the vertebrate FRS2 protein, constitutively binds the intracellular domains of both *Drosophila* FGFRs (Wilson et al., 2004; Csiszar et al., 2010) (Figure 7). Dof does not show a homology to FRS2, but is related to other vertebrate adaptor proteins BCAP and BANK, which are responsible for B-cell receptor signaling (Battersby et al., 2003). Upon binding the activated FGF receptor, Dof becomes phosphorylated at several tyrosine residues and recruits a

tyrosine phosphatase (PTP) Corkscrew (Csw) (Perkins et al., 1992; Petit et al., 2004). This interaction is essential for downstream activation of the MAPK pathway via repression of Spry (Jarvis et al., 2006). In contrast to Dof, which is shown to function only downstream of FGF receptors, Csw is not specific for FGF signaling and was reported to regulate other RTK pathways, including EGFR and Torso signaling (Perkins et al., 1996; Jarvis et al., 2006). In addition, Dof contains a putative consensus motif for PI3K binding that was shown to be phosphorylated upon RTK activation. However, it is not clear whether this phophorylation activates the PI3K pathway (Csiszar et al., 2010).

Drk (downstream of receptor kinase) is the *Drosophila* homolog of the vertebrate Grb2 adaptor protein and was shown to interact with RasGEF Son of sevenless (Sos) (Raabe et al., 1995) (Figure 7). It is probably recruited by the Dof protein upon FGFR activation. It was shown that *Drosophila* RasGAP (Ras GTPase activating protein) directly binds activated Btl and Htl receptors. This interaction attenuates FGFR-mediated signal transduction and was implicated in regulation of FGF signaling strength through the Ras/MAPK pathway (Woodcock and Hughes, 2004). However, since null mutants for the gene encoding *Drosophila* RasGAP, demonstrate no lethality, RasGAP function seems not to be essential for FGF signaling (Botella et al., 2003).

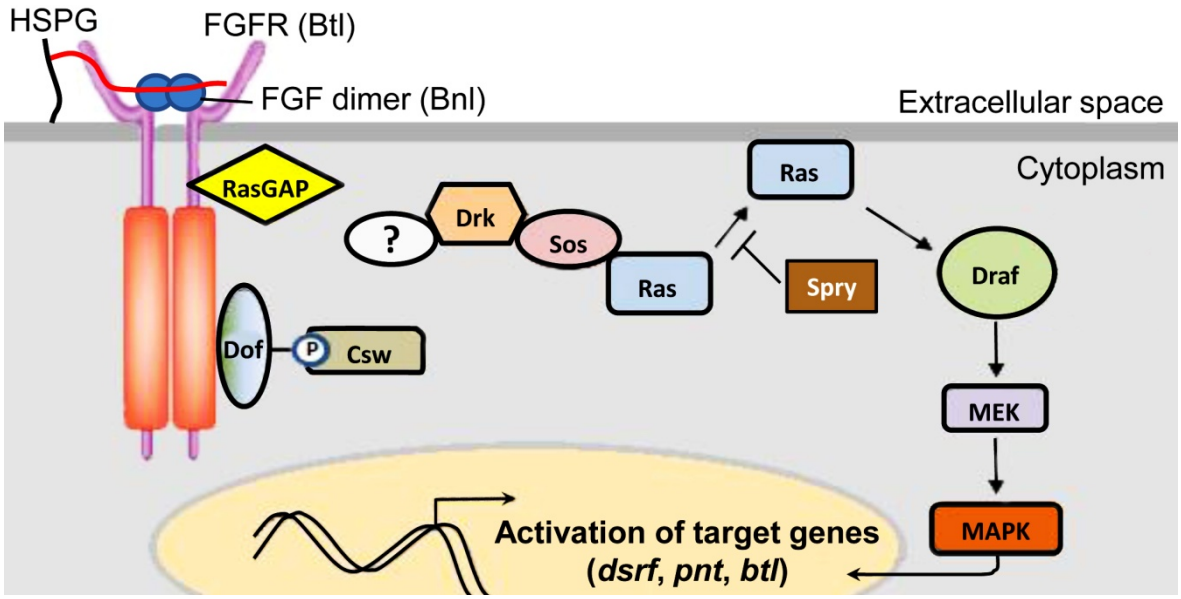

Figure 7: FGF signaling pathway in *Drosophila* (adapted from Petit et al., 2004). A schematic representation of the Bnl/Btl signaling pathway.

Not all FGF pathway routes have been identified to date and there are still some missing links to discover in the future. However, many identified proteins required for vertebrate FGF signaling appear to be highly conserved and functional in flies, proving high biological relevance of this pathway preserved through evolution.

1.4 FGF signaling in *Drosophila* development

Drosophila melanogaster represents an excellent model for studying the role of FGF signal transduction during embryogenesis due to the limited number of possible ligand-receptor interactions (Huang and Stern, 2005). FGF signaling is known to regulate formation and specification of the *Drosophila* mesoderm and branching morphogenesis during tracheal system development (Kadam et al., 2009; Samakovlis et al., 1996a).

1.4.1 FGF signaling in *Drosophila* mesoderm formation

Mesoderm spreading in *Drosophila* relies on FGFR Heartless (Htl) and two FGFs, Thisbe (Ths) and Pyramus (Pyr). Lack of both FGF ligands causes embryonic lethality, whereas single mutants are semilethal and show defects in mesoderm invagination and differentiation (Stathopoulos et al., 2004; Gryzik and Müller, 2004; Kadam et al., 2009; Klingseisen et al., 2009). Gastrulation in *Drosophila* occurs with invagination of the ventral part of the blastoderm and formation of the mesoderm primordial structure that undergoes further cell movements and rearrangements, which require several factors (Figure 8). The fate of future mesodermal cells is defined by high nuclear level of the transcription factor Dorsal (DL) on the ventral site of the blastula (Leptin and Affolter, 2004). DL activates the expression of Twist (Twi) and Snail (Sna). Twi acts as a transcriptional activator and induces the expression of mesodermal markers in the ventral blastoderm. In contrast, Sna functions as a transcriptional repressor of ectodermal markers in the mesodemal primordium. The invagination of mesoderm is accompanied by changes in cell shape that is induced by Twi and Sna (Leptin, 1991; Leptin, 1999).

Once inside the embryo, mesodermal cells first form an epithelial tube. However, later the cells lose their epithelial characteristics and intercellular contacts. They collectively migrate in the dorsolateral direction and spread out on the embryonic ectoderm forming a mesodermal monolayer (Leptin and Affolter,

2004). The disintegration of the mesodermal tube and spreading of the cells occur under the control of Htl signaling within the mesodermal cells (Figure 8). It was shown that Pyr is expressed in the dorsal ectoderm and provides an instructive cue for the migrating mesodermal cells (Kadam et al., 2009; Klingseisen et al., 2009). However, it seems that Pyr and Ths may function in a redundant manner in this process, since *pyr* mutant embryos show a weaker migration phenotype compared to *htl* mutants (Kadam et al., 2009; Klingseisen et al., 2009). Moreover, both FGF ligands are required in specification of the muscle progenitors during *Drosophila* development (Klingseisen et al., 2009).

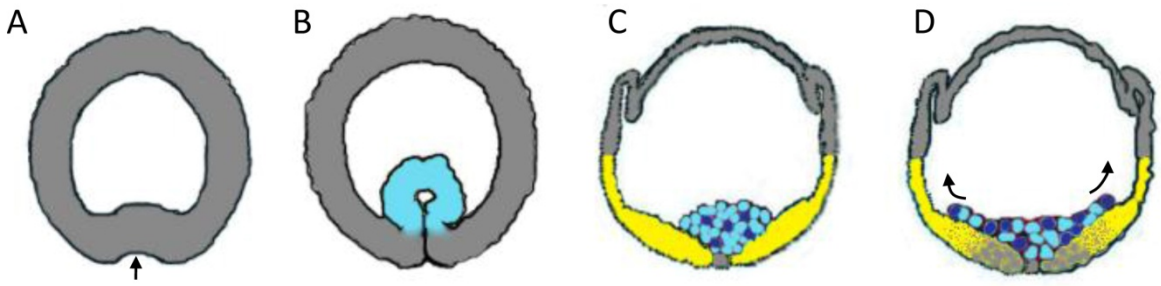

Figure 8: *Drosophila* gastrulation (adapted from Wilson and Leptin, 2000 and Stathopoulos et al., 2004). Schematic representation of gastrulation events in the embryo. Optical transverse crossections are shown. Arrows indicate the directions of gastrulational movement and mesoderm migration. **(A)** Invagination of the ventral blastoderm. **(B)** Mesoderm internalization and formation of the epithelial tube. Cells expressing the Htl receptor are marked in blue. **(C)** Disintegration of the tube and **(D)** spreading of the mesodermal cells along the embryonic ectoderm. The Pyr and Ths expressing cells are in yellow, The Htl-positive mesodermal cells are shown in blue (dark blue: cells with an activated MAPK cascade).

Despite the overlapping functions during gastrulation, Ths and Pyr demonstrate distinct activities during mesoderm specification (Kadam et al., 2009; Klingseisen et al., 2009). Pyr was shown to be required for the localized induction of *even-skipped* (Eve) expression in the dorsal mesoderm. This transcription repressor is involved in specification of subsets of pericardial and muscle cells on the dorsal side of the embryo (Smallhorn et al., 2004; Klingseisen et al., 2009). In addition, only Pyr was found to be essential for the formation of segment border muscles (SBMs) in *Drosophila*. These data suggest that Pyr function is more specialized compared to the function of Ths during early embryonic development (Klingseisen et al., 2009).

Furthermore, it was reported that *Drosophila* adaptor protein Dof also contributes to the mesodermal spreading (Petit et al., 2004; Wilson et al., 2004; Klingseisen et al., 2009), indicating that the conserved FGF signaling is essential for gastrulation. Furthermore, the RhoGEF Pebble functions downstream of Htl,

indicating that FGF signaling directly affects cell shape changes (Schumacher et al., 2004).

1.4.2 Role of FGF signaling in *Drosophila* tracheal development

Drosophila Bnl/Btl signaling is essential for the morphogenesis of the tracheal system. Tracheal development is a complex morphogenetic process that relies on the crosstalk of many signaling pathways. Therefore, first an introduction to general steps of the *Drosophila* tracheal system development will be given, and then the molecular mechanisms underlying this process will be described.

1.4.2.1 Development of Drosophila tracheal system

Drosophila tracheal system development involves a number of developmental events including generation of epithelial tubes, their consequent elongation and branching. The fly respiratory organ represents a bilaterally symmetric system of interconnected epithelial tubules of different diameter, which deliver oxygen to almost every cell of a body. Air enters the system through special openings called spiracles (Uv et al., 2003; Cabernard et al., 2004; Affolter and Caussinus, 2008).

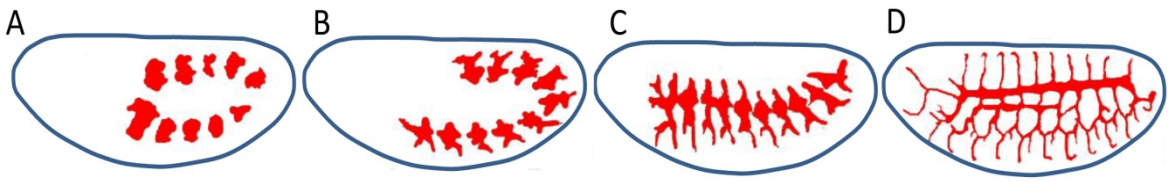

Figure 9: Development of *Drosophila* tracheal system (adapted from Cabernard et al., 2004). (A-D) Steps of the trachea formation in *Drosophila* embryo. Developing trachea is shown in red. Ten epithelial placodes arise on the both sides of the embryo. After two rounds of cell devision each metameric tracheal unit consists of ~80 cells. **(A)** Six primary branches grow out of the placode. **(B-D)** They elongate in different directions and some of them fuse together to form interconnected tubular network.

Tracheal system development starts during *Drosophila* embryogenesis (embryonic stage 10) with the formation of 10 pairs of bilaterally symmetric epithelial clusters called tracheal placodes, each containing ~20 cells (Figure 9). The cells of each placode divide twice to generate about 80 tracheal cells. These cells do not divide again until the metamorphosis (Sato and Kornberg, 2002; Cabernard et al., 2005). Previously it was thought that the number of the tracheal cells remains stable, however, it was shown recently that some cells of the developing tracheal system

undergo apoptosis during their migration (Baer et al., 2009). All 20 tracheal pits invaginate to form inner epithelial sacs that give rise to tracheal tubes. This internalization is not complete, since the short stalk connects the tracheal sac to the body surface forming spiracular branches. The development of each tracheal unit occurs in a highly stereotypic manner and includes elongation of epithelial tubes (primary branch formation), bifurcation (secondary branch formation), sprouting of terminal branches and branch fusion (Uv et al., 2003; Cabernard et al., 2004; Affolter and Caussinus, 2008).

At stage 11 of embryogenesis cells of the tracheal pits start migrating in different directions and form six primary branches: the dorsal branch (DB), the dorsal trunk anterior and posterior (DTa and DTp), the visceral branch (VB), lateral branches anterior and posterior/ganglionic branch (LBa and LBp/GB) (Figures 10 and 11). Spiracular branches (SB) on each side on the body close later during embryogenesis. Primary tracheal branches build up the basic framework of the respiratory organ. During development every tracheal branch follows a certain growing pattern. Dorsal branches migrate dorsally towards the developing cardiac tissue. DTa and DTp branches grow in anterior and posterior directions respectively and eventually fuse together to form the dorsal trunk. Visceral branches grow towards the inner organs to deliver oxygen to the gut, whereas ganglionic branches elongate ventrally towards the central nervous system (CNS) (Samakovlis et al., 1996a; Uv et al., 2003) (Figure 10).

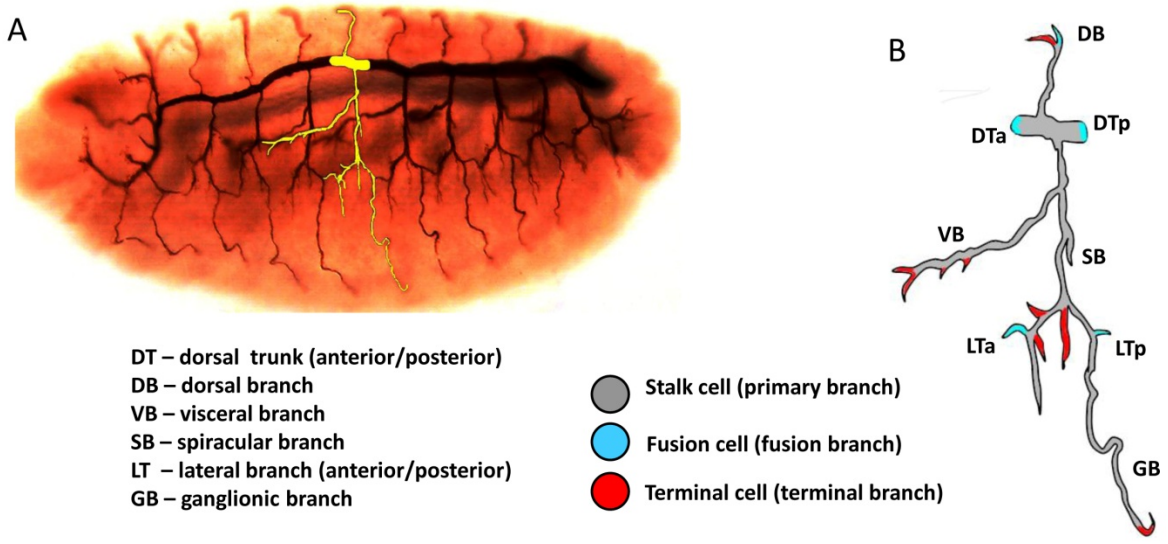

Figure 10 *Drosophila* respiratory system (adapted from Uv et al., 2003). (A) Tracheal system of the late embryo visualized by the antibody against lumenal antigen. One of the tracheal metamers is shown in yellow. **(B)** Schematic drawing of the individual tracheal metamer. Multicellular primary branches are marked in grey. Unicellular terminal branches are in red. Fusion branches that interconnect tracheal metamers are in blue.

The process of branch growth includes cell elongation and rearrangement. During tube formation neighboring tracheal cells located side by side undergo controlled intercalation. This event is based on changes of cellular shape and remodeling of the adhesive junctions (AJ) and results in an assumption of an end-to-end cell configuration (Ribeiro et al., 2004).

At stage 14 tracheal cells at the tip of each primary branch (leading cells) send unicellular outgrowths (secondary branches) that elongate and eventually form terminal branches (Figure 10). They represent blind-ended capillaries with an intracellular lumen that directly contact target tissues (Samakovlis et al., 1996a; Uv et al., 2003). However, some secondary branches contact and fuse with tracheal cells of the neighboring metamere to generate an interconnected tubular network (Uv et al., 2003). These branches are called fusion branches (Figure 10). Branch fusion is a complex process that involves cell recognition and the formation of an intracellular lumen within the fusion cells (Samakovlis et al., 1996b).

Morphogenesis of the *Drosophila* respiratory system continues after embryonic development during larval and pupal stages. During the late larval period embryonic tracheal branches undergo extensive remodeling and give rise to the specialized structure called air sac primordium, whose cells proliferate and migrate to form the adult tracheal system (Sato and Kornberg, 2002; Cabernard et al., 2005; Chanut-Delalande et al., 2007).

1.4.2.2 Regulation of tracheal system development in Drosophila

Specification of tracheal precursor cells is under the control of several transcription factors including Tango (Tgo), Trachealess (Trh) and Ventral veinless (Vvl, also called Drifter) (Anderson et al., 1997; Llimargas and Casanova, 1997), whose expression starts at the stage 10 of *Drosophila* embryogenesis. Trh forms a heterodimer with Tgo and the expression of these factors determines tracheal cell fate (Boube et al., 2000; Brodu and Casanova, 2006).

The exact position of future placode invagination was shown to be strongly region-specific and is defined by the localized activity of several factors (Figure 11). One of them is the zinc-finger transcription factor Spalt (Sal) (Kühnlein et al., 1994), whose activity restricts the area of the forming tracheal placode. Additionally, Sal participates in the dorsal trunk formation during later stages of

Drosophila embryogenesis (Kühnlein and Schuh, 1996). Trh also induces the expression of Rhomboid (Rho), a transmembrane protein that specifically cleaves and activates the EGF ligand Spitz (Lee et al., 2001a). EGF activity is responsible for the proper cellular movements during placode invagination and for subsequent migration of the tracheal cells (Figure 11). This pathway is also essential to maintain epithelial integrity during tracheal migration via cadherin-based cell-cell adhesion (Cela and Llimargas, 2006). Components of EGF signaling including Spitz ligand (Spi), *Drosophila* EGF receptor (DER) and Rho are involved in the regulation of the directional migration of tracheal cells along the AP body axis via induction of Sal expression. Thus, EGF signaling controls formation of the dorsal trunk and visceral branches (Llimargas and Casanova, 1999; Wappner et al., 1997).

Furthermore, the TGFβ homolog Dpp is expressed dorsally and ventrally of the initial place of placode invagination (Figure 11). Dpp signaling is required for the tracheal migration along the dorso-ventral axes and causes inhibition of Spalt function in the dorsal branches. Dpp interacts with receptor serine/threonine kinases Thick veins (Tkv) and Punt (Put) and locally controls Sal expression via the induction of Knirps (Kni) and Knirps-related (Knrl) zink finger transcription factors (Chen et al., 1998). Dpp signaling is required for the formation of dorsal branches, lateral trunk branches and ganglionic branches (Affolter et al., 1994; Vincent et al., 1997) (Figure 11). It was shown that *rho* and *tkv* double mutants demonstrate loss of all tracheal branches, consistent with the determined functions of these signaling pathways in tracheal development (Wappnes et al., 1997).

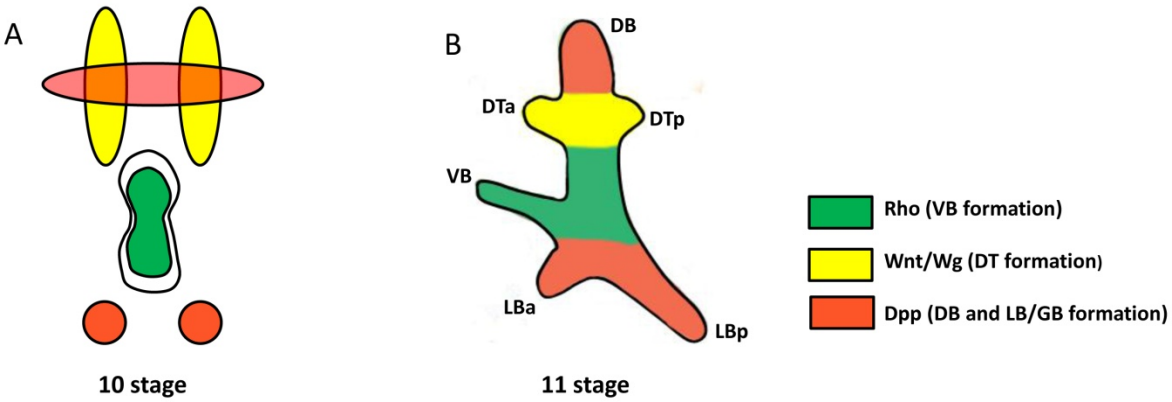

Figure 11: Involvement of patterning genes in specification of tracheal branches (adapted from Uv et al., 2003). (A) Localized expression of the signaling components of EGF (green), Wnt (yellow) and Dpp (red) pathways during early tracheal development. **(B)** Each patterning factor controls distinct subsets of tracheal branches.

Moreover, Wingless (Wg) signaling was shown to specify cell fate in the dorsal trunk via induction of Sal expression. Wg also promotes cell differentiation in all fusion branches (Chihara and Hayashi, 2000; Llimargas, 2000) (Figure 11). Furthermore, the components of Wnt/Wg, EGF or Dpp/TGF-β signaling pathways were shown to regulate the size, shape and branching pattern of individual tracheal branches.

FGF signaling is essential for the directional migration of the tracheal branches and determination of branch-specific cell fate during *Drosophila* tracheal development. In the absence of one of the pathway components such as the Btl receptor, the Bnl ligand or protein tyrosine phosphatese Csw, tracheal branches do not migrate in the stereotypically defined manner and mutant embryos fail to form a normal tracheal system (Klämbt et al., 1992; Sutherland et al., 1996; Perkins et al., 1996). Moreover, mutations of *sugarless* and *sulfatless*, genes encoding enzymes involved in the synthesis and modification of heparan sulfate proteoglycans (HSPGs), also result in a migration disorder (Lin et al., 1999). Furthermore, similar tracheal phenotypes were observed in embryos lacking functional Dally-like, cell-surface bound HSPG (Yan and Lin, 2007).

Starting from stage 10 of embryogenesis all tracheal cells start to express the Btl receptor. At the same time Bnl is expressed in cell clusters surrounding the tracheal metamere. The Bnl ligand activates Btl in the nearby tracheal cells and induces directed migration and formation of the primary tracheal branches (Sutherland et al., 1996).

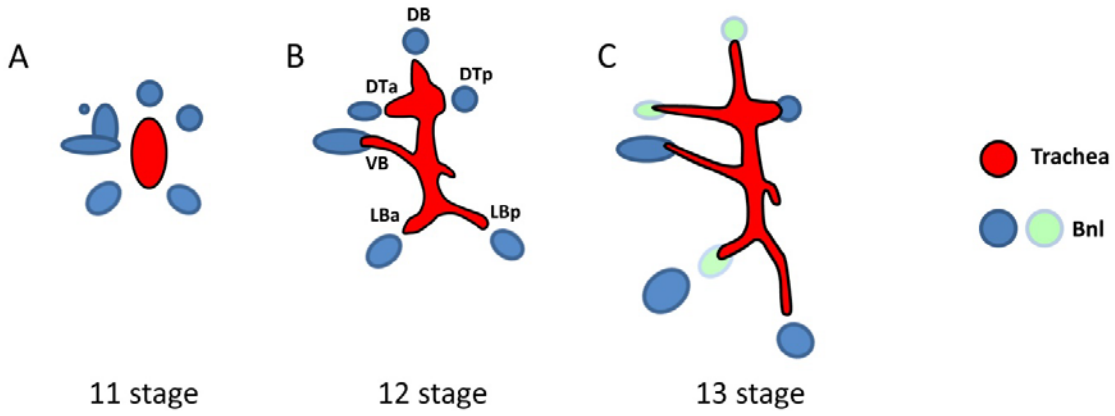

Figure 12: Directional migration of the primary branches controlled by Bnl/Btl signaling (adapted from Uv et al., 2003). (A-C) Schematic representation of the developing tracheal metamere. Tracheal epithelium expressing the Btl receptor is shown in red; the Bnl FGF ligand is shown in blue. **(A)** Tracheal cells migrate in different directions and form six primary branches: the dorsal branch (DB), the dorsal trunk anterior and posterior (DTa and DTp), the visceral branch (VB), lateral branches anterior and posterior (LBa and LBp). **(B, C)** Once the tracheal branch reaches the source of Bnl, its expression fades (light blue circles) and appears in other developmentally programmed place.

In other words, Bnl serves as a chemoattractant for the tracheal cells (Figure 12). Once the leading cell of the branch reaches the source of Bnl expression, its synthesis starts in other place according to the developmental pattern (Sutherland et al., 1996). Thus, Bnl/Btl signaling provides spatially and temporally regulated molecular cues critical for the stereotyped formation of the tracheal branches. Based on *in vivo* imaging experiments, it was shown that FGF-mediated signaling induces the generation of dynamic filopodia in tracheal cells, which probably contributes to the oriented cellular movements. Dynamic filopodia fail to form in animals, which lack Btl, Bnl or Dof activity. Moreover, ectopic expression of Bnl in the tracheal cells results in multiple filopodia formation (Ribeiro et al., 2002). Interestingly, the deletion analysis of the Dof adaptor protein suggests that MAPK activation is not required for the tracheal cell migration. This indicates that other FGF-mediated signaling pathways, including PI3K activation or PLCγ/calcium dependent intracellular cascade, may be involved in tracheal migration (Petit et al., 2004).

FGF signaling is also required for secondary branching via induction of ETS-transcription factor Pointed (Pnt) expression in the leading cells of the trachea, which is supposed to undergo bifurcation (Scholz et al., 1996). Pnt also plays a permissive role for the formation of terminal branches (Klämbt, 1993; Samakovlis et al., 1996a). The inhibitor of FGF signaling Spry is also involved in the secondary branching. Its expression is activated in the tracheal leading cells by Bnl/Btl signaling pathway. It functions non-autonomously and provides spatial restriction of FGF signaling in stalk cells preventing formation of additional branches (reviewed in Kim and Bar-Sagi, 2004). Embryos lacking Spry activity show formation of multiple ectopic terminal branches, suggesting that all tracheal cells assume the leading cell fate (Hacohen et al., 1998; Jarvis et al., 2006).

During tracheal morphogenesis some of the leading cells become specialized as fusion cells (Tanaka-Matakatsu et al., 1996). Upon contact with the leading cell of the other branch the two branches fuse together with the consequent formation of the common lumen. Notch signaling functions as a negative regulator of fusion cell fate by the inhibition of MAPK activation and the loss of Notch activity was reported to cause ectopic branch fusions in *Drosophila* (Steneberg et al., 1999; Llimargas, 1999; Ikeya and Hayashi, 1999).

Migration and fusion of the dorsal trunk branches, in addition to Bnl signals, require special mesodermal cells (bridge cells) that express the transcription factor Hunchback (Hb) (Wolf and Schuh, 2000). These cells are localized at the places where DTa and DTp branches meet and *hb* mutants demonstrate DT fusion defects.

Also, the terminal tracheal branches receive their specification through FGF-mediated induction of Blistered (Bs, also Pruned and DSRF) expression. Bs promotes branch elongation and formation of fine cellular protrusions with an internal lumen that penetrate the target tissue (Guillemin et al., 1996). Slit/Robo signaling provides an additional control of terminal branch migration and was shown to repel tracheal cells from ventral midline (Englund, et al., 2002).

Furthermore, the Bnl/Btl signaling was shown to play an essential role as mitogen and chemoattractant during larval trachea remodeling, shaping and guiding the newly appearing tracheal branches to their developmentally predetermined positions (Sato and Kornberg, 2002). However, formation of larval tracheal branches is additionally regulated by oxygen demand in the surrounding tissues. It was shown that Bnl expression is upregulated under hypoxic conditions and that induces additional tracheal growth towards the oxygen-starving tissue (Jarecki et al., 1999). Furthermore, FGF signaling in larvae is regulated by *Drosophila* matrix metalloproteinase 2 (Mmp2). Similar to Spry, it inhibits Bnl signaling in stalk cells in a non-autonomous manner. The target of the protease remains unknown, however, it was reported that the expression of Mmp2 in the tracheal cells is induced in response to FGF signaling building up the negative feedback loop (Wang et al., 2010).

Taken together, the morphogenesis of the fly tracheal system involves the interplay of numerous instructive and limiting factors, whose spatial and temporal control helps to generate and shape an elaborated and highly ordered tubular organ. FGF signaling plays an essential role in this process and its modulated biological activity induces diverse cellular responses during the entire process. In this work, the developing trachea of *Drosophila melanogaster* serves as a model system to study the biological relevance of Bnl processing for its morphogenetic function.

2 MATERIALS AND METHODS

2.1 Molecular cloning

2.1.1 Polymerase chain reaction

Polymerase Chain Reaction (PCR) was used to produce DNA fragments for succeeding cloning. PfuUltra High-Fidelity DNA Polymerase (Stratagene) and PfuUltra II Fusion HS DNA Polymerase (Stratagene) were used for generation of the PCR product for cloning. HotStarTaq DNA Master Mix Kit (Qiagen) was used for analytical PCR. The chosen annealing temperature for each reaction was generally 5°C below the melting temperature of the designed primer pair. All PCRs were performed using Gene Amp 9700 PCR cycler (Applied Biosystems).

2.1.2 DNA/RNA electrophoresis in agarose gel

For purification or analysis of DNA or RNA fragments, they were subjected to electrophoresis in 0.8–2 % agarose gels with addition of ethidium bromide (Roth) in 0.5 % TBE buffer (Sambrook et al. 1989). DNA/RNA samples were loaded next to GeneRuler 1kb Plus DNA Ladder (Fermentas) to estimate relative size of the fragments. Stained DNA/RNA was visualized using UV-transilluminator (Raytest) at 366 nm.

2.1.3 DNA gel extraction

Desired DNA fragments were cut out from an agarose gel using a scalpel. DNA was extracted from the gel using QIAquick Gel Extraction Kit (Qiagen), according to the manufacturer's protocol.

2.1.4 Determination of DNA concentration

1µl aliquots of DNA aqueous solution were used to estimate the concentration of DNA. All measurements were performed at 260 nm using NanoDrop 1000 Spectrophotometer (Thermo Scientific), according to the manufacturer's manual.

2.1.5 DNA digestion with restriction endonucleases

The reactions were carried out as described (Sambrook et al. 1989). For analytical purposes 1 µg of DNA was incubated with respective enzymes in total volume of 20 µl for 1–2 h. In preparative reactions 5 to 10 µg of DNA was digested in 50 µl volumes for 4h. All enzymatic digestion reactions were performed at 37°C. After restriction reaction DNA samples were purified using QiAquick Nucleotide Removal Kit (Qiagen), according to the manufacturer's protocol, and eluted in 30–50 µl volume.

2.1.6 Dephosphorylation of linearized vector DNA

In order to prevent linearized vector DNA from self-ligation, 5' phosphate groups were removed by treatment of DNA with an alkaline phosphatase (according to the protocol adapted from Sambrook et al., 1989). 1 µl of Shrimp alkaline phosphatase (SAP) (USB) was added to digested vector DNA samples in appropriate amount of SAP buffer (USB) and incubated at 37°C for 30 minutes. Afterwards, SAP was inactivated by heating DNA vector samples at 65°C for 15 minutes.

2.1.7 DNA ligation

For a ligation reaction (adapted from Sambrook et al., 1989), 50–100 ng of linearized dephosphorylated vector was combained with a purified PCR fragment in a molar ratio 1:5, 1 µl of T4 DNA ligase (Fermentas) and appropriate volume of T4 DNA ligase buffer (Fermentas) in total volume of 10 to 30 µl. DNA ligation reactions were generally performed at room temperature for 1–2 h or overnight at 18°C.

2.1.8 Gateway TOPO cloning

For a directional cloning of blunt-end PCR fragments, pENTR Directional TOPO Cloning Kit (Invitrogen) was used. Cloning reactions were set up according to the manufacturer's protocol. One Shot Top10 chemically competent *E. coli* cells, provided with the pENTR Directional TOPO Cloning Kit (Invitrogen) were used for further transformation of the cloning constructs.

2.1.9 Gateway LR recombination

For a LR recombination reaction, 50–100 ng of pENTR/D-TOPO vector containing the desired DNA insertion in the rfa-recombination cassette was combined with 100–150 ng of destination vector carrying a promoter sequence and 5' or 3' fusion tags. The reaction was set up and performed using LR Gateway recombination kit (Invitrogen) according to the manufacturer's protocol. One Shot Top10 chemically competent *E. coli* cells (Invitrogen) were used for further transformation of the recombination constructs.

2.1.10 Preparation of chemically competent *E. coli* cells

Generation of chemically competent *E. coli* cells was performed according to Inoue et al., 1990. A single colony of XL1-blue *E. coli* cells was inoculated in 5 ml of LB bacterial medium overnight at 37°C and agitation 200 rpm. 1 ml of overnight culture was transferred to 250 ml of fresh LB medium and cultured until an OD_{600} reaches 0.5–0.6. Then the culture was incubated on ice for 10–15 minutes. All further steps were carried out on ice or at 4°C. *E. coli* cells were collected by centrifugation at 3500 rpm for 10 minutes. The cell pellet was resuspended in 10 ml of TB solution (10 mM PIPES, 15 mM $CaCl_2$, 250 mM KCl, pH adjusted to 6.7 with KOH, then added 55 mM $MnCl_2$). 70 ml of TB was added and the cells were kept on ice for 10–15 minutes. The cells were pelleted by centrifugation at 3500 rpm for 10 minutes and resuspended in 20 ml of TB with 7% DMSO. After 10-15 minutes of incubation on ice the cells were aliquoted and flash-frozen in liquid nitrogen. The aliquotes were kept at -80°C until used for the transformation.

2.1.11 Transformation of chemically competent *E. coli* cells

A heat-shock transformation was carried out according to Inoue et al., 1990. An aliquot of chemically competent *E. coli* cells was thawed on ice and 5–10 µl of ligation reaction or TOPO cloning mixture were added to the cells. After 30 minutes of incubation on ice, the cells were subjected to the heat shock at 42°C for 30 seconds and transferred back onto ice. The cells were incubated for 1 hour in 800 µl of LB medium at 37°C with constant agitation. Then 100 µl of culture were plated on LB agar plates containing an appropriate antibiotic.

2.1.12 Site-directed mutagenesis

Point mutations of Bnl furin sites were introduced using Quick Change Site-Directed Mutagenesis Kit (Stratagene). Oligonucleotides designed for mutagenesis contain desirable mutations and 15-17 nucleotides complementary flanking regions. Site-directed mutagenesis procedure was performed according to the manufacturer's manual. Plasmid DNA isolated from resulting bacterial clones was sequenced to control for the presence of the nucleotide substitutions.

2.1.13 Isolation of plasmid DNA

Plasmid DNA was isolated using QIAprep Plasmid Mini Kit (Qiagen) or QIAfilter Plasmid Midi Kit (Qiagen). A single colony of transformed *E. coli* cells was inoculated overnight at 37°C with constant agitation in 3–5 ml of LB medium containing selective antibiotic. Next day the cells were collected by centrifugation at 4000 rpm for 15 minutes. The plasmid preparation procedure was performed according to the protocol supplied by manufacturer.

2.1.14 Sequencing of DNA

DNA samples for sequencing contained each 0,7–1 µg of plasmid DNA that was either lyophilized or diluted in 15 µl of pure water. Oligonucleotides were diluted to 2 pmol/µl and supplied in volume of 15 µl. DNA sequencing was performed in sequencing facility of MWG-Biotech AG.

2.1.15 Generation of cDNA library from *Drosophila* Kc cells

Total RNA was isolated form *Drosophila* cultured cells using RNeasy Mini RNA purification Kit (Qiagen), according to the manual provided by the manufacturer. QuantiTect Reverse Transcription Kit (Qiagen) was utilized for *in vitro* cDNA synthesis. The reaction was set up and performed according to the manufacturer's protocol.

2.1.16 Semi-quantitative PCR

To estimate the efficiency of dsRNA silencing of furin genes in *Drosophila* Kc cells, semi-quantitative PCR was performed using 10 ng of different Kc cDNA

library samples as templates. The PCR reactions were set up using gene-specific primer pairs and HotStarTaq DNA Master Mix Kit (Qiagen), according to the manufacturer's manual. Resulting PCR products were analyzed in 1,5-2% agarose gel as described in section 2.1.2. The acquired image of DNA bands was subjected to quantitative analysis of DNA intensity as described in section 2.5.3.

2.1.17 Preparation of single-stranded RNA *in situ* probes

5-10 µg of plasmid DNA containing gene of interest and 3' RNA polymerase promoter was linearized using a unique restriction site within the insert located 500-1000 bp upstream of RNA promoter. The digestion reaction was performed as described in section 2.1.5. The linearized plasmid was purified with QiAquick Nucleotide Removal Kit (Qiagen), according to the manufacturer's protocol, and eluted in 30–50 µl volume. The digoxygenin (DIG) labeled RNA probe was generated using linearized DNA template and DIG RNA labeling kit (Sp6/T7) (Roche), according to the protocol provided by the manufacturer. The synthesized single-stranded RNA probe was purified using RNeasy Mini kit (Qiagen), according to the manufacturer's manual. The RNA probe was visualized on 2% agarose gel as described in section 2.1.2. The probe was mixed with one volume of Hybe buffer (50% Formamide, 5x SSC, 5 µg/ml Heparin, 0,2 mg/ml sonicated salmon testis DNA, 0,1 mg/ml tRNA) and kept at -20/-75ºC.

2.1.18 Preparation of double-stranded RNA for transfection of Kc cells

The DNA templates for dsRNA synthesis were generated by PCR. Resulting short PCR products contain two opposing T7 promoters. *In vitro* synthesis of dsRNA was performed using MEGAscript T7 Transcription Kit (Ambion) according to the manual supplied by manufacturer. Resulting dsRNA was purified with RNeasy mini RNA purification kit (Qiagen) according to the manufacturer's protocol.

2.2 Cell biology methods

2.2.1 Maintenance of *Drosophila* cultured cell lines

Drosophila Kc167 (Drosophila Genomics Resource Center (DGRC), Echalier and Ohanessian, 1970) embryonic cell line was maintained in Schneider's *Drosophila* medium (Gibco) supplemented with 100 μg/ml of penicillin/streptomycin (PAA Labs) and 10% of fetal calf serum (Sigma Aldrich). The cells were cultured in 25 cm^2 flasks or 10 cm^2 plates at 25ºC.

2.2.2 Transient transfection of *Drosophila* Kc cells

Confluent *Drosophila* Kc cells were plated at a concentration of $1x10^5$–$5x10^5$ cells/ml on 6-well (2 ml per well) or 12-well (1 ml per well) cell culture plates. The cells were grown overnight before the transfection. The transfection was performed next day using the Effectene Transfection Kit (Qiagen). The manufacturer's protocol was adjusted for *Drosophila* cells. 1 μg of plasmid DNA was combined with 200 μl of EC buffer, 20 μl of Enhancer reagent, 8 μl of Effectene reagent and the appropriate volume of cell medium per one well of 6-well plate. The amount of DNA and reagents was scaled down by half for the transfection of 12-well plate. The resulting mixture was added drop-wise onto the cells. Next day, the cells were carefully washed with 1x PBS buffer (1,7 mM KH_2PO_4, 5,2 mM Na_2HPO_4, 150 mM NaCl) and serum-free medium with or without proteinase inhibitor cocktail (Complete Proteinase Inhibitor Cocktail Tablets, Roche) was added. The cells were incubated at 25ºC for 1 or 2 days. Then the supernatant and cells were harvested for further analysis.

2.2.3 Knock-down of endogenous gene expression by dsRNA

Drosophila Kc cells were split and plated onto 12-well plate at a concentration 1-1,5$x10^6$ cells/ml. The cells were allowed to settle for 45 minutes in serum-free medium. Then the medium was substituted with the complete Schneider's medium with 10% of fetal calf serum, which contained 10 μg of dsRNA. The cells were incubated at 25ºC. After 3-4 days dsRNA treated cells were either additionally transfected with plasmid DNA as described in section 2.2.2 or harvested for subsequent analysis.

2.2.4 Receptor-ligand binding assay in *Drosophila* embryonic cells

Kc cells were transfected separately with receptor (pUbi-FLAG-Btl) or Bnl (pUbi-EGFP-Bnl-Myc) DNA constructs as described in section 2.2.2. One day before the assay, the receptor-expressing cells were plated on the cover slips and allowed to settle overnight. Next day, cell supernatants containing secreted Bnl molecules were collected and centrifuged at 1500 rpm for 10 minutes to get rid of the residual cells. The conditioned medium of receptor expressing cells were substituted with the cell-free Bnl supernatants and the cells were incubated at 4ºC for 2 hours with slow agitation to allow specific binding of Bnl ligands to the cell-surface Btl receptors. Afterwards, the cells were subjected to the fluorescent immunostaining.

2.2.5 Immunostaining of *Drosophila* cells

The cells on the cover slips were washed 3 times with ice-cold 1x PBS buffer and fixed in 4% paraformaldehyde (PFA) solution in 1x PBS at room temperature for 10 minutes. Afterwards, the cells were thoroughly washed 3 times for 15 minutes with 1x PBT buffer and subsequently blocked using 1x PBT with 10% of goat serum (Sigma Aldrich). Then the cover slips were incubated for 30 minutes with primary anti-GFP and anti-FLAG antibodies in 1x PBT with 5% goat serum at room temperature with slow agitation. The cells were subsequently washed 3 times for 15 minutes in 1x PBT and incubated for 30 minutes with fluorescently coupled secondary antibody at room temperature with slow agitation. Finally, the stained cells were washed 3 times for 15 minutes in 1x PBT and the cover slips were mounted on the microscopic slides in Vectashield mounting medium with DAPI (Vector Laboratories). The slides were sealed with transparent nail polish and kept at 4ºC until used for fluorescent microscopy.

2.2.6 Fluorescent scanning confocal microscopy of *Drosophila* cells

The stained Kc cells were analyzed on Leica TCS SP2 LSM confocal microscope (Leica Microsystems) using 488 nm and 568 nm excitation light. The images were acquired with 40x magnification oil objective.

2.2.7 Preparation of cell lysates for Western blot analysis

Transfected cells were washed twice with 1x PBS buffer. Then the cells were harvested and lysed in 1x loading buffer (50 mM Tris-HCl pH 6.8, 1% SDS, ~0,01% bromphenol blue, 50 mM Dithiothreitol (DTT), 5% Glycerol) and kept at -20ºC until analysed by Western blot.

2.2.8 Preparation of cell supernatants for Western blot analysis

Drosophila cells were grown and transfected as described in section 2.2.2. Afterwards, supernatants of transfected cells were collected and centrifuged at 1500 rpm at room temperature to get rid of residual cells. Then the supernatants were concentrated using Vivaspin 2 centrifugal protein concentrators (10.000 MWCO PES, Vivascience AG). Alternatively, cell-free supernatants were concentrated using trichloracetic acid (TCA) protein precipitation. 100% TCA (500 g TCA, 227 g water) was added to 10-15% concentration to the supernatant samples and mixed well. The samples were kept at -20ºC for 30 minutes to induce protein precipitation. The precipitates were collected by centrifugation at 15000 rpm at 4ºC for 10 minutes. The resulting pellets were washed with ice-cold acetone (Merck Chemicals), air-dried for 5 minutes and dissolved in 50-100 µl of 1x loading buffer. The concentrated supernatant samples were subsequently analyzed by Western blot (see Materials and methods sections 2.3.2-2.3.4).

2.3 Proteomic methods

2.3.1 Enzymatic protein N-deglycosylation

Enzymatic N-deglycosylation reaction (according to Tarentino and Plummer, 1994) was employed to remove sugar moieties attached to asparagine residues of the protein chain. Protein N-deglycosydase F (PNGase F, Sigma Aldrich, Plummer et al., 1984) was used for this purpose. 45 µl of concentrated cell supernatant was mixed with 5 µl of the denaturing buffer (0,2% SDS, 100 mM 2-mercaptoethanol). The solution was heated at 100ºC for 10 minutes to denature the proteins and then cooled down to the room temperature. Then 5µl of 15% Triton-X100 and 5 µl of PNGase F were added to the solution. The mixture was incubated at 37ºC for 1-2 hours. The enzymatic reaction was stopped by heating at 100ºC for 5 minutes. Deglycosylated supernatant samples were subjected to Western blot analysis.

2.3.2 SDS protein electrophoresis (modified from Laemmli, 1970)

Protein polyacrylamide gels (PAGEs) containing different concentrations of acrylamide were precast using 8%, 10% or 15% resolving gel solution (375 mM Tris-Cl pH 8.8, 0,1% SDS, 0,1% ammonium persulfate (APS), 0,08% tetramethylethylendiamin (TEMED), appropriate percentage of 30% acrylamide-bisacrylamide solution) and stacking gel solution (4% acrylamide, 130 mM Tris-Cl pH 6.8, 0,1% SDS, 0,1% APS, 1µg/ml TEMED). Protein samples were mixed with 4x loading buffer and heat at 95ºC for 5 minutes. Then the samples were run on PAAG along with PageRuler Plus Prestained Protein Ladder (Fermentas) using Mini Protean II System (Bio Rad). Protein electrophoresis was performed at a constant voltage of 80-110 V in 1x Tris-Glycine buffer (25 mM Tris, 250 mM Glycine, 0,1% SDS) until the dye front reached the gel bottom.

2.3.3 Tricine-SDS protein electrophoresis

Tricine-SDS PAGE electrophoresis (according to Schägger and Von Jagow, 1987) was employed for the efficient separation of low molecular weight proteins. The 15% polyacrylamid gel was precast as described in section 2.2.10. The electrophoresis was run using 1x Cathode buffer (0,1M Tris, 0,1M Tricine, 0,1% SDS) and 1x Anode buffer (0,2 M Tris-Cl pH 8.9) in Mini Protean II System (Bio Rad) at a constant voltage of 90-150 V.

2.3.4 Protein immunodetection by Western blot

Protein gels after electrophoresis were blotted on a polyvinylidenfluorid (PVDF) (Millipore) membrane activated by 30 seconds incubation in methanol. Protein blotting was performed in 1x Transfer buffer (25 mM Tris, 250 mM Glycine, 10% methanol) using Mini Protean II System (Bio Rad) at a constant voltage of 45 V for 1 hour 40 minutes. All subsequent steps were performed on a shaker unless mentioned otherwise. The membrane was shortly washed in 1x PBT buffer (1x PBS with 0,01% Tween-20) and blocked for 2 hours in 1x Blocking buffer (Sigma Aldrich) to diminish a cross-reactivity of antibody. The membrane was incubated overnight at 4ºC with primary antibody at appropriate concentration in 1x Blocking buffer. Next day, the membrane was washed 3 times for 15 minutes with 1x PBT and subsequently incubated with HRP-coupled secondary antibody for 1 hour. Finally, the membrane was washed 3 times for 15

minutes in 1x PBT buffer. The specific chemiluminescent signal was developed using SuperSignal West Dura Extended Duration Substrate (Thermo Scientific), according to the manufacturer's protocol. The image was acquired using LAS 1000Plus IDX2 Intelligent Dark Box II luminescence detector (Fujifilm). In order to reprobe the same membrane with different primary and secondary antibodies, it was subjected to the stripping procedure to wash away bound antibody using Western blot striping buffer (Thermo Scientific). Then the membrane was washed 3 times for 15 minutes with 1x PBT buffer and incubated with the new antibody as described above.

2.4 *Drosophila* techniques

2.4.1 Maintenance of *Drosophila melanogaster* strains

Fruit flies were maintained and bred in the fly vials on a food medium containing corn flour-soya, flour-molasses and dry yeast. The vials were kept at 25ºC and 20-30% humidity.

2.4.2 Generation of stable transgenic fly lines

Transgenic *Drosophila* lines were generated using site-specific P-element mediated germline transformation (Bischof et al., 2007) at the cytolocation 86F on the third chromosome. Plasmid DNA for injection was isolated and purified as described in section 2.1.13. Embryo injections were performed in BestGene Inc. (California, USA). Freshly eclosed transformed flies were identified by the red eye color introduced by a *mini-w*$^{+}$ marker gene in the P-element insertion. The flies were further crossed to a "balancer" fly lines for the third chromosome w^{1118}*;; D3/TM6B Hu* or w^{1118}*;; D3/TM3 Ser*.

2.4.3 UAS/GAL4 system for ectopic gene expression

UAS/GAL4 system was utilized to induce spatially- and temporary-specific gene expression in *Drosophila* embryo (Brand and Perrimon, 1993). The system relies on the yeast transcription factor GAL4 that interacts with upstream Activating Sequence (UAS) and activates expression of a downstream target gene. During the experiment, transgenic flies carrying *gal4* coding sequence downstream of a tissue-specific promoter were mated with a fly line encoding gene of interest fused downstream of UAS element. The resulting progeny show

certain temporal and spatial pattern of target gene expression controlled by a specific promoter upstream of *gal4* sequence.

2.4.4 Collection and fixation of *Drosophila* embryos

Drosophila embryos were collected on agar-apple juice plates supplemented with yeast for 14-20 hours at 25ºC. The embryos were harvested from the plates using a brush and thoroughly washed with 1x Embryo wash buffer (10 mM NaCl, 0,01% Triton X-100) to get rid of the residual yeast. Then the embryos were dechorinated with 50% bleach and washed again with 1x Embryo wash buffer. Afterwards, they were fixed in 1 ml of RNA-fix solution (10% paraformaldehyde, 50 mM EGTA) with addition of 6 ml of heptane for 20 minutes on a rocking platform. Then the aqueous fixing solution was discarded and the embryos were devitellinized by adding of 5 ml of methanol to the residual heptane phase and thoroughly mixing for 15 seconds. Devitellinized embryos were washed 3 times with methanol and stored at 4ºC

2.4.5 Embryo immunostaining

All steps were performed at room temperature with constant rotation unless mentioned otherwise. Fixed *Drosophila* embryos were rehydrated by washing 3 times with 1x PBT buffer (described in section 2.3.4). Then the embryos were incubated with primary antibody at appropriate concentration overnight at 4ºC on a rotator. Next day the embryos were washed several times with 1x PBT buffer and blocked for 1 hour using 10% goat serum to prevent cross-reactivity of antibody. Afterwards, secondary antibodies at appropriate dilution were added and the embryos were incubated for 2 hours. Then the embryos were washed 3 times for 15 minutes with 1x PBT buffer. For the signal amplification, the embryos were incubated with ABC Elite PK6100 Kit (Vector Laboratories). The reaction was prepared by mixing of 10 µl of solution A and 10 µl of solution B in 500 µl of 1x PBT buffer half an hour in advance. The embryos were incubated with the reaction mixture for 30-45 minutes. After thorough washing with 1x PBT a specific staining was developed with SIGMAFAST^{TM}3,3'-Diaminobenzidine tablets (Sigma Aldrich) detecting peroxidise activity of HRP-coupled secondary antibody. The reaction was terminated by washing 3 times with 1x PBT buffer. In case when alkaline phosphatise-coupled secondary antibodies were used, the embryos were additionally washed with 1 ml of alkaline phosphatase (AP) buffer (200 mM Tric-Cl pH 9.5, 100 mM NaCl, 50 mM $MgCl_2$) and a specific blue staining was developed by

incubation of the embryos with 4,5 µl 4-Nitro blue tetrazolium chloride (NBT, Roche)/3,5 µl 5-Bromo-4-chloro-3-indolyl-phosphate (X-phosphate, Roche) mixture in 1 ml of AP-buffer for 10-45 minutes without rotation. The precipitation reaction was stopped by washing 3 times with 1x PBT buffer. The immunostained embryos were dehydrated in absolute ethanol and individually mounted in Canada balsam (Sigma Aldrich).

2.4.6 Whole-mount RNA *in situ* hybridization of *Drosophila* embryos

All steps were performed at room temperature with rotation unless mentioned otherwise. Fixed embryos were washed with methanol and then with 50% methanol in 1x PBT buffer. Then the embryos were additionally fixed for 20 minutes with RNA-fix solution half diluted with 1x PBT. After washing 3 times with 1x PBT buffer, the embryos were rinsed with 250 µl of HybeB solution (50% Formamide, 5x SSC) for prehybridization. Then HybeB solution was substituted with 250 µl of Hybe solution (described in section 2.1.17). Afterwards, the embryos were incubated for 1 hour with 500 µl of fresh Hybe at 68ºC in the water bath. Then Hybe solution was discarded and 1-5 µl of DIG labelled RNA probe in 30 µl of Hybe was added to the embryos. Hybridization was performed overnight at 68ºC in water bath. Next day embryos were washed twice with 500 µl of warm Hybe solution at 68ºC and once with HybeB solution. Then embryos were transferred to room temperature and washed several times with 1x PBT for 5-15 minutes to remove the residual RNA probe. Anti-DIG alkaline phosphatise-coupled secondary antibody was added and the embryos were incubated for 2h on a rotator. After thorough washing with 1x PBT buffer, the embryos were rinsed and washed with 1 ml of AP buffer. Alkaline phosphatase staining was developed as described in section 2.4.5. The reaction was terminated by washing of the embryos with 1x PBT several times for 15 minutes. Stained embryos were then dehydrated in absolute ethanol and mounted in Canada balsam.

2.4.7 Preparation of embryo lysates for Western blot analysis

Drosophila embryos were collected from the agar-juice plates and washed with 1x embryo wash buffer. The embryos were dechorionated in 50% bleach for 3 minutes and thoroughly washed with 1x embryo wash buffer. The residual liquid was removed and the tubes with embryos were flash-frozen in liquid nitrogen. The embryos were stored at -20ºC until used. Frozen embryos were squashed in cold 1x PBS supplemented with protease inhibitor cocktail and subjected to

ultrasound treatment using Bioruptor (Diagenode). The sonication was performed several times for 30 seconds with 1 minute intervals and total time of 5-7 minutes. Then 4x loading buffer was added to the samples. The lysates were vortexed well and heat at 95ºC for 10 minutes. Finally, the samples were centrifuged for 30 minutes at 15.000 rpm at 4ºC. Resulting pellets and supernatants were separated and kept at -20ºC before analyzed by Westen blot with appropriate antibody.

2.4.8 Bright field microscopy of *Drosophila* embryos

Stained embryos were analysed using Zeiss Axiophot microscope (Carl Zeiss AG) with x10 or x20 magnification objectives.

2.5. Computed methods

2.5.1 Primer design

Oligonucleotides for molecular cloning and site-directed mutagenesis were designed using Primer3Plus online tool (Untergasser et al. 2007).

2.5.2 Alignment of protein sequences

In silico alignment of protein sequences and estimation of their homology was performed using ClustalW2 (EBI) (Mackey et al., 2002) and Blastp 2.2.18 (Altschul et al., 1997) online recourses.

2.5.3 Quantitative analysis of intensity of DNA bands

Digital image of DNA bands after semi-qantitative PCR reaction (described in section 2.1.16) was analysed using ImageJ software (Abramoff et al., 2004). The intensity of each band was quantified and the resulting reference and test values were compared with each other to estimate the efficiency of gene silencing.

2.5.4 Prediction of N- and O-linked glycosylation sites

Prediction of potential sites for N-linked protein glycosylation was performed using the NetNGlyc 1.0 Server online resource (Gupta et al., 2004). O-linked protein

glycosylation sites were predicted using the OGPET 1.0 online prediction tool (http://ogpet.utep.edu/OGPET; University of Texas at El Paso).

2.6 List of oligonucleotides

Oligo number	Oligonucleotide name	Sequence (5'-3')
TKO1	ol.bnl-entry F	CACCATGCCCCTCATGGCCATGGA
TKO2	ol.bnl-entry R	CAGGATGGCTCTTTTTCGGA
TKO3	ol.bnlFL-entry F	CACCATGCGAAGAAACCTGCGC
TKO4	ol.WgSP F	GACACTAGTATGGATATCAGCTATATCTT
TKO5	ol.WgSP R	GTAGCTAGCCATGGAGCCCCGGCCCCTTC
TKO6	ol.btl-entry F	CACCTGCGATTATGGCCATCATCG
TKO7	ol.btl-entry R	ATTAAACTTATAGGTGTACTG
TKO8	ol.bnlN-entry R	CTAGGACTGTGGCACCGTGGA
TKO9	ol.bnlFGFstop-entry R	CTAGATGGCGTTCGTGTAGGT
TKO10	ol.bnlFGF-entry R	GATGGCGTTCGTGTAGGT
TKO11	ol.bnlSSL-entry F	CACCAGTAGTCTTAACATAAATA
TKO12	ol.bnlSSN-entry F	CACCAGCAGTAACACGCCCATCAG
TKO13	ol.bnlSNL-entry F	CACCAGCAATCTGGACCGTAACGA
TKO14	ol.bnlNER-entry F	CACCAACGAACGATCCACGGTGCC
TKO15	ol.bnlSTV-entry F	CACCTCCACGGTGCCACAGTCCC
TKO16	ol.bnlHLA-entry F	CACCCATTTGGCCTGGACCTCGCG
TKO17	ol.bnlR233G F	GCCCATCAGCAATCTGGACGGTAACGAACGATCC ACGGTGC
TKO18	ol.bnlR233G R	GCACCGTGGATCGTTCGTTACCGTCCAGATTGCTG ATGGGC
TKO19	ol.bnlR236G F	GCAATCTGGACCGTAACGAAGGATCCACGGTGCC ACAGTC

TKO20	ol.bnlR236G R	GACTGTGGCACCGTGGATCCTTCGTTACGGTCCA GATTGC
TKO21	ol.bnlR233GR236G F	CCATCAGCAATCTGGACGGTAACGAAGGATCCAC GGTGCCACA
TKO22	ol.bnlR233GR236G R	TGTGGCACCGTGGATCCTTCGTTACCGTCCAGATT GCTGATGG
TKO23	ol.dfur1_RT F	TCGGACACTATACCCAC
TKO24	ol.dfur1_RT R	CGCGATCGTCGTCATCC
TKO25	ol.dfur2_RT F	GTTTGGGCCTCTGGCAAC
TKO26	ol.dfur2_RT R	CATGTCGACGGTGGCGAC
TKO27	ol.bnlR164S F	TCCTGTCGCGTACCGAAAGCAGCATTCGTCACCAG
TKO28	ol.bnlR164S R	CTGGTGACGAATGCTGCTTTCGGTACGCGACAGG A
TKO29	ol.bnlR642GR645G F	CAAATCCATTTCCGGTGGCAAGGGGAAGCATGGG AAATTGGATGCAAGTACCAC
TKO30	ol.bnlR642GR645G R	GTGGTACTTGCATCCAATTTCCCATGCTTCCCCTT GCCACCGGAAATGGATTTG
TKO31	ol.bnlR687GR690G F	GAAACCAGCGATAGGGTGGAGGGCAACGTGGGC ATGAGCAGCGGCGAGGAGCAG
TKO32	ol.bnlR687GR690G R	CTGCTCCTCGCCGCTGCTCATGCCCACGTTGCCCT CCACCCTATCGCTGGTTTC
TKO33	ol.bnlSTV-KpnI-F	GACGGTACCTCCACGGTGCCACAGTCC
TKO34	ol.bnlSTV-KpnI-R	ACGGTACCTTACAGGATGGCTCT
TKO35	ol.bnlGGKKpnI-R	GACGGTACCCTTGCCACCGGAA
TKO36	ol.bnlSP-BglII-F	GCAGATCTATGCGAAGAAACCTG
TKO37	ol.bnlSP-XhoI-R	ATCTCGAGCGCAGATACAAGGCC
TKO38	ol.bnlN-XhoI R	ATCTCGAGGGATCGTTCGTTACGGTCCAG
TKO39	ol.EGFP-XhoI F	AGCTCGAGATGGTGAGCAAGGGCGAG
TKO40	ol.EGFP-XhoI R	TACTCGAGCTTGTACAGCTCGTCCA

TKO41	ol.XhoI-STV	ATCTCGAGTCCACGGTGCCACAGTCC
DRSC31247_R	ol.sec23#47 F (from Mathias Beller)	gtaatacgactcactataggGTTCGGCGAGTACTCAAAGG
DRSC31247_S	ol.sec23#47 R (from Mathias Beller)	gtaatacgactcactataggTGGCATGTCCTGGTATTTGA
DRSC31248_S	ol.sec23#48 R (from Mathias Beller)	gtaatacgactcactataggCTCGGAAATGGCAGCATATT
DRSC31248_R	ol.sec23#48 F (from Mathias Beller)	gtaatacgactcactataggTTACCAGCCTTTGAAGGAGC

2.7 List of plasmid DNA

Plasmid number	Insert	Vector	Preparation
TKP1	*bnl* ORFΔ1-93 bps	pENTR/D-TOPO	PCR with TKO1/2, TOPO-cloning
TKP2	WgSP	pUbi-EGFP-rfA	PCR with TKO4/5, cloning via SpeI
TKP3	10x Myc tag	pUbi-WgSP-EGFP-rfA	Subcloning via NheI site
TKP4	10x Myc tag	pUbiP-rfA	Subcloning via NheI site
TKP5	*bnl* ORF Δ1-93 bps	pUbi-WgSP-EGFP-rfA-Myc	LR recombination of TKP3 with TKP1
TKP6	*bnl* ORF	pENTR/D-TOPO	PCR with TKO2/3, TOPO-cloning
TKP7	*bnl* ORF	pUbi-rfA-Myc	LR recombination of TKP4 with TKP6
TKP8	WgSP-EGFP-rfA-Myc cassette	pUASTattB	Cloning via XbaI site
TKP9	*bnl*N (bnl ORF 94-726 bps)	pENTR/D-TOPO	PCR with TKO1/8, TOPO cloning
TKP10	*bnl*FGFstop (bnl ORF 94-1131 bps with Stop-codon)	pENTR/D-TOPO	PCR with TKO1/9, TOPO cloning
TKP11	*bnl*FGF (bnl ORF	pENTR/D-TOPO	PCR with TKO1/10, TOPO

	94-1131 bps)		cloning
TKP12	*bnl*N (bnl ORF 94-726 bps)	pUbi-WgSP-EGFP-rfA-Myc	LR recombination of TKP9 with TKP3
TKP13	*bnl*FGFstop (bnl ORF 94-1131 bps with Stop-codon)	pUbi-WgSP-EGFP-rfA-Myc	LR recombination of TKP10 with TKP3
TKP14	*bnl*FGF (bnl ORF 94-1131 bps)	pUbi-WgSP-EGFP-rfA-Myc	LR recombination of TKP11 with TKP3
TKP15	3x FLAG tag	pUbi-rfA-Myc	Cloning via SpeI
TKP16	WgSP	pUbi-FLAG-rfA-Myc	PCR with TKO4/5, cloning via SpeI
TKP17	*bnl*SSL	pENTR/D-TOPO	PCR with TKO11/2, TOPO cloning
TKP18	*bnl*SSN	pENTR/D-TOPO	PCR with TKO12/2, TOPO cloning
TKP19	*bnl*SNL	pENTR/D-TOPO	PCR with TKO13/2, TOPO cloning
TKP20	*bnl*NER	pENTR/D-TOPO	PCR with TKO14/2, TOPO cloning
TKP21	*bnl*STV	pENTR/D-TOPO	PCR with TKO15/2, TOPO cloning
TKP22	*bnl*HLA	pENTR/D-TOPO	PCR with TKO16/2, TOPO cloning
TKP23	*bnl*SSL	pUbi-WgSP-FLAG-rfA-Myc	LR recombination of TKP16 with TKP17
TKP24	*bnl*SSN	pUbi-WgSP-FLAG-rfA-Myc	LR recombination of TKP16 with TKP18
TKP25	*bnl*SNL	pUbi-WgSP-FLAG-rfA-Myc	LR recombination of TKP16 with TKP19
TKP26	*bnl*NER	pUbi-WgSP-FLAG-rfA-Myc	LR recombination of TKP16 with TKP20
TKP27	*bnl*STV	pUbi-WgSP-FLAG-rfA-Myc	LR recombination of TKP16 with TKP21
TKP28	*bnl*HLA	pUbi-WgSP-FLAG-rfA-Myc	LR recombination of TKP16 with TKP22
TKP29	*bnl*SSL	pUbi-WgSP-EGFP-rfA-Myc	LR recombination of TKP17 with TKP3
TKP30	*bnl*SSL(R233G)	pUbi-WgSP-EGFP-	Site-directed mutagenesis

		rfA-Myc	using TKO17/18
TKP31	*bnl*SSL(R236G)	pUbi-WgSP-EGFP-rfA-Myc	Site-directed mutagenesis using TKO19/20
TKP32	*bnl* ORF Δ1-93 bps (R164S)	pUbi-WgSP-EGFP-rfA-Myc	Site-directed mutagenesis using TKO27/28
TKP33	*bnl* ORF Δ1-93 bps (R233G;R236G)	pUbi-WgSP-EGFP-rfA-Myc	Site-directed mutagenesis using TKO21/22
TKP34	*bnl* ORF Δ1-93 bps (R642G;R645G)	pUbi-WgSP-EGFP-rfA-Myc	Site-directed mutagenesis using TKO29/30
TKP35	*bnl* ORF Δ1-93 bps (R687G;R690G)	pUbi-WgSP-EGFP-rfA-Myc	Site-directed mutagenesis using TKO31/32
TKP36	*bnl* ORF Δ1-93 bps (R164S;R233G; R236G)	pENTR/D-TOPO-bnlORF Δ1-93 bps	Site-directed mutagenesis using TKO27/28 and then TKO21/22
TKP37	*bnl* ORF Δ1-93 bps (R164S;R233G; R236G)	pUbi-WgSP-EGFP-rfA-Myc	LR recombination of TKO3 with TKO36
TKP38	*bnl* ORF Δ1-93 bps (R642S;R645G; R687G;R690G)	pUbi-WgSP-EGFP-rfA-Myc	Site-directed mutagenesis using TKO29/30 and then TKO31/32
TKP39	*bnl* ORF Δ1-93 bps (with all 4 furin sites mutated)	pENTR/D-TOPO-bnlORF Δ1-93 bps	Site-directed mutagenesis using TKO27/28, TKO21/22, TKO29/30 and TKO31/32
TKP40	*bnl* ORF Δ1-93 bps (with all 4 furin sites mutated)	pUbi-WgSP-EGFP-rfA-Myc	LR recombination of TKP3 with TKP39
TKP41	*bnl* ORF Δ1-93 bps	pUASTattB-WgSP-EGFP-rfA-Myc	LR recombination of TKP1 with TKP8
TKP42	3x FLAG	pUbi-rfA-EGFP	Cloning via SpeI
TKP43	WgSP	pUbi-FLAG-rfA-EGFP	PCR with TKO4/5, cloning via SpeI
TKP44	WgSP-FLAG-rfA-EGFP cassette	pUASTattB	Cloning of the cassette via XbaI
TKP45	*bnl* ORF Δ1-93 bps	pUASTattB-WgSP-FLAG-rfA-EGFP	LR recombination of TKP1 with TKP44
TKP46	*bnl* ORF Δ1-93 bps (with all 4 furin sites mutated)	pUASTattB-WgSP-FLAG-rfA-EGFP	LR recombination of TKP39 with TKP44
TKP47	*bnl*N(bnl ORF 93-711 bps)	pUASTattB	PCR with TKO36/38, cloning via BglII/XhoI

TKP48	*bnl*C(bnlORF 709-2310 bps)	pUASTattB-bnlN	PCR with TKO41/34, cloning via XhoI/KpnI
TKP49	*egfp* ORF	pUASTattB-bnlN-bnlC	PCR with TKO39/40, cloning via XhoI
TKP50	rfA cassette	pUASTattB	Subcloning via XbaI site
TKP51	*bnl* ORF	pUASTattB-rfA	LR recombination of TKP6 with TKP50
TKP52	*bnl* ORF(R164S; R233G;R236G)	pENTR/D-TOPO-bnlORF	Site-directed mutagenesis using TKO27/28 and then TKO21/22
TKP53	*bnl* ORF with all 4 furin sites mutated	pENTR/D-TOPO-bnlORF(R164S; R233G;R236G)	Site-directed mutagenesis using TKO29/30 and then TKO31/32
TKP54	*bnl* ORF(R164S; R233G;R236G)	pUASTattB-rfA	LR recombination of TKP50 with TKP52
TKP55	*bnl* ORF with all 4 furin sites mutated	pUASTattB-rfA	LR recombination of TKP50 with TKP53
TKP56	*bnl* SP sequence (1-93 bp of ORF)	pUASTattB	PCR with TKO36/37, cloning via BglII/XhoI
TKP57	bnlSTV	pUASTattB-bnlSP-rfA	PCR with TKO33/34, cloning via KpnI
TKP58	*bnl*STV-GGK	pUASTattB-bnlSP-rfA	PCR with TKO33/35, cloning via KpnI
TKP59	α1-PDX ORF	pUASTattB	Cloning via EcoRI and XhoI
TKP60	*btl* ORF Δ1-66 bps	pENTR/D-TOPO	PCR with TKO6/7, TOPO cloning
TKP61	3x FLAG	pUbi-rfA	Cloning via SpeI
TKP62	WgSP	pUbi-FLAG-rfA	PCR with TKO4/5, cloning via SpeI
TKP63	*btl* ORF Δ1-66 bps	pUbi-WgSP-FLAG-rfA	LR recombination of TKP60 with TKP62

2.8 List of fly stocks generated for this work

Stock number	Genotype	Description
TKF1	*y*w*;;P{w[+mC]UAST-WgSP-EGFP-bnlΔ1-31-10xMyc}/TM3,Ser*	Transgene TKP41
TKF2	*y*w*;;P{w[+mC]UAST-WgSP-FLAG-bnlΔ1-31-EGFP}/TM3,Ser*	Transgene TKP45
TKF3	*y*w*;;P{w[+mC]UAST-WgSP-FLAG-bnlΔ1-31 MFS 1-4-EGFP}/TM3,Ser*	Transgene TKP46
TKF4	*y*w*;;P{w[+mC]UAST-bnl/TM3,Ser*	Transgene TKP51
TKF5	*y*w*;;P{w[+mC]UAST-bnlMFS1,2}/TM3,Ser*	Transgene TKP54
TKF6	*y*w*;;P{w[+mC]UAST-bnlMFS1-4}/TM3,Ser*	Transgene TKP55
TKF7	*y*w*;;P{w[+mC]UAST-bnlSTV}/TM3,Ser*	Transgene TKP57
TKF8	*y*w*;;P{w[+mC]UAST-bnlSTV-GGK}/TM3,Ser*	Transgene TKP58
TKF9	*y*w*;;P{w[+mC]UAST-α1-PDX}/TM3,Ser*	Transgene TKP59
	w^{1118}*;Df(3R)Exel6202,P{w[+mC]=XP-U}Exel6202/TM6B,P{ubx-lacZ},Hu*	Balanced line (Gerd Vorbrüggen)
	ry^{506} *P{PZ}Fur1*^{rL205}*/TM6B,P{ubx-lacZ},Hu*	Balanced line (Gerd Vorbrüggen)

2.9 List of other fly stocks used

Stock number	Genotype	Source
8164	*w*^{1118}	Bloomington
109128	*y*^{1} *w*^{67c23}*; P{GAL4-btl.S}2*	Kyoto Stock Center
NP2211	*w*;P{GawB}NP2211/ TM3, Sb*^{1} *Ser*^{1}	Kyoto Stock Center
Gö1339	w*;P{w[+mC]=tubP-GAL4}/CyO	Departmental stock
1774	*w*; P{GawB}69B*	Bloomington
6384	*ry*^{506} *P{PZ}bnl*^{00857}*/TM3, Sb*^{1}	Bloomington
7681	*w*^{1118}*;Df(3R)Exel6202,P{w[+mC]=XP-U}Exel6202/TM6B, Tb*^{1}	Bloomington
10341	*ry*^{506} *P{PZ}Fur1*^{rL205}*/TM3, ry*^{RK} *Sb*^{1} *Ser*^{1}	Bloomington

2.10 List of primary antibodies

Antibody	Source	Producer	Epitope	Dilution
Anti-GFP	rabbit	Synaptic Systems	EGFP	1:2000 (for Western blot) 1:500 (for cytofluorescense)
ab290	rabbit	Abcam	EGFP	1:1000
Anti-Myc	mouse	Iowa-Hybridoma Bank	Myc tag	1:30
Anti-FLAG M2	mouse	Sigma Aldrich	FLAG	1:5000 (for Western blot) 1:1000 (for cytofluorescense)

2A12	mouse	Iowa Hybridoma Bank	Tracheal lument	1:200
β-galactosidase	rabbit	Cappel	β-galactosidase	1:1000
Anti-BnlN	rabbit	Gift from Mark Krasnow	Bnl	1:100

2.11 List of secondary antibodies

Epitope	**Source**	**Producer**	**Label**	**Dilution**
Mouse IgG	goat	Peirce	HRP	1:2000
Rabbit IgG	goat	Pierce	HRP	1:2000
Mouse IgG	goat	Molecular Probes	Alexa 568	1:500
Rabbit IgG	goat	Molecular Probes	Alexa 488	1:500
Mouse IgM	goat	Jackson ImmunoResearch Laboratories	Biotinylated	1:400
DIG	sheep	Roche	Alkaline phosphatase	1:2000
Rabbit IgG	goat	Vector Laboratories	Biotinylated	1:400
Rabbit IgG	donkey	Jackson ImmunoResearch Laboratories	Alkaline phophatase	1:400

3 RESULTS

3.1 Observation of Bnl cleavage

3.1.1 Bnl protein is proteolytically cleaved in *Drosophila* embryonic cells

Interactions between extracellular signaling molecules and the cellular surface play a key role in cell-to-cell communication within a multicellular organism during processes of development, tissue repair, homeostasis and immune response. Heparan sulphate proteoglycans (HSPGs) are exactly positioned in the place where this complex communication takes place – in the extracellular matrix (ECM) (reviewed in Häcker et al., 2005). HSPGs were implicated in different signaling events including Wingless/Wnt, transforming growth factor-β (TGF- β), Hedgehog (Hh) as well as fibroblast growth factor (FGF) signal-transduction pathways (Han et al., 2005; Belenkaya et al., 2004; Bellaiche et al., 1998; Freeman et al., 2008; Yan and Lin, 2009). However, the mechanism and specificity of their action remain elusive. It was shown recently that one of *Drosophila* membrane bound HSPGs, Dally-like (Dlp) (Gallet et al., 2008) interacts with the Branchless (Bnl) protein, one of the three *Drosophila* FGF homologues, *in vivo* and modulates its activity in the embryonic tracheal system (Yan and Lin, 2007). Based on the experimental evidence, it was proposed that Dlp directly binds Bnl and facilitates its interaction with the FGF receptor Breathless (Btl). The aim of the current study is to analyze functional domains of the Bnl protein and investigate, how cell surface bound HSPGs modulate the Bnl/Btl signaling during tracheal system development.

In order to establish a cell culture based assay to detect direct interactions of *Drosophila* cell surface HSPGs with extracellular Bnl, a tagged Bnl protein was overexpressed in *Drosophila* Kc cell culture. The construct for *bnl* expression was created employing the Gateway recombination cloning technology (Invitrogen) by recombining the *bnl* ORF without the N-terminal signal sequence (*bnl*Δ1-93 bp) into a destination vector with a constitutive *ubiquitin* promoter. The resulting construct contains the *bnl*Δ1-93 ORF fused with the *wg* signal sequence, EGFP ORF and a 57 bp linker sequence on the N-terminus and a 10x Myc tag, separated from the *bnl* sequence by a 61 bp linker on the C-terminus (Figure 13A). This construct was used for transient transfection in *Drosophila* embryonic cell culture. Kc cells overexpressing tagged Bnl protein and cell supernatants were harvested and efficiency of protein expression and secretion was estimated by Western blot analysis with both anti-GFP and anti-Myc antibodies.

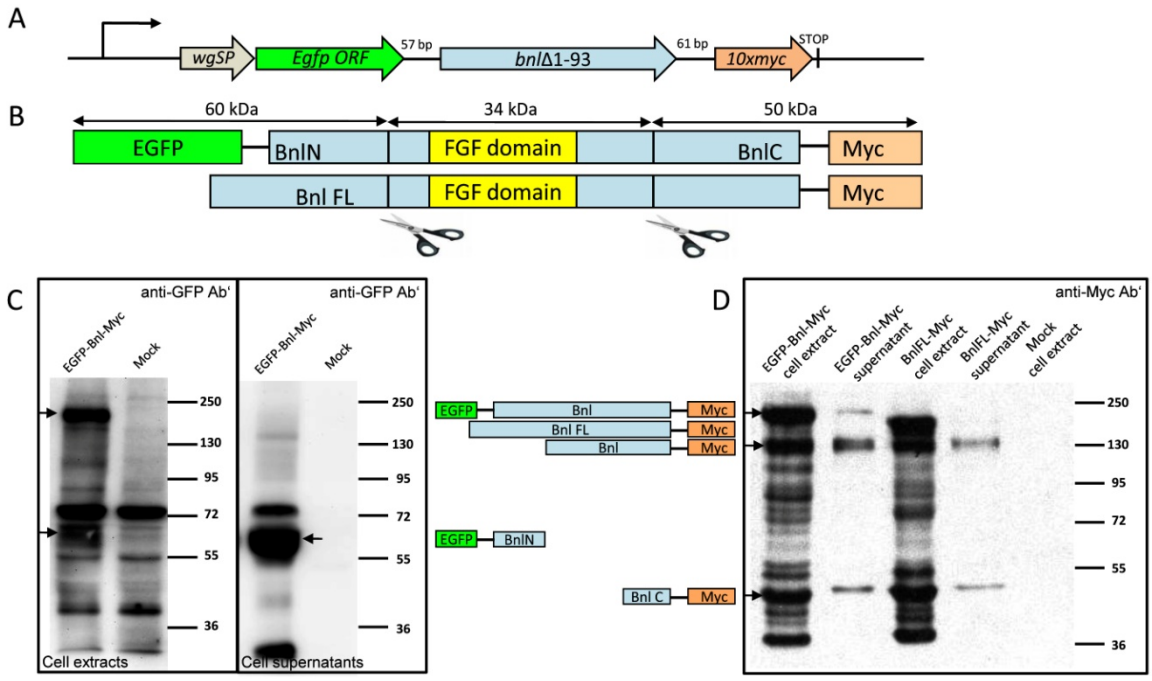

Figure 13: EGFP-Bnl-Myc cleavage in Kc cells and supernatants. (A) A schematic drawing of the recombinant tagged Bnl expression construct. **(B)** A schematic drawing of the EGFP-Bnl-Myc and Bnl FL-Myc proteins with two potential cleavage sites. **(C)** Western blot analysis of the overexpressed EGFP-Bnl-Myc and its cleavage products in cell extracts and cell supernatants. Arrows indicate the revealed Bnl protein. A schematic representation of the detected Bnl forms is shown between the Western blot panels.The cleaved off N-terminal domain is detected in both cell extract and cell supernatant, whereas the full length protein can be only revealed in cell extract with the anti-GFP antibody. **(D)** Western blot analysis of overexpressed EGFP-Bnl-Myc and Bnl FL-Myc. Full length proteins as well as the products of the N- and C-terminal cleavage are detected with the anti-Myc antibody both in cell extracts and cell supernatants.

Surprisingly, not only the full length tagged Bnl protein (~200 kDa, further also referred to as EGFP-Bnl-Myc) was detected in cell supernatants as well as in cell extracts. Additionally, a 60 kDa N-terminal peptide was revealed with the anti-GFP antibody mostly in cell supernatant and two C-terminal peptides of 130 kDa and 50 kDa were detected with the anti-Myc antibody in both cell extract and supernatant (Figure 13B, C and D). This finding indicated that the EGFP-Bnl-Myc protein was cleaved into three parts in Kc cells. Moreover, all three cleavage products could be detected in cell extracts, pointing out that the cleavage occured intracellularly. Further experiments described in this manuscript were carried out to explore the unusual behavior of the Bnl ligand.

In order to exclude that the addition of ectopic *wingless* signaling peptide (*wg*SP) and the EGFP sequence could be responsible for this cleavage, the Bnl protein carrying its own signal sequence and only tagged at the carboxy-terminus with 10x Myc tag was expressed in cell culture and analyzed by Western blot. Similar to the

previous observation, two peptides of 130 kDa and 50 kDa were detected with the anti-Myc antibody (Figure 13D), proving that also the wild type Bnl protein is cleaved in Kc cells and the addition of *wg*SP and EGFP does not have any impact on EGFP-Bnl-Myc cleavage.

An additional experiment was performed to exclude the possibility that cleavage of the recombinant Bnl protein occurs extracellularly as a result of non-specific proteolytic activity. If the cleavage would occur after the secretion process, the peptides would have to stick to the cellular surface, as the cleaved peptides could be detected within the cell extracts (Figure 13). To inhibit extracellular protease activity, a protease inhibitor cocktail (Complete Mini Protease Inhibitor, Roche) was added to the medium of Kc cells transiently transfected with the EGFP-Bnl-Myc construct and cell supernatants were analyzed by Western blot.

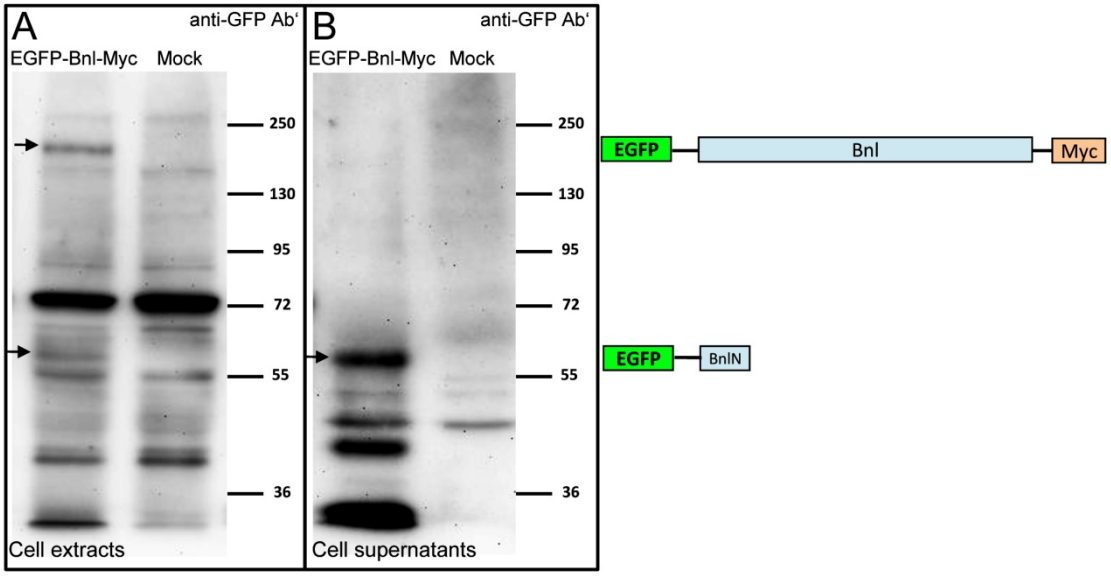

Figure 14: Intracellular cleavage of EGFP-Bnl-Myc in the presence of protease inhibitors. Western blot analysis of EGFP-Bnl-Myc expression **(A)** and secretion **(B)** with or without the addition of the protease inhibitor to conditioned medium. Arrows indicate the revealed Bnl protein. A schematic drawing of the detected protein forms is shown on the right. The cleaved off N-terminal domain of Bnl is detected in both cell extract and cell supernatant, whereas the full length protein can be only revealed in cell extract with the anti-GFP antibody.

The result represented in Figure 14 shows that the product of EGFP-Bnl-Myc amino-terminal cleavage is still present in cell extract as well as in supernatant in the presence of protease inhibitors, excluding Bnl unspecific cleavage outside the cells.

Taken together, the results obtained clearly show that the Bnl protein is cleaved intracellularly into three peptides by an unknown protease in *Drosophila* cell culture. Since the Bnl molecule carries unusually large domains flanking a conserved FGF domain which are not found in all known FGF homologues from vertebrates (Introduction 1.2.3 and Sutherland et al., 1996) and there are several reports that

some of vertebrate FGFs undergo proteolytic processing (Bellosta et al., 1993; Antoine et al., 2000; Fukumoto et al., 2005), the results correspond to a model in which the Bnl protein cleavage observed is carried out by a specific protease.

3.1.2 Bnl undergoes proteolytic cleavage in *Drosophila* embryos

In order to verify whether Bnl/FGF cleavage occurs not only in *Drosophila* cell culture but also in a living organism, the UAS/GAL4 system (Brand and Perrimon, 1993) was utilized to induce tissue specific expression of EGFP-Bnl-Myc protein in *Drosophila* embryos. Flies carrying homozygous *btl*GAL4 driver, activating expression of UAS transgenes in embryonic tracheal cells, were crossed to UAS-EGFP-Bnl-Myc transgenic flies. Embryo extracts of F1 progeny were subjected to Western blot analysis. The result shown in Figure 15 clearly indicates that the EGFP-Bnl-Myc protein is proteolytically cleaved *in vivo* as well. It was possible to visualize a 60 kDa cleaved N- terminal peptide with the anti-GFP antibody (Figure 15A) and the anti-Myc antibody revealed in addition to the full length EGFP-Bnl-Myc protein a 130 kDa cleaved variant as a result of the amino-terminal cleavage and 55 kDa cleaved carboxy-terminal peptide (Figure 15B). A minor increase in molecular mass of the C-terminal cleavage product can be explained by a higher degree of post-translational protein modifications taking place in *Drosophila* embryos compared to cell culture conditions.

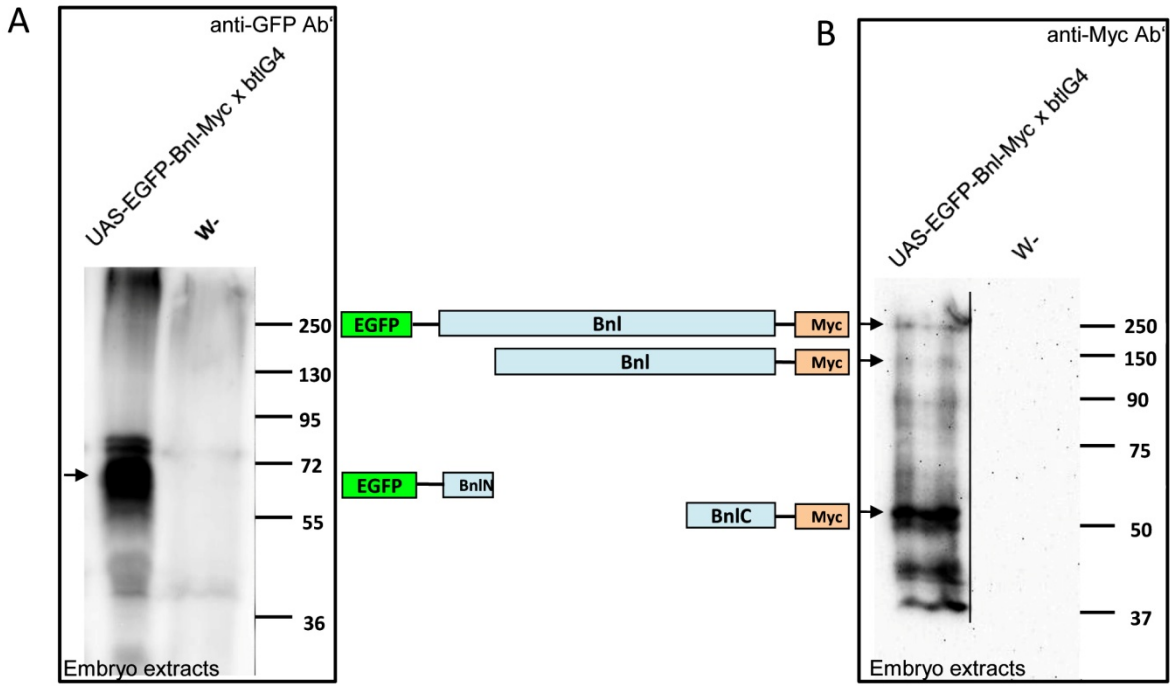

Figure 15: Cleavage of the EGFP-Bnl-Myc protein in *Drosophila* embryos. Western blot analysis of the embryos expressing the recombinant Bnl protein in the tracheal cells. Full length protein and the cleavage products are detected with the anti-GFP **(A)** and anti-Myc antibodies **(B)**. Arrows and a schematic drawing between the panels show the revealed forms of Bnl.

Taken together, all results shown strongly indicate that Bnl is proteolytically cleaved within the secreting cells both in embryonic cell culture and in *Drosophila* embryos resulting in three cleavage products: a N-terminal peptide (approximately 30 kDa when untagged), middle part carrying an intact or truncated FGF domain (~34-37 kDa) and a small C-terminal peptide (~22 kDa when untagged). However, without precise identification of the cleavage sites it is not yet clear whether Bnl cleavage represents a propeptide activation step releasing the conserved FGF domain or, in opposite, it may serve as a mechanism of the growth factor inactivation if the cleavage occurs within the FGF domain.

3.1.3 *Drosophila* Bnl is N-glycosylated

Whereas the anti-Myc antibody could reveal the full length EGFP-Bnl-Myc protein in cell extracts as well as in supernatants, the anti-GFP antibody fails to detect the secreted full length protein (Figure 13). This could be caused by protein modifications which are masking the antibody epitope. It is known, that mammalian FGFs show a varying degree of glycosylation that is important for their stability and secretion and in some cases for the activity of growth factors (Bates et al., 1991; Asada et al., 1999).

N-glycosylation is the most frequent post-translational modification for secreted eukaryotic proteins. It occurs at asparagin residues of the polypeptide chain (Walsh et al., 2005). To analyze whether EGFP-Bnl-Myc carries post-translational N-glycosylation, supernatant of overexpressing Kc cells was treated with peptide-N-glycosydase F (PNGase F) to remove N-linked sugar moieties from the polypeptide chain. Deglycosylated and control cell supernatant samples were subjected to Western blot analysis. As shown in Figure 16, treatment with PNGase F results in a clear reduction of the apparent molecular weight of the cleaved amino-terminal protein portion. Furthermore, after glycosidase treatment the second GFP-positive band of 150 kDa, corresponding to the C-terminally cleaved Bnl can be detected.

This result shows that, similar to mammalian FGFs, Bnl is N-glycosylated and this modification is at least partially responsible for the dramatically increased apparent molecular weight of the Bnl full length protein observed on SDS PAGE. Furthermore, the N-glycosylation seems to be the cause for the impaired binding of the anti-GFP antibody to high molecular weight Bnl forms. However, since the treatment with PNGase F did not help to reveal the full length Bnl protein, further Western blot experiments were carried out using the anti-Myc antibody for the tagged protein detection.

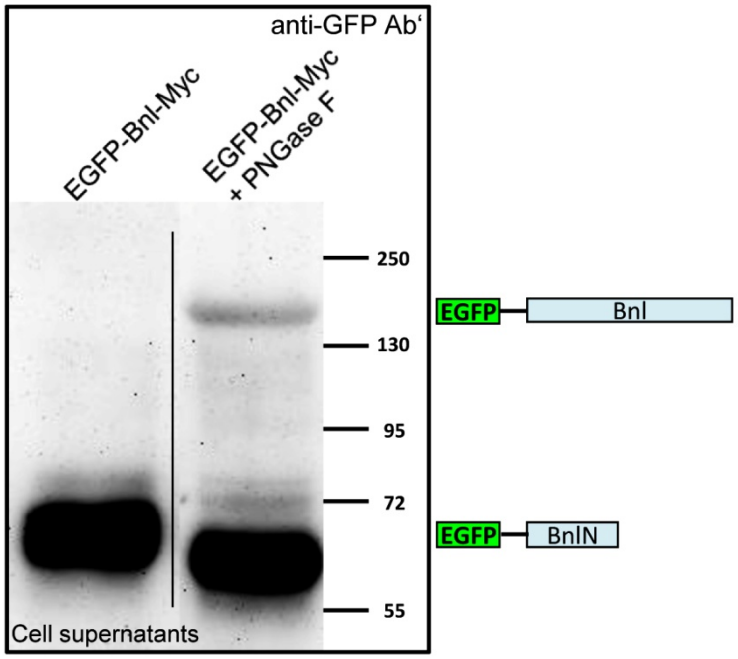

Figure 16: Deglycosylation of EGFP-Bnl-Myc. Western blot analysis of the EGFP-Bnl-Myc supernatants with or without treatment with PNGase F enzyme. The products of the N-terminal Bnl cleavage are detected with the anti-GFP antibody. A schematic representation of the revealed Bnl forms is shown on the right. N-linked glycosylation of Bnl increases its apparent molecular weight and partially masks the anti-GFP antibody epitope.

3.1.4 Anterograde trafficking is required for Bnl cleavage

The majority of secreted eukaryotic proteins containing an amino-terminal signal sequence peptide utilizes the classical intracellular secretory pathway, which leads them from the endoplasmic reticulum (ER) to the Golgi apparatus and further in secretory vesicles to the plasma membrane and eventually to the extracellular environment (Reynaud and Simpson, 2002; Abrahamsen and Stenmark, 2010). According to the available data, a proteolytic cleavage of cargo proteins may occur in each of these transportation steps (Boddey et al., 2010; Wallis et al., 2003). Moreover, it was previously described that some of mammalian FGFs utilize an unconventional secretory pathway for their secretion (Zehe et al., 2006; Nickel and Rabouille, 2009). In order to investigate whether the ER to Golgi transport is essential for EGFP-Bnl-Myc cleavage and secretion, anterograde trafficking was blocked in Kc cells using siRNA knockdown approach. Two different dsRNAs containing the *sec23* sequence were co-transfected with EGFP-Bnl-Myc in Kc cells. Sec 23 is essential for the coat-protein complex II (COPII) vesicle assembly (reviewed in Fromme et al., 2008) and depletion of this protein leads to the blockage of anterograde vesicle trafficking. Under these conditions all secreted proteins synthesized by the cell are retained in the ER. Cell extracts and supernatants from Sec23 dsRNA treated or control Kc cells were harvested and analyzed by Western blot. The result shows that

inhibition of anterograde vesicle trafficking completely blocks both the protein cleavage and secretion (Figure 17).

This indicates that the EGFP-Bnl-Myc protein utilizes the classical secretory pathway within the cell and has to enter the Golgi apparatus for its secretion. Furthermore, dsRNA treatment inhibits Bnl cleavage as well, suggesting that the protease activity is localized and processing occurs downstream of the ER, either in the Golgi or even further downstream.

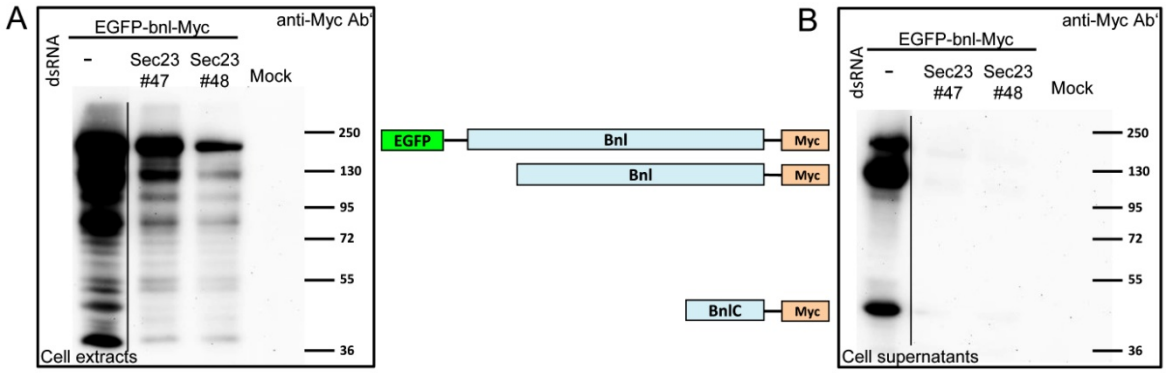

Figure 17: Inhibition of anterograde trafficking in Kc cells. Western blot analysis of *Drosophila* Kc cell extracts **(A)** and supernatants **(B)**, treated with the two different dsRNAs (#47 and #48) against Sec23 and transiently expressing the EGFP-Bnl-Myc protein. Bnl protein is detected with the anti-Myc antibody. A schematic drawing of the revealed protein forms is shown between the panels. Blockage of anterograde protein trafficking prevents Bnl cleavage and secretion.

3.2 Identification of Bnl cleavage sites and the cleaving protease

3.2.1 Amino-terminal Bnl cleavage occurs upstream of the FGF domain

The observed Bnl cleavage may serve two different purposes. It can either represent the process of proteolytic protein activation releasing its biologically functional central FGF domain, or alternatively, the cleavage can reveal the mechanism of regulation of signaling activity and contribute to the growth factor degradation and turn over. It is reasonable to assume that activating Bnl cleavage has to preserve the integrity of the conserved FGF domain. Conversely, an inactivating cleavage would preferentially occur within this domain. According to molecular masses of the cleavage products observed, Bnl N-terminal cleavage takes place directly upstream or within the FGF domain. In order to identify the location of the Bnl N-terminal cleavage site, three C-terminally truncated Bnl variants were generated.

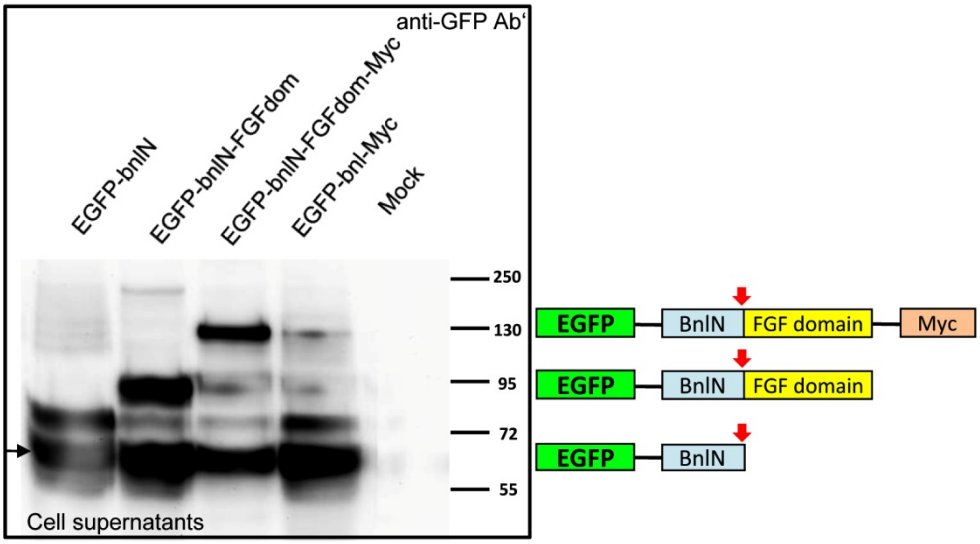

Figure 18: Analysis of the Bnl truncated variants. Western blot analysis of cell supernatants from Kc cells overexpressing truncated variants of Bnl. Detection of tagged proteins is performed with the anti-GFP antibody. A schematic representation of Bnl protein variants is shown on the right. Location of the N-terminal cleavage site is marked with red arrows. N-terminal cleavage of Bnl occurs upstream of the Bnl FGF domain.

The first construct represents the EGFP ORF fused to the Bnl N-terminal sequence up to the FGF domain (EGFP-Bnl N), the second construct contains the EGFP sequence, the Bnl N-teminal sequence and the full length FGF domain (EGFP-Bnl N-FGFdom.), the third variant has an additional C-terminal Myc tag (EGFP-Bnl N-FGFdom-Myc). The three truncated variants were transiently expressed in *Drosophila* cell culture and secreted fusion proteins were visualized by Western blot. As shown in Figure 18, an amino-terminal 60 kDa peptide was detected in all protein variants tested, proving that the N-terminal cleavage occurs upstream of the conserved FGF domain of Bnl. Consequently, this experiment supports the idea that Bnl cleavage represents the mechanism of growth factor maturation.

3.2.2 N-terminal Bnl cleavage occurs between S229 and N234

The three deletion constructs allowed to narrow down the localization of the Bnl amino-terminal cleavage site to the region of the 28 amino acids adjacent to the FGF domain. In order to identify the cleavage site within this area, an additional series of N-terminally truncated Bnl variants were generated (Figure 19A). To avoid undesirable background from non-specific EGFP cleavage and to visualize even minor differences in molecular masses of the cleaved fragments, a small 3x FLAG-tag was used to mark N-terminal parts of the constructs. The resulting Bnl variants were expressed in cell culture and supernatants were subjected to Western blot analysis.

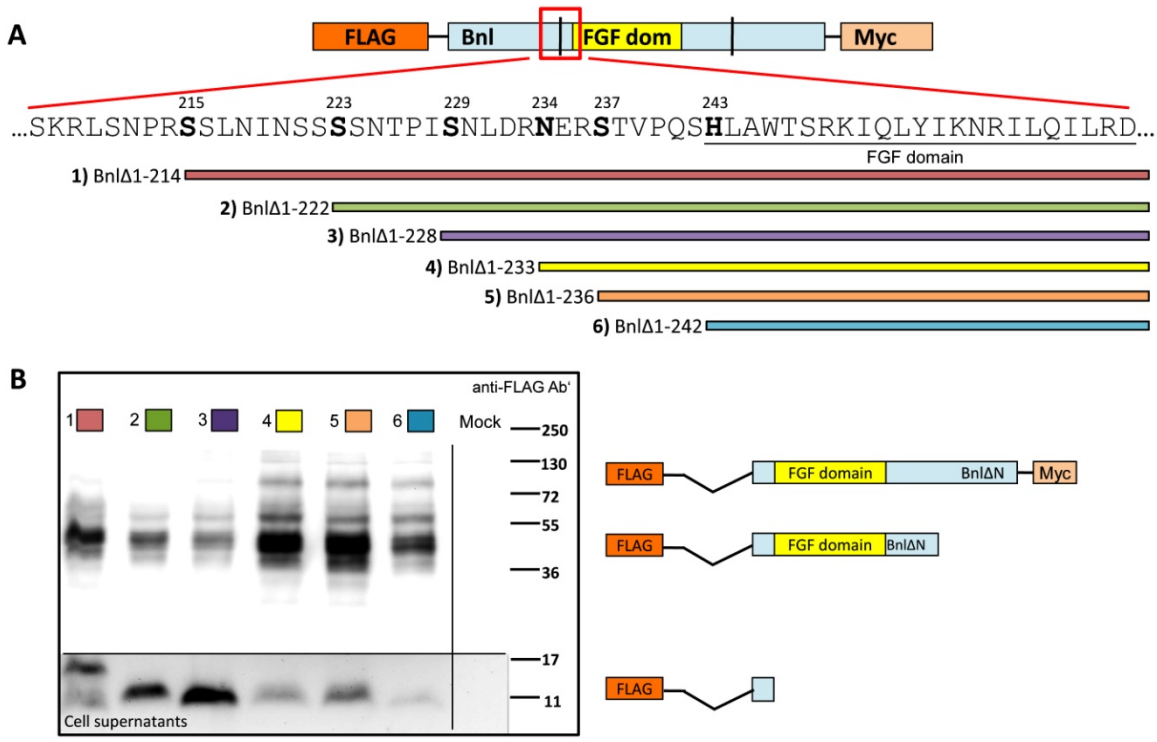

Figure 19: Bnl N-terminal cleavage occurs between S229 and N234. (A) A schematic representation of the Bnl N-terminal cleavage region and the N-teminal truncation constructs showed in different colors. **(B)** Western blot analysis of cell supernatants from Kc cells overexpressing Bnl truncated variants. The tagged proteins are detected with the anti-FLAG antibody. A schematic drawing of the revealed protein forms is on the right. Numbers and colored boxes mark the lanes corresponding to the truncated Bnl variants depicted in (A). Lower part of the blot shows low molecular weight peptides with a longer exposition of the same membrane.

Protein gel electrophoresis was performed using a 15% Tricine gel to achieve an appropriate separation of small amino-terminal peptides. The detection of Bnl variants was carried out with the anti-FLAG antibody. As represented on Figure 19B, samples 1, 2 and 3 contain the small cleaved off FLAG-positive bands (11-15 kDa) showing the expected molecular weight differences corresponding to the length of the constructs. In contrast, samples 4, 5 and 6 reveal the high molecular weight bands of approximately 85 kDa, corresponding to the uncleaved fusion protein but no clear bands in the range of the cleaved FLAG-tag. According to the output of this experiment, it is possible to conclude, that the N-terminal cleavage takes place between S229 and N234 of the Bnl protein sequence. However, it is necessary to take into account that in the represented experimental setup, the FLAG-tag localizes in close proximity to the cleavage site and could interfere with an efficient cleavage process. Moreover, the cleavage site could be destroyed due to truncation. Therefore further approaches were applied to identify the precise position of the N-teminal Bnl cleavage site.

3.2.3 Bnl is cleaved between R236 and S237 by a furin protease

In order to precisely identify the N-terminal cleavage site, *in silico* analysis of the Bnl protein sequence was performed to screen for a potential protease recognition site in the region of interest. This approach revealed the presence of a furin protease recognition motif (–R–N–E–R–) between D232 and S237 of the Bnl sequence. Moreover, three more potential furin recognition sites were identified in the Bnl protein sequence: one was found N-terminally of the already mentioned furin site, and two – in the C-terminus beyond the conservative FGF domain (Figure 20A). Furin is a highly conserved subtilisine-like proprotein convertase (SPC) found in a broad range of organisms from yeast to humans. As it was shown previously, furin protease resides in the *trans*-Golgi network (TGN) and represents the major processing enzyme of the cellular secretory pathway (Molloy et al., 1994; Steiner, 1998). Furins are highly specific endoproteases that have a recognition sequence –R–X–K/R–R↓– (where X is any amino acid and the arrow represents the cleavage point). However it was shown in many cases that these proteases can also effectively cleave the so-called minimal furin recognition motif –R–X–X–R↓– (Thomas, 2002), that was actually detected in the Bnl sequence.

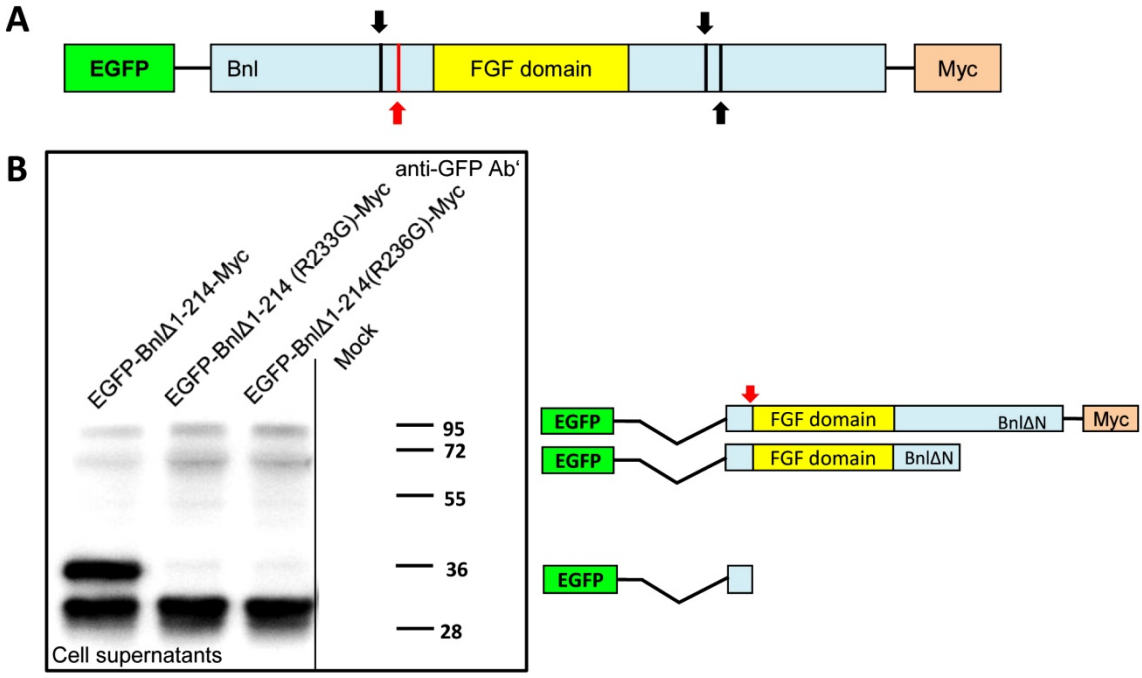

Figure 20: Bnl N-terminal cleavage is performed by a furin protease. (A) A chematic drawing of the Bnl protein with potential furin cleavage sites identified *in silico*. Furin site confirmed by the mutagenesis is shown by the red arrow. Other three furin motives are shown by black arrows **(B)** Western blot analysis of cell supernatants from Kc cells overexpressing the N-truncated variants of Bnl with Arg to Gly substitutions within the furin recognition site. Tagged proteins are detected with the anti-GFP antibody. A schematic drawing of the revealed Bnl protein forms is shown next to the Western blot panel. Location of the cleavage site is indicated by the red arrow. Site-directed mutagenesis of the identified furin recognition motif prevents processing of truncated Bnl.

To examine whether furin subtilisin-like proteases are indeed involved in Bnl cleavage, a site-directed mutagenesis approach was employed in order to disrupt the N-terminal furin cleavage site in the recombinant Bnl protein. Two EGFP- and Myc-tagged mutated Bnl variants were designed. Each of them carries a single Arg to Gly substitution (either R233G or R236G) in the mapped –R–X–X–R↓– Bnl recognition motif. Moreover, both protein variants are N-terminaly truncated (BnlΔ1-214) in order to prevent Bnl cleavage via an additional N-terminal furin recognition site. The constructs were expressed in cell culture and secreted proteins were detected in the supernatants by Western blot analysis. The result represented in Figure 20B shows, that the 36 kDa EGFP-positive peptide cleaved off from the non-mutated protein variant is absent when either of the two arginines of the furin recognition site is mutated.

This data clearly shows that Bnl is processed within its N-terminus between R236 and S237 by a *Drosophila* furin proprotein convertase. However, since three additional potential furin protease recognition sequences were identified within the Bnl protein, it is still to be explored if all of these sites contribute to the Bnl cleavage and if the observed C-terminal processing requires furin proprotein convertase activity.

3.2.4 Alpha1-PDX inhibitor blocks N- and C-terminal Bnl processing

Another widely used approach to identify proteases and their targets is to employ a specific protease inhibitor. Alpha1-antitrypsin variant Portland (α1-PDX) – is a potent and selective inhibitor of the SPC family of proteases. It was bioengineered from a mammalian α1-antitrypsin protease variant and contains a minimal furin consensus motif in its reactive loop. When expressed in cell culture, this protein effectively inhibits proprotein convertase related proteolytic activity (Benjannet et al., 1997; Jean et al., 1998).

In order to examine whether furin protease is indeed implicated in both N- and C-terminal Bnl cleavage, an α1-PDX coding sequence (a gift from G. Thomas) was co-expressed together with EGFP-Bnl-Myc in cell culture under control of a constitutive actin5C promoter. Resulting cell supernatants were analyzed by Western blot using the anti-Myc antibody. As represented in Figure 21, both the 50 kDa and the 130 kDa Bnl forms corresponding to the C- and N-terminal cleavage are absent in the presence of the α1-PDX inhibitor. In contrast, the 200 kDa full length form of Bnl becomes more apparent. This independent approach shows that the specific SPC inhibitor α1-PDX is able to effectively block Bnl cleavage. Thus, our data strongly indicates, that

Drosophila furin proprotein convertase is involved in both amino- and carboxy-terminal Bnl processing.

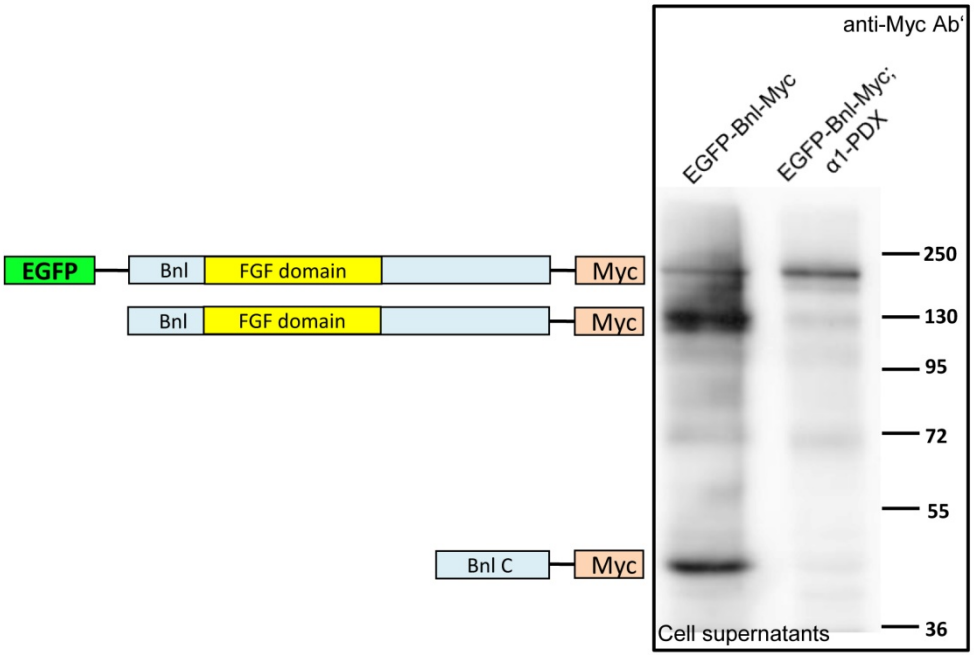

Figure 21: Alpha1-PDX inhibits the Bnl cleavage in cell culture. Western blot analysis of cell supernatants from Kc cells co-expressing EGFP-Bnl-Myc and α1-PDX inhibitor of SPC proteases. Tagged proteins are revealed with the anti-Myc antibody. A schematic representation of the detected Bnl forms is on the left. The inhibitor blocks both N- and C-terminal protein cleavage, suggesting that furin is involved in N- and C-terminal processing of Bnl.

3.2.5 *Drosophila* Furin1 activity is necessary for Bnl cleavage in cell culture

According to the available data and the genome annotation, there are two genes encoding furin proteases in *Drosophila melanogaster* (Roebroek et al., 1991; Roebroek et al., 1992; Flybase data), which are designated as *dfur1* and *dfur2*. Like their homologues from other organisms, *Drosophila* furins are involved in the processing of secreted signaling molecules. For example, it was shown previously that both Dfur1 and Dfur2 proteins participate in the proteolytic processing of the *Drosophila* TGF-β homolog Decapentaplegic (Dpp) (Panganiban et al., 1990). However, they reveal different affinity towards the three furin recognition motives found in this protein. (Künnapuu et al., 2009). Since each of these two proteases is present in *Drosophila* Kc cells, it was interesting to investigate, whether both of them are required for Bnl processing, as it was shown for Dpp.

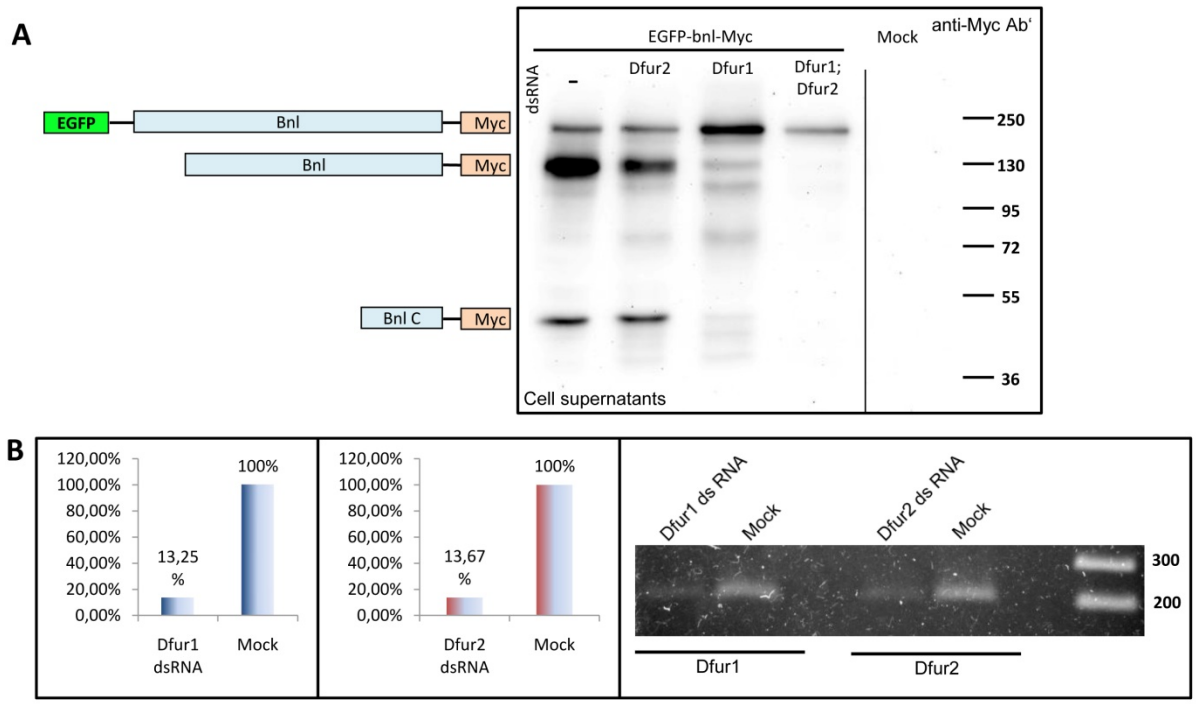

Figure 22: *Drosophila* furin 1 is responsible for Bnl cleavage in cell culture. (A) Western blot analysis of cell supernatants from Kc cells overexpressing EGFP-Bnl-Myc and treated with dsRNAs inhibiting either the Dfur1 or Dfur2 expression. Tagged Bnl is detected with the anti-Myc antibody. A schematic drawing of the revealed protein forms is shown on the left. Inhibition of Dfur1 activity is able to prevent Bnl processing. **(B)** Semi-quantitative PCR analysis for evaluation of dsRNAs silencing efficiency. On the left: quantitation of relative intensity of the gel bands in percents. Silencing efficiency for both Dfur1 and Dfur2 expression is ~85%.

In order to specifically inhibit the expression of one or the other of *Drosophila* furins, dsRNAs containing 150 bp of either *dfur1* or *dfur2* sequence were co-expressed with the EGFP-Bnl-Myc construct in Kc cell culture. Supernatants from dsRNA treated or control cells were subjected to Western blot analysis. As represented in Figure 22A, samples treated with dsRNA against Dfur1 show dramatically reduced Bnl cleavage in comparison with the control, whereas no significant difference was detected in the supernatants from the cells with the silenced Dfur2 expression, although both proteases show relatively similar RNA level (Figure 22B). The efficiency of dsRNA silencing was estimated by semi-quantitative PCR using a cDNA library prepared from Dfur1 or Dfur2 dsRNA treated Kc cells. According to quantitative analysis of DNA band intensity, it was possible to decrease the expression rate of furins by more than 85% (Figure 22B).

Thus, this experiment clearly shows that only Dfurin 1 is required for Bnl cleavage. Our data also indicates that the two *Drosophila* furin proteases have different specificity towards recognition motives and their functions are not redundant in the cell, consistently with the previous report of Künnapuu et al., 2009.

3.2.6 Bnl cleavage sites are conserved in FGF homologues from other *Drosophila* species

According to performed computed analysis, there are four furin consensus motives in the Bnl protein sequence. Two of them are found upstream of the conserved FGF domain in the amino-terminal region, whereas the other two are positioned within the C-terminal part of the protein. For convenience, all furin recognition sites were designated with numbers from 1 to 4 (Figure 23).

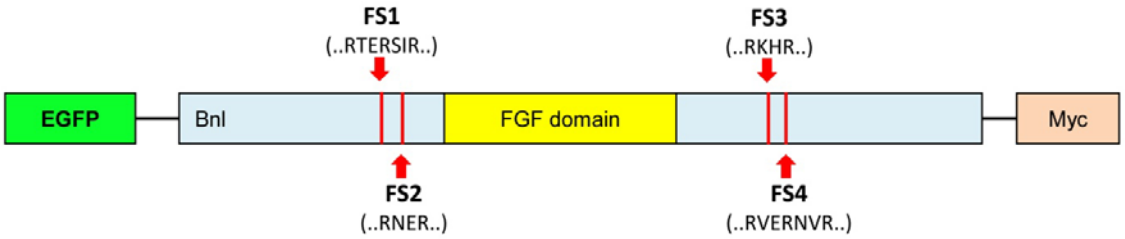

Figure 23: Furin recognition motives identified in Bnl protein. A schematic representation of the Bnl protein with furin consensus motives marked with red lines and arrows. Bnl containes two N-terminal and two C-terminal furin cleavage sites.

Furin recognition site1 (FS1) is located between S160 and H168 of the Bnl protein sequence. It is the most distal N-terminal motif and is separated from FS2 by 65 amino acids, containing stretches of repeated residues (groups of serine, glutamine and histidine), of unknown purpose. Interestingly, FS1 consists of two minimal furin recognition motives (–R–X–X–R–) fused together and building double furin site –R–T–E–R–S–I–R–. However, it is not known whether such duplication of the protease recognition motif leads to more efficient cleavage of the site.

The amino-terminal Bnl recognition site FS2 that was identified first (Results 3.2.3) is located between D232 and S237 and represents a minimal furin recognition motif (–R–N–E–R–). The site is only six amino acids upstream of the beginning of the conserved FGF domain. FS3 is positioned far downstream of the FGF domain and occupies residues K641 to K646. Similar to FS2, it represents a minimal furin consensus motif (Figure 23). The most C-terminally localized furin site 4 is separated from FS3 by 38 amino acids and is located between D683 and M691. This recognition motif (–R–V–E–R–N–V–R–) is duplicated as well as furin site 1. Thus, the Bnl protein has two double minimal furin motives located distally and two single minimal sites located proximally to the conserved FGF domain. Such an extra duplication of the motives and a symmetric disposition of furin recognition sites within the Bnl protein sequence has to be based on certain cellular (and/or organismic) needs and seems to represent a mechanism for the reliable FGF cleavage in the secreting cells.

In order to check whether similar furin cleavage sites can be found in FGF homologues from other *Drosophila* species, a protein sequence alignment of Bnl was performed. An on-line service tool Blastp 2.2.18 was employed for this purpose (Altschul et al., 1997). The result of the alignment is summarized in Table 1.

Species	Protein	FS1	FS2	FS3	FS4
D. melanogaster	Bnl	...VLSRTERSIRHQN...	...NLDRNERSTV...	...GGKRKHRKLD...	...TSDRVERNVRMSS...
D. simulans	GD20101-PA	...VLSRTERSIRHQN...	...NLDRNERSTV...	...GGKRKHRKLD...	...TSDRVERNVRMSS...
D. yakuba	GE25113-PA	...VLSRTERSIRHRN...	...NLDRNERSTV...	...GGKRKHRKVD...	...TSDRVERNVRMSS...
D.erectus	GG15841-PA	...VLSRTERSIRHQS...	...NLDRNERSTV...	...GGRRKHRKLD...	...TSDRVERNVRMSS...
D.sechellia	GM26894-PA	...VLSRTERSIRHQN...	...NLDRNERSTV...	...GGKRKHRKLD...	...TSDRVERNVRMSS...
D. persimilis	GL11947-PA	...VLSRTERSIRHQQ...	...NLDRNERSTV...	...GKQRKQRPST...	...TSDRVERNVRMSS...
D.pseudoobscura	GA18297-PA	...VLSRTERSLRHQQ...	...NLDRNERSTV...	...GKQRKQRPST...	...TSDRVERNVRMSS...
D. ananassea	GF17357-PA	...VLSRTERSIRHQE...	...NLDRNERSTV...	...GSKRRQRKME...	...TSDRVERNVRMSS...
D. virilis	GJ10186-PA	...ILSRTERSIRHQH...	...NLDRNERSTI...	...VTKRLQR LLE...	...TSDRVERNVRMPP...
D. mojavensis	GI10332-PA	...ILSRTERSIRHQH...	...NLDRNERSTI...	----------	...TSDRVERNVRMSH...
D. wilistoni	GK22814-PA	...ILSRTERSIRHQH...	...NLDRNERSTH...	...GGKRKHR TTT...	...TSDRVERNVRRLD...

Table 1: Conservation of Bnl furin cleavage sites within *Drosophilidae* family. Alignment of Bnl furin recognition motives with those of the FGF homologues from other *Drosophila* species. FS1, FS2 and FS4 are highly conserved amon Bnl homologues, whereas FS3 shows sequence variability and is absent in Bnl homologue from *D.mojavensis*.

Interestingly, all four furin recognition motives similar to Bnl cleavage sites were found in 9 out of 11 tested FGF homologues from different *Drosophila* species, despite a diverse protein length and organization. Another homolog from *D. mojavensis* contains only 3 of 4 found furin motives whereby FS3 is missing. Surprisingly, there was no Bnl homologous protein sequence found in *D. grimshavi*.

Taken together, the alignment data indicates, that Bnl cleavage sites are highly conserved among *Drosophila* species despite the difference in the length of the homologues. It is still to be explored, whether each of them have distinct relevance for the growth factor processing, secretion and functionality.

3.2.7 Mutagenesis of Bnl cleavage sites in *Drosophila* cell culture

In order to investigate the contribution of each of the identified furin cleavage sites for Bnl cleavage, a site-directed mutagenesis approach was employed to mutate sequentially each of the four recognition sites. One or two cleavage sites were mutated at the same time on either the N- or C-termini of the Bnl protein. A list of the amino acid substitutions is represented in Table 2. In the duplicated FS1 the central arginine was substituted to serine in order to destroy both recognition sequences at the same time (R164S). FS2 has both consensus arginine residues mutated to glycine (R233G and R236G). Also both arginines are mutated in the minimal furin recognition

motif number 3 (R642G and R645G). The duplicated FS4 contains two amino acid substitutions affecting the second and third arginines of the cleavage site (R687G and R690G).

	Furin cleavage sites (FSs)	Mutated furin sites (MFSs)
FS 1	...VLSRTERSIRHQN...	...VLSRTE**S**SIRHQN...
FS 2	...NLDRNERSTV...	...NLD**G**NE**G**STV...
FS 3	...GGKRKHRKLD...	...GGK**G**KH**G**KLD...
FS 4	...TSDRVERNVRMSS...	...TSDRVE**G**NV**G**MSS...

Table 2: Amino acid substitutions in furin consensus motives of Bnl. Sequence of Bnl furin recognition motives and amino acid substitutions introduced by site-directed mutagenesis (furin consensus motives are marked in red; amino acid substitutions are in bold).

In order to investigate the function of each recognition site alone and in combination, seven mutated Bnl variants were generated. The constructs were supplied with amino-terminal EGFP and carboxy-terminal Myc tags for effective detection of the modified proteins and their cleavage products. The variants were designated with the letters MFS (for “mutated furin site”) and the numbers corresponding to the mutated furin site number. The following MFS combination constructs were generated: EGFP-Bnl MFS 1-Myc; EGFP-Bnl MFS 2-Myc; EGFP-Bnl MFS 3-Myc; EGFP-Bnl MFS 4-Myc; EGFP-Bnl MFS 1,2-Myc (both N-terminal sites are mutated); EGFP-Bnl MFS 3,4-Myc (both C-terminal sites are mutated) and EGFP-Bnl MFS 1-4-Myc (all furin sites are mutated). The above-listed Bnl variants including non-mutated EGFP-Bnl-Myc as a control were expressed in Kc cell culture and supernatants of these cells were subjected to Western blot analysis using both anti-GFP and anti-Myc antibodies.

The output of the experiment is represented in Figure 24. It shows that in the FS1 mutated variant the 60 kDa GFP-positive band corresponding to the amino-terminal cleavage vanishes, whereas another band of 75 kDa appears, indicating that under these circumstances the amino-terminal Bnl cleavage can occur only via the second furin site. The 75 kDa GFP-positive peptide was previously detected on some of the blots. This band was left unattended since it was considered to be a background (Figures 13C). It is possible now to identify it as a product of the furin site (FS2) cleavage (Figure 24B). The third lane of the same figure shows that mutation of FS2 leads to the amino-teminal Bnl cleavage using non-mutated FS1, resulting in the

appearance of the usual 60 kDa band. However, when both amino-terminal furin consensus sequences were mutated, neither 75 kDa nor 60 kDa GFP-positive bands were detected, suggesting that no amino-terminal Bnl cleavage could occur in the absence of valid furin recognition sites.

A different situation was observed when the third and the fourth Bnl cleavage sites were mutated. The mutation of FS3 did not result in a difference in the masses of the cleaved C-terminal fragments (Figure 24C), whereas the mutation of the fourth furin recognition motif inhibited Bnl carboxy-terminal cleavage completely. The same result was observed when both C-terminal sites were mutated. This data strongly suggests that although FS3 represents a consensus furin recognition motif, it seems not to be cleaved by a furin protease in *Drosophila* cell culture. Eventually, the Bnl variant with all four furin sites mutated did not show any apparent cleavage (Figure 24C), proving that the identified furin recognition motives are responsible for the Bnl processing.

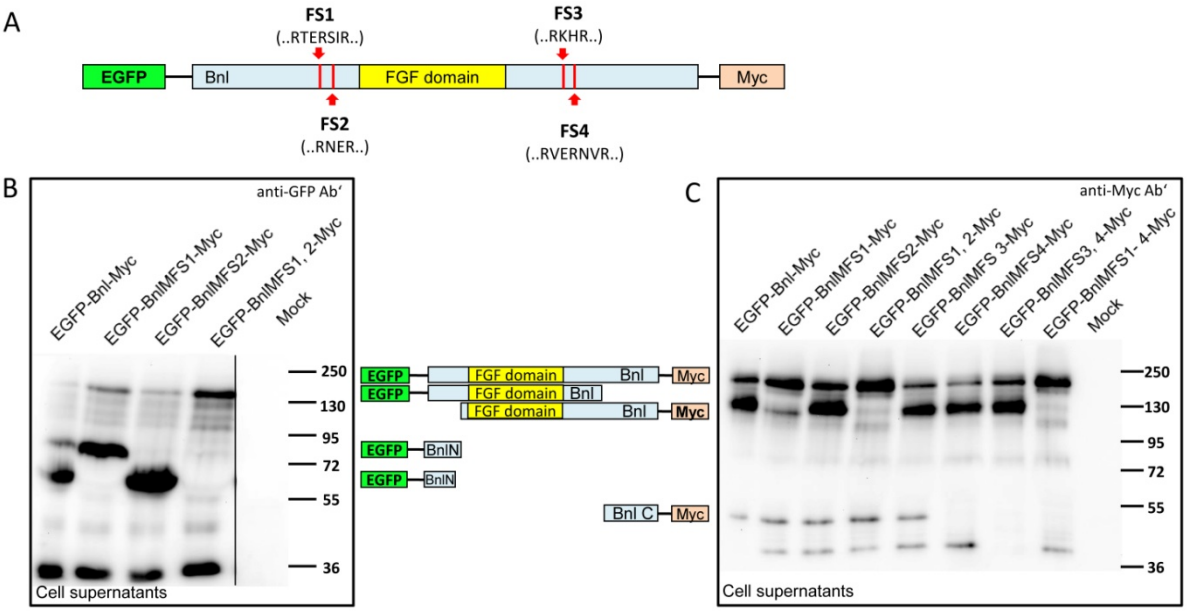

Figure 24: Site-directed mutagenesis of furin cleavage sites. (A) A schematic representation of furin cleavage sites localization in the Bnl protein. **(B)** Western blot analysis of supernatants from cells expressing the EGFP-Bnl-Myc constructs with mutated N-terminal cleavage sites. Bnl N-terminal domain is detected with the anti-GFP antibody. A schematic drawing of the revealed Bnl forms is shown between the panels. Only the mutagenesis of both N-terminal furin sites prevents the N-terminal protein processing. **(C)** Western blot analysis of supernatants from cells expressing the EGFP-Bnl-Myc constructs with mutated N- and C-terminal cleavage sites. Tagged protein forms are detected with the anti-Myc antibody. Site-directed mutagenesis of the FS4 alone blocks Bnl C-terminal cleavage. Mutagenesis of all four recognition motives prevents Bnl processing from both termini.

According to the represented data, the four furin consensus motives identified within the Bnl protein have a differential impact on its cleavage. Both the first and the second furin cleavage sites located on the amino-terminus are clearly utilized for the Bnl cleavage, since the mutagenesis of either site leads to the protein processing using the residual cleavage sequence. When both N-terminal cleavage sites are preserved, the FS1 is utilized for the cleavage as revealed by the EGFP tagged N-terminal protein of 60 kDa. However, since FS2 is cleaved as well as shown by the FS1 mutation, it is not clear if actually both recognition sites are used in Bnl. Regarding the carboxy-terminal cleavage, the FS4 site is clearly processed, whereas the mutation of the FS3 site had no effect, indicating that FS4 is the only used C-terminal furin cleavage site. Although it cannot be excluded, that FS3 might only be used if both C-terminal recognition sites are present.

3.2.8 Mutagenesis of Bnl cleavage sites in *Drosophila* embryos

To confirm the observed cleavage of Bnl by furin proteases *in vivo*, the effect of the site-directed mutagenesis of all furin cleavage sites within Bnl was investigated in *Drosophila* embryos. In order to analyze this, a transgenic fly line was generated that allowed the expression of the mutated Bnl protein using the GAL4/UAS system (Brand and Perrimon 1993). The Bnl variant containing wild type furin cleavage sites was compared with Bnl that carries the earlier described amino acid substitutions impairing all four furin recognition motives. Both constructs contain the N-teminal FLAG- and the C-terminal EGFP-tags for the detection of ectopically expressed Bnl proteins. The two transgenic fly lines, carrying either of the constructs, were crossed to the *tub*GAL4 line, inducing strong ubiquitous transgene expression. Embryos of F1 progeny were harvested and subjected to Western blot analysis and the expressed protein variants were detected with the anti-FLAG antibody.

The result of the experiment, shown in Figure 25, clearly shows, that the small FLAG-positive 28 kDa peptide, corresponding to amino-terminal Bnl cleavage, is not present in the protein sample in which furin recognition sites were mutated. Furthermore a band, representing the full length 200 kDa protein becomes slightly more intensive, indicating that the mutation of the furin recognition sites inhibits Bnl cleavage *in vivo* as well.

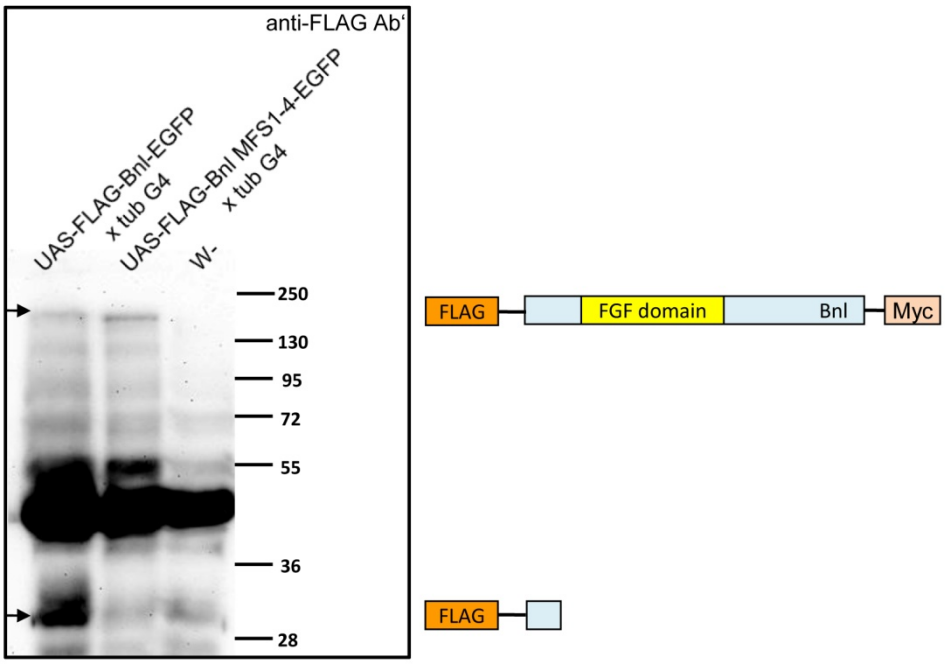

Figure 25: The effect of site-directed mutagenesis of Bnl furin sites in *Drosophila* embryos. Western blot analysis of the embryos expressing FLAG-Bnl-EGFP with the wild type or mutated furin recognition motives. Bnl protein is visualized with anti-FLAG antibody. Arrows indicate the cleaved and intact protein forms. A schematic drawing of the detected Bnl is shown on the right. Site-directed mutagenesis of all furin sites prevents Bnl processing in *Drosophila* embryos.

Thus, the represented data strongly suggests that Bnl is proteolytically processed by a furin proprotein convertase in both *Drosophila* cells and embryos. Furthermore, the specific cleavage can be inhibited by the site-directed mutagenesis of the furin recognition motives. However, it is not yet understood, whether the correct processing of Bnl protein within the secreting cells is relevant for its biological activity. The experiments described below were carried out in order to clarify this issue.

3.3 Relevance of Bnl processing for its biological function

3.3.1 Bnl with mutated furin recognition sites is able to bind Btl receptor in cell culture

A basic biological function of all known fibroblast growth factors is their ability to bind FGFRs and cause their dimerization that represents the first step of receptor tyrosine kinase signaling (Eswarakumar et al., 2005; Polanska et al., 2009). It is also known that Bnl regulates FGF signaling by direct interaction with its receptor Breathless (Btl) (Sutherland et al., 1996). Therefore, it was interesting to verify whether the Bnl variant with impaired furin cleavage sites would show a specific binding to its receptor Btl. A cell culture based assay was employed to investigate the

direct binding of the secreted Bnl variants to the cell-surface localized Btl receptor. *Drosophila* Kc cells expressing FLAG-Btl (a FLAG-tag was introduced N-terminally of *breathless* ORF) were incubated with conditioned medium containing either tagged wild type Bnl or non-cleavable Bnl protein carrying mutated furin sites (Material and methods 2.2.4). In order to detect the conserved FGF domain of the cleavable Bnl variant, a full length EGFP sequence was introduced directly downstream of the second amino-terminal Bnl furin site (FS2) (Figure 26A). EGFP- and Myc-tagged construct containing the described amino acid substitutions impairing all four furin recognition motives was used for expression of the non-cleavable Bnl variant, designated as EGFP-BnlMFS1-4-Myc (Figure 26B). After incubation of the supernatants containing mutated and non-mutated Bnl with FLAG-Btl-expressing cells, the latter were fixed and stained with anti-FLAG and anti-GFP antibodies to visualize the binding partners on the cellular surface.

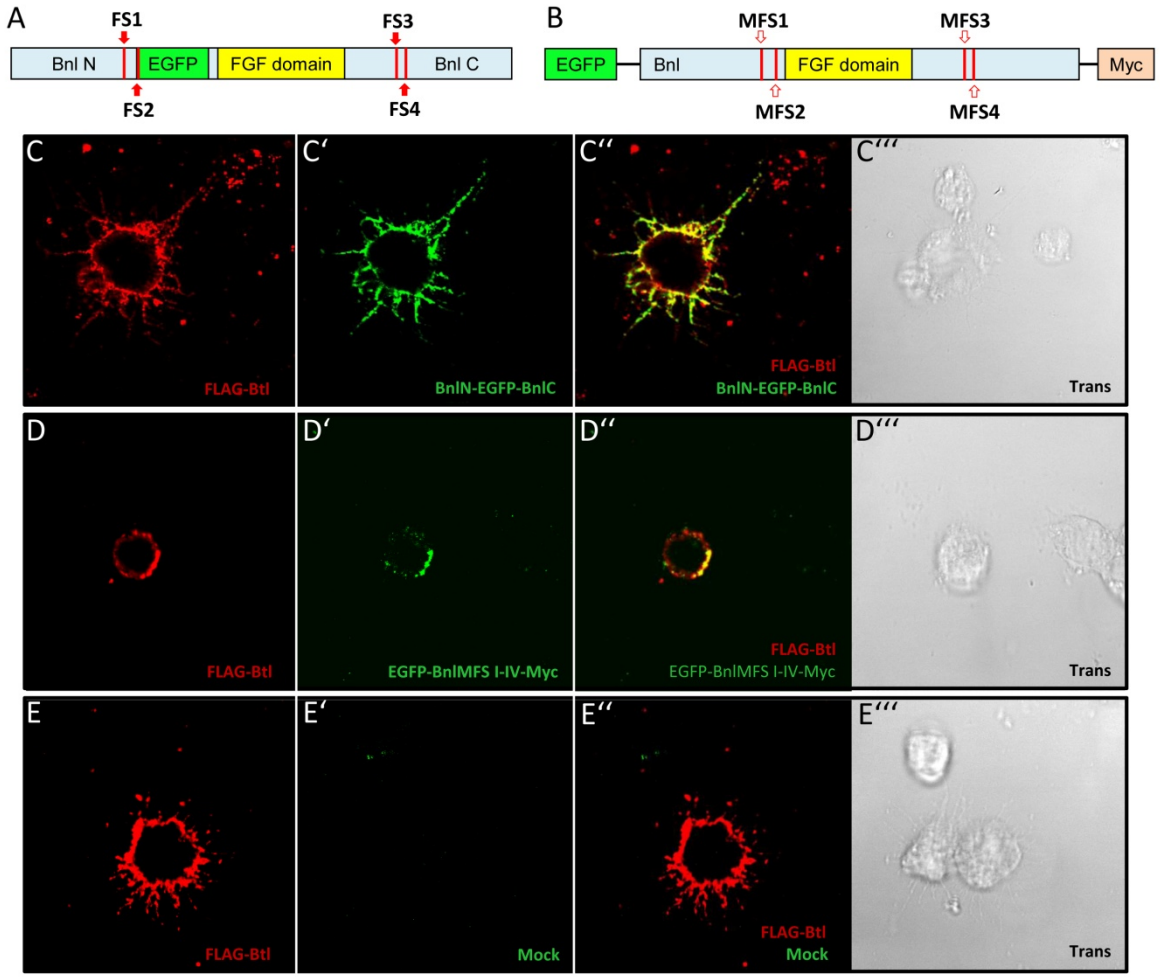

Figure 26: Non-cleavable Bnl specifically binds the Btl receptor in *Drosophila* cells. Schematic representation of the cleavable BnlN-EGFP-BnlC (A) and the non-cleavable EGFP-BnlMFS1-4-Myc (B) Bnl variants (**FS** – furin sites; **MFS** – mutated furin sites). Binding of the cleavable Bnl **(C–C''')**, the non-cleavable Bnl **(D–D''')** and mock control **(E–E''')** to FLAG-Btl in cell culture (**C, D, E** – FLAG-Btl expression detected with the anti-FLAG antibody; **C', D', E'** – bound Bnl protein detected with the anti-GFP antibody; **C'', D'', E''** – overlay of the FLAG and GFP channels; **C''', D''', E'''** – transmitted light image).

The cells were further subjected to the laser scanning confocal microscopy. As shown on Figure 26C–C''', the GFP-marked FGF domain of the cleavable Bnl variant apparently co-localizes with the FLAG-Btl receptor on the surface of Kc cells. This observation proves that the secreted Bnl protein carrying wild type furin recognition sequences interacts only with surface of the cells expressing Btl receptor (Figure 26C–C'''). Therefore, the binding of wild type Bnl was considered to be specific. Interestingly, similar to the cleavable Bnl variant, the secreted EGFP-BnlMFS1-4-Myc protein was found co-localized with Btl-expressing cells. No interaction with cells that do not express the FLAG-tag could be observed (Figure 26D–D''') , indicating that despite the impaired furin cleavage sites, this Bnl variant still shows strong and specific binding to the receptor. The supernatants from mock-treated Kc cells were used as a control for the specificity of the anti-GFP antibody in this assay and showed no background staining (Figure 26E–E''').

Taken together, the described ligand-receptor binding experiment argues strongly that the processing of the Bnl protein is not required for its specific interaction with Btl receptor in *Drosophila* cell culture.

3.3.2 Bnl with impaired furin recognition sites shows dominant negative activity in *Drosophila* embryos

The described above experimental data showed that the unprocessed Bnl protein is still able to bind its receptor. However, this experiment does not demonstrate if the pre-mature growth factor can also cause FGFR activation and induce downstream signaling *in vivo*.

Bnl has two central functions during *Drosophila* embryonic development: (i) it is required for the guidance of embryonic tracheal branches in order to create and shape an elaborated net of epithelial tubules, which will later supply oxygen to different tissues and organs of emerging larvae and (ii) Bnl regulates the final intracellular outgrowth of the terminal branches towards the target cells (Introduction 1.2.3, 1.4.2; Samakovlis et al., 1996a; Uv et al., 2003). In the absence of functioning FGF signaling tracheal branches fail to migrate accordingly to the developmental pattern and do not form secondary and other lower range branches (Sutherland et al., 1996). However, in case when Bnl protein is expressed ectopically in wild type background, tracheal branches change their usual direction of growth and start migrating towards the new growth factor source (Sutherland et al., 1996). Furthermore, upon overexpression, Bnl introduces the fate of terminal cells within the majority of tracheal cells resulting in the massive outgrowth of terminal branches.

Therefore, developing trachea of *Drosophila* embryo represents a perfect model system to study the biological function of Bnl protein variants both by loss-of-function experiments but also in gain-of-function experiments. Due to the highly dynamic Bnl protein expression during embryogenesis it was not possible to rescue the *bnl* loss-of-function (LOF) tracheal phenotype using the GAL4/UAS system (Brand and Perrimon, 1993). Therefore, an ectopic expression approach was employed in order to trace Bnl biological activity.

The GAL4/ UAS expression system (Materials and methods 2.4.3; Brand and Perrimon, 1993) was utilized to provide tissue-specific ectopic expression of transgenic Bnl constructs. The 69BGal4 fly line was employed to induce UAS-controlled gene expression all over the embryonic ectoderm. Three different UAS fly lines were utilized in this experiment. The full length wild type *bnl* sequence (UAS-*bnl*) provides a positive control for the ectopic Bnl activity. Another transgenic line carries *bnl* ORF with impaired N-terminal furin cleavage sites (UAS-*bnl*MFS1,2), so N-terminal processing of this Bnl variant cannot occur. The third transgenic line enables the expression of the non-cleavable Bnl variant with all four furin consensus motives mutated (UAS-*bnl*MFS1-4). All constructs were generated without fusion tags to avoid phenotypes that might be caused by the tags. The three described Bnl transgenic fly lines were crossed with the ectodermal 69BGal4 driver line. F1 progeny embryos were harvested and chemically stained with 2A12 antibody in order to visualize lumen of the developing tracheal system. Further the immunostained embryos were subjected to the bright-field microscopy.

As shown in Figure 27A, a wild type embryonic tracheal system represents a highly-ordered pattern of the tracheal branches. The ectopic expression of the wild type Bnl transgenic protein all over in the embryonic ectoderm almost completely destroys this pattern as a result of a mis-positioned FGF signaling. The abnormally thickened “chain-like” dorsal trunk and the appearance of multiple densely localized tracheoles are the characteristic features of the 69BGal4 induced tracheal misguidance phenotype, which is caused by the transformation of almost all tracheal cells into terminal unicellular branches (Figure 27B). However, when UAS-*bnl*MFS1,2 Bnl variant with two impaired amino-terminal cleavage sites was ectopically expressed in the same tissue, none of these changes was detected, the tracheal system pattern of these embryos looks as in wild type animals (Figure 27C). Similar to this, the misexpression of completely non-cleavable UAS-*bnl*MFS1-4 showed no tracheal misguidance phenotype. (Figure 27D). These results clearly indicate that Bnl processing is required to provide proper FGF signaling in gain-of-function experiments.

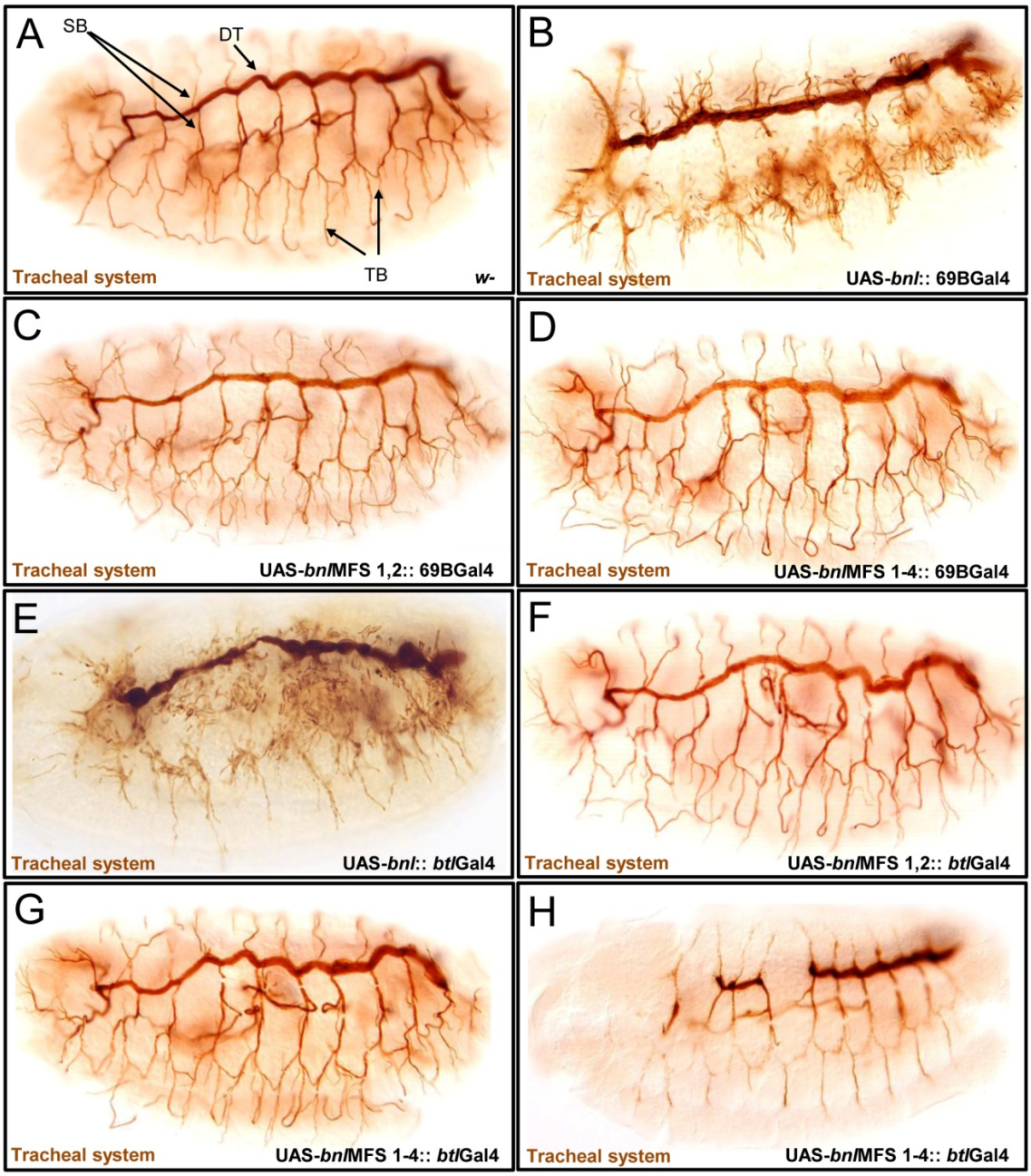

Figure 27: Bnl processing is required for its activity in *Drosophila* embryos. (A) Wild type tracheal system visualized with the 2A12 antibody (DT – dorsal trunk (primary branch); SB – secondary branches; TB – terminal branches (tracheoles). **(B)** Tracheal misguidance phenotype caused by ectopic expression of the wild type Bnl in the embryonic ectoderm. Ectopic ectodermal expression of the N-terminally uncleavable (UAS-*bnl*MFS1,2) **(C)** and the uncleavable Bnl variant (UAS-*bnl*MFS1-4) **(D)** introduces no tracheal misguidance phenotype. **(E)** Ectopic expression of UAS-*bnl* in the tracheal system also results in tracheal misrouting. Ectopic expression of UAS-*bnl*MFS1,2 **(F)** and UAS-*bnl*MFS1-4 **(G)** Bnl variants in the trachea cells does not introduce the misguidance, but instead causes the *bnl* loss-of-function phenotype **(H)**.

The loss of activity of the two mutated Bnl variants can be explained by two mechanisms: first, the processing may be needed for the effective transport of the ligand. In the wild type situation the Bnl protein is secreted by epidermal cells and has to travel certain distance in the extracellular matrix in order to eventually interact with the Btl receptor of the tracheal tip cells (Sutherland et al., 1996; Imam et al., 1999). It is possible that in the represented experimental setup the mutated Bnl protein variants could not migrate to interact with Btl receptor. Another possible explanation of the ineffective signaling caused by non-cleaved Bnl variants could be that the too long and thus misfolded ligands are not able to provide receptor dimerization and thus trigger FGF signal transduction.

In order to distinguish between the described models, the three Bnl constructs were ectopically expressed in the embryonic tracheal system cells using *btl*Gal4 driver line, so that the Btl receptor and the Bnl protein variants are co-expressed within the same cell, excluding the necessity of ligand transportation. As shown in Figure 27E, embryos resulting from *btl*Gal4 female flies crossed to male animals carrying the cleavable wild type Bnl variant, show severe tracheal misguidance phenotype, similar to that seen with 69BGal4 induced FGF expression. However, when either of the two mutated Bnl constructs was expressed in the trachea, no misrouting phenotype was detected (Figure 27F, G).

This observation indicates that the uncleaved FGF ligands fail to induce Btl receptor activation. Moreover, in some of the embryos expressing the non-cleavable Bnl variant severe breaks in the dorsal tracheal trunk were revealed (Figure 27H). Such interruptions in the dorsal trunk are not the cause of gain-of-function experiments but they represent one of the characteristic traits of the *bnl* LOF phenotype (Sutherland et al., 1996). The appearance of this phenotype may indicate that the uncleaved Bnl protein is able to act as a dominant negative form of the ligand. It is secreted from the tracheal cells, readily binds to the Bnl receptor of the same cells and blocks it, thus preventing the receptor from interaction with endogenous Bnl ligands and thereby causing the observed *bnl* LOF phenotype.

Taken together, the represented data strongly suggests, that proteolytic processing is required for the proper biological activity of Bnl *in vivo*. Moreover, though the uncleavable Bnl protein is able to bind the Btl receptor, the dominant negative effect observed in *Drosophila* embryos indicated that the Bnl precursor is unable to induce downstream signaling.

3.3.3 Non-cleavable Bnl variants are expressed but not functional in *Drosophila* embryos

Since there was no apparent gain-of-function FGF activity detected in embryos expressing mutated Bnl variants, it is necessary to prove, that these transgenic proteins were expressed. Therefore, whole mount *in situ* RNA hybridization was performed to detect ectopically expressed mRNA encoding Bnl protein variants. As represented in Figure 28A, an ectopic expression of a control UAS-*bnl* transgene with *btl*Gal4 driver can be revealed in the developing trachea with a *bnl* antisense RNA probe. Similar tracheal staining was detected when both UAS-*bnl*MFS1,2 and UAS-*bnl*MFS1-4 mutated Bnl variants were expressed with the *btl*Gal4 driver line (Figure 28B and C). Moreover, anti-Bnl immunostaining was carried out in embryos expressing the non-cleavable Bnl construct to further prove the protein expression. The antiserum detecting the amino-terminal part of the Bnl protein was kindly provided by Mark Krasnow (Stanford, USA; Jarecki et al., 1999). The immunostainig clearly detects presence of the ectopically expressed mutated Bnl protein in tracheal cells (Figure 28D).

Thus, the results show that the non-cleavable Bnl variants are effectively expressed in the embryos as well as the wild type protein, suggesting that the mutations of the furin cleavage sites are responsible for the lack of Bnl biological activity.

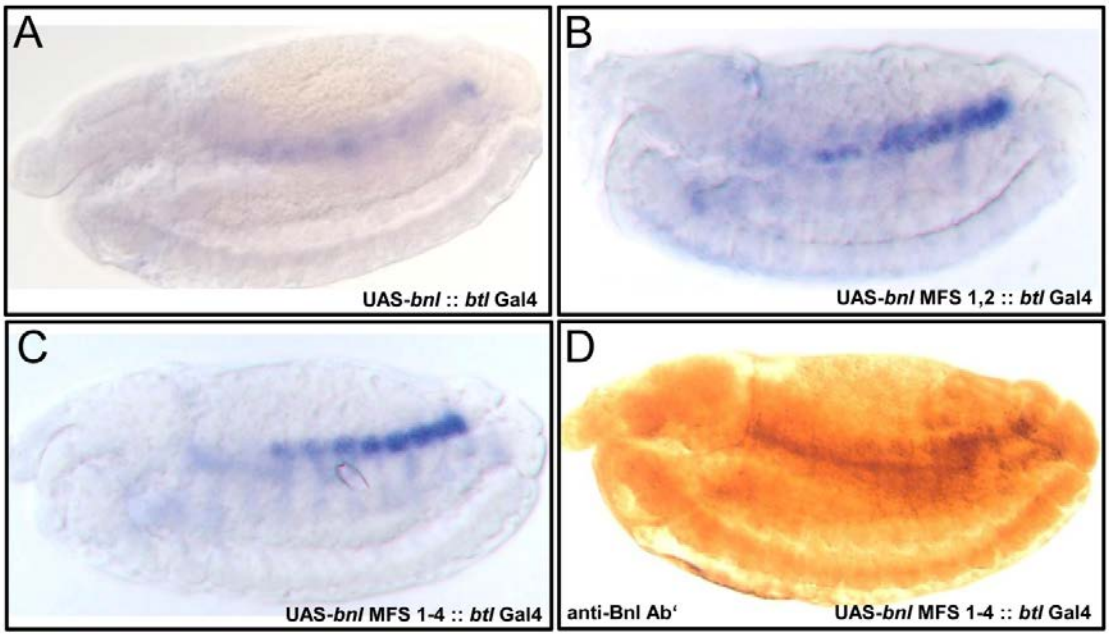

Figure 28: Mutated Bnl variants are expressed in *Drosophila* embryos. (A) *In situ* hybridization of wild type Bnl ectopically expressed in the trachea. **(B)** Ectopic expression of UAS-*bnl*MFS1,2 construct detected in the tracheal system. **(C)** Ectopic expression of the uncleavable Bnl variant (UAS-*bnl*MFS1-4) in the tracheal cells revealed by *in situ* hybridization. **(D)** Ectopic tracheal expression of UAS-*bnl*MFS1-4 detected with the anti-BnlN antibody.

3.3.4 N- and C-terminal parts of Bnl protein are not required for its in vivo activity

The experiments revealed that the uncleavable Bnl protein is not active, indicating the the proteolytic processing is indeed required for the activation of Bnl. If this is the case, the released central part of the protein with the conserved FGF domain should be biologically active.

To explore this hypothesis, two additional transgenic lines were generated that allow the expression of a N-terminal shortened Bnl protein and a N- and C-terminal shortened protein that would represent the fully processed Bnl protein. The first fly line contains an untagged bnl sequence lacking the amino-terminal region up to the second cleavage site (FS2) starting exactly with the amino acids following the furin recognition motif (UAS-BnlSTV) (Figure 29A). The second line carries the fully truncated Bnl form with both the N- and the C-termini deleted (UAS-BnlSTV-GGK) (Figure 29B). The tissue-specific ectopic expression of truncated UAS Bnl constructs was induced using 69BGal4 and *btl*Gal4 driver lines described in the section 3.3.2. Embryos resulting from this cross were harvested and stained using the 2A12 antibody to visualize the tracheal lumen. The immunostained embryos were screened for the tracheal misguidance phenotype using bright-field microscopy.

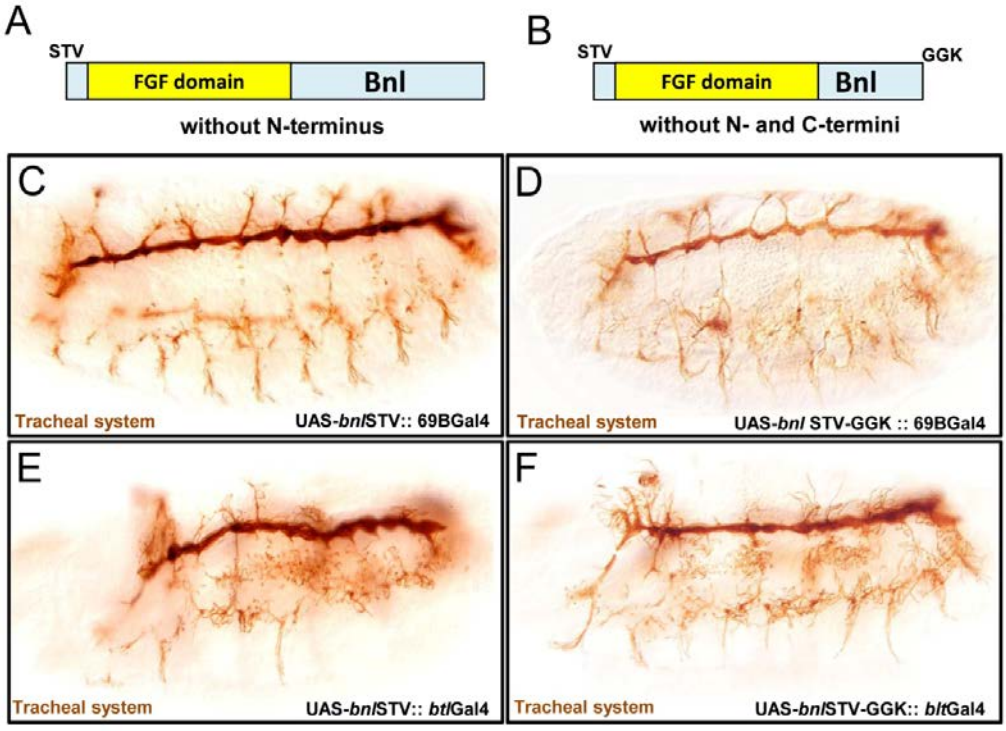

Figure 29: Bnl truncated variants show FGF activity in *Drosophila* embryos. (A) Schematic representations of the N-terminally truncated (UAS-*bnl*STV) and **(B)** both N- and C-terminally truncated (UAS-*bnl*STV-GGK) Bnl transgenic variants. Ectopic ectodermal expression of UAS-bnlSTV **(C)** and UAS-*bnl*STV-GGK **(D)** causes misgudance of tracheal branches. Tracheal expression of UAS-*bnl*STV **(E)** and UAS-*bnl*STV-GGK **(F)** with *btl*Gal4 also results in the tracheal misguidance phenotype. In **C-F** embryonic tracheal system is visualized with the 2A12 antibody.

As represented in Figure 29, the truncated Bnl variant mimicking the N-terminally processed protein shows a clear tracheal misguidance phenotype when ectopically expressed using both 69BGal4 (Figure 29C) and *btl*Gal4 (Figure 29E) driver lines. Similar to this, the misexpression of the Bnl variant with N- and C-termini truncated causes the remarkable rerouting of the tracheal branches (Figure 29D and F).

Brought together, the represented data strongly indicates that the amino- and carboxy-terminal Bnl protein parts, including furin recognition motives, are not required for the proper FGF signaling *in vivo* and the proteolytic processing serves to release the functional FGF domain.

3.3.5 Bnl processing is required in the secreting tissue

The gain-of-function experiments clearly showed that the proteolytic processing is required to activate the Bnl protein and that only the central part including the FGF conserved domain is required for the activation of the Btl receptor. However, these experiments do not allow to conclude that also the endogenous Bnl protein has to be processed to become active.

In order to investigate this issue, the processing of the endogenous Bnl protein was selectively blocked by the expression of α1-PDX protease inhibitor in different embryonic tissues. A tissue-specific expression of the inhibitor was achieved by employing the UAS/Gal4 inducible expression system (Brand and Perrimon, 1993). The cell culture results clearly proved that Bnl is processed during its synthesis within the secreting cells. Therefore, the processing should be specific to the epidermis that include the *bnl*-expressing cells but should not be required in the signal receiving cells of the tracheal system. Therefore, the specific furin inhibitor α1-PDX was first expressed within the tracheal cells using the *btl*-Gal4 driver line as a control. As expected, no tracheal system phenotype could be observed (Figure 30A and C). Flies carrying the *bnl*Gal4 driver were utilized to provide an expression of the UAS-*α1-PDX* transgenic construct selectively in Bnl secreting ectodermal cells, although based on the highly dynamic expression changes and the time delay of expression using the Gal4/UAS system only weak effects could be expected. As shown in Figure 30D, embryos resulting from this cross have gaps in the main dorsal tracheal trunk that are characteristic of the *bnl* loss-of-function phenotype (Figure 30B). This phenotype becomes more apparent, when UAS-*α1-PDX* is expressed throughout the embryonic ectoderm under control of the 69BGal4 driver (Figure 30E).

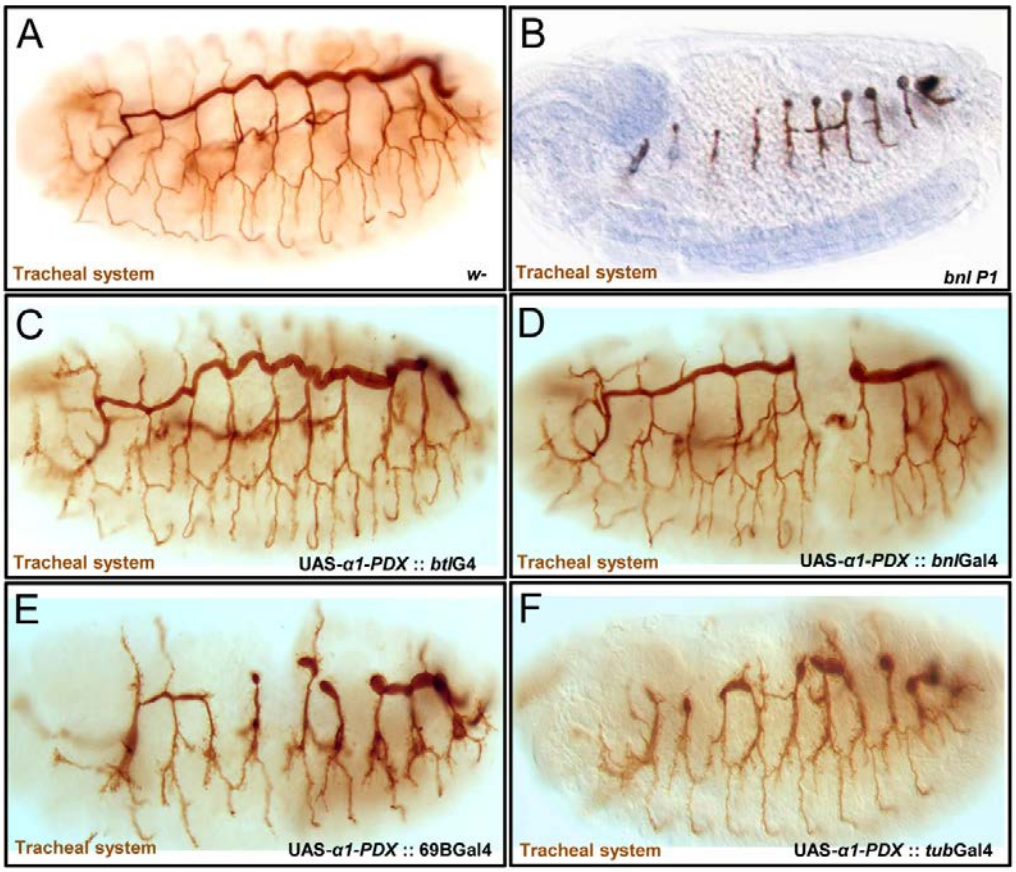

Figure 30: Bnl processing is required in the secreting cells. Embryonic tracheal system is stained with the 2A12 antibody **(A)** Wild type tracheal system. **(B)** Strong *bnl* loss-of-function tracheal phenotype (dorsal tracheal trunk is not formed). **(C)** Tracheal expression of the α1-PDX inhibitor does not cause any tracheal phenotype. **(D)** A1-PDX expression in Bnl secreting cells introduces the weak *bnl* LOF phenotype. Expression of α1-PDX in the ectoderm **(E)** and ubiquitously in the embryo **(F)** results in the strong *bnl* LOF phenotype.

Moreover, a strong and ubiquitous inhibition of Bnl cleavage with the *tub*Gal4 driver resulted in a further increase of the phenotype. As shown in Figure 30F, the dorsal trunk failed to form in these animals, as it is observed in embryos with a strong *bnl* mutant alleles (Sutherland 1996).

Thus, the experimental data supports the cell culture results proving also *in vivo*, that Bnl protein processing occurs only in the secreting tissue and is not required in the target tracheal cells. Furthermore, the represented experiment is *in vivo* evidence, that an impairment of Bnl processing by the inhibition of the furin protease activity has a negative impact on the embryonic tracheal development. This result therefore, strongly indicates that the proteolytic processing is also required for the activation of the endogenous Bnl protein.

3.3.6 *Drosophila* Furin1 expression overlaps with that of Bnl

As was shown in section 3.2.5, *Drosophila* Furin1 proprotein convertase was identified as a protease required for Bnl processing in cell culture. Therefore, it is interesting to investigate, whether *dfur1* and *bnl* genes would demonstrate a temporally and spatially overlapping expression pattern in *Drosophila* embryo. *bnl* gene expression becomes detectable in the ectoderm in multiple spots surrounding the arising tracheal pits at stage 11 of embryogenesis (Sutherland et al., 1996). During stages 12 and 13 *bnl* expression dynamically changes, corresponding to formation and growth of primary tracheal branches (Figure 31A). At stage 14 the ectodermal *bnl* expression is diminished and eventually cut off. In order to correlate the *dfur1* expression pattern with that of *bnl*, whole mount RNA *in situ* hybridization with a *dfur1* antisense probe was performed using w^{1118} *Drosophila* embryos of different stages to trace the localization of *dfur1* mRNA. Stained embryos were mounted on slides and *dfur1* expression was visualized using bright-field microscopy. According to the previous observation, embryos of early stages show ubiquitous *dfur1* mRNA localization, so that it is not possible to distinguish any specific expression pattern (Roebroek et al., 1993). However, at stage 13 *dfur1* expression accumulates laterally in epidermal spots, in the area where *bnl* is expressed at the same time point (Figure 31A and B; Roebroek et al., 1993; Sutherland et al., 1996).

Thus, the observed overlapping expression pattern of *bnl* and *dfur1* strongly indicates, that Dfur1 proprotein convertase could be the protease required for the Bnl processing in *Drosophila* embryos as well as in cell culture.

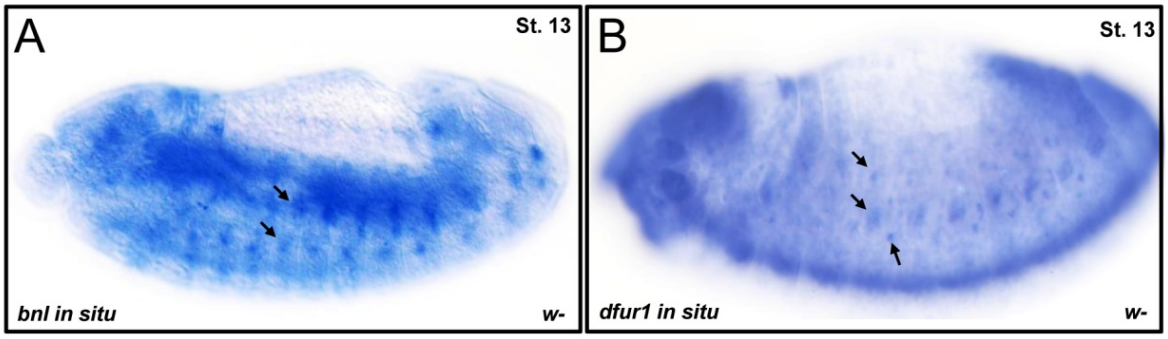

Figure 31: *dfur1* and *bnl* RNA *in situ* hybridization. (A) Whole mount *in situ* hybridization with the *bnl* antisense RNA probe carried out in *w-* embryos. **(B)** *dfur1* gene expression detected in stage 13 embryos. Both genes are dynamically expressed in the lateral epidermis of late embryo.

3.3.7 Embryos lacking Dfur1 demonstrate impaired tracheal development

In order to further investigate relevance of Dfur1 protease for Bnl signaling *in vivo*, *Drosophila* embryos lacking a functional *dfur1* gene were screened for the *bnl* tracheal phenotype. Since no strong alleles of *dfur1* gene are available, embryos of a cross of a *dfur1* gene deficiency *in trans* with a P-element insertion in the 5'-UTR of the *dfur1* gene were analyzed. The mutant embryos were identified using β-galactosidase marked balancer chromosomes of the two parental strains. The embryos were harvested and stained with the 2A12 antibody to visualize the developing tracheal system. In addition, anti-β-Galactosidase staining was performed to identify mutant embryos. The immunostained embryos showing no β-Galactosidase staining were subjected to the bright field microscopy. About 15% of the explored embryos showed defects in tracheal system development. As represented in Figure 32, numerous breaks in the main trunk were detected in these animals. Moreover, some of the dorsal tracheal branches were missing as a result of impaired Dfur1 activity. The observed phenotypes resemble the weak *bnl* loss-of-function phenotype. However, it was previously shown, that *Drosophila* furins participate in the processing of Decapentaplegic (Dpp) proprotein, another signaling molecule required for embryonic tracheal system formation (Myat et al., 2005; Künnapuu et al., 2009).

Therefore, it is not yet clear if the observed phenotype represents the result of a reduced *bnl* activity or, alternatively, both Bnl and Dpp signaling pathways are impaired. Further *in vivo* experiments are required to explore this issue.

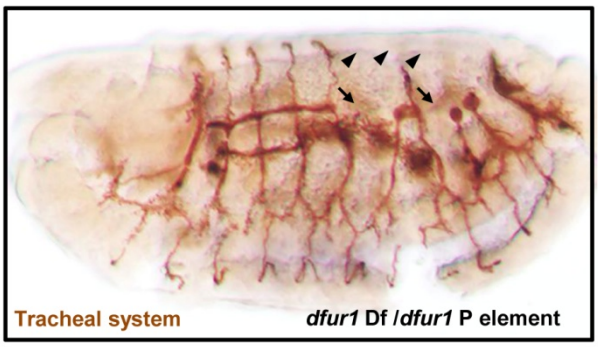

Figure 32: *dfur1* mutant embryos show the impaired tracheal development. *Drosophila* embryo lacking functional Dfur1 protein demonstrates numerous breaks in dosal trunk (arrows) and missing dorsal brunches (arrowheads). Embryonic tracheal system is stained with the 2A12 antibody.

3.3.8 Dfur1 activity is required for Bnl signaling during embryonic tracheal system development

One of the commonly utilized approaches to connect the activities of two gene activities to the same signaling pathway *in vivo* is the genetic interaction assay. For this purpose, the dosage of the corresponding genes is decreased by 50% in the organism. Such a reduction of the gene dosage by itself has normally no effect. However, if the two proteins functionally belong to the same biological process, simultaneous reduction of their gene dosage will result in a phenotype that resembles a homozygous loss-of-function phenotype of each of these genes, despite that both of them are in fact in the heterozygous state.

In order to check whether Dfur1 proprotein convertase indeed participates in the Bnl signal-transduction pathway, a *dfur1* deficiency heterozygous fly line was crossed with flies carrying the *bnlP1* loss-of-function mutation. As was earlier described by Sutherland et al., 1996, in homozygous state this mutation causes a complete failure of the tracheal branching and dorsal trunk formation (Figure 30A), whereas heterozygous mutants do not show a tracheal phenotype (Sutherland et al., 1996). F1 embryos resulting from the genetic interaction cross were harvested and stained with the 2A12 antibody for tracheal lumen detection and with the anti-β galactosidase antibody to visualize the wild type balancer chromosome. Embryos lacking one copy of each gene were screened for the tracheal system phenotype. 25% of the observed trans-heterozygous embryos showed impaired tracheal development. In particular, in some animals the anterior and posterior dorsal trunk branches failed to fuse together (Figure 33A), additionally, in other cases dorsal or ganglionic tracheal branches were missing (Figure 33B). This result strongly indicates that Dfur1 protease activity is required for the function of the Bnl signaling pathway in the tracheal system.

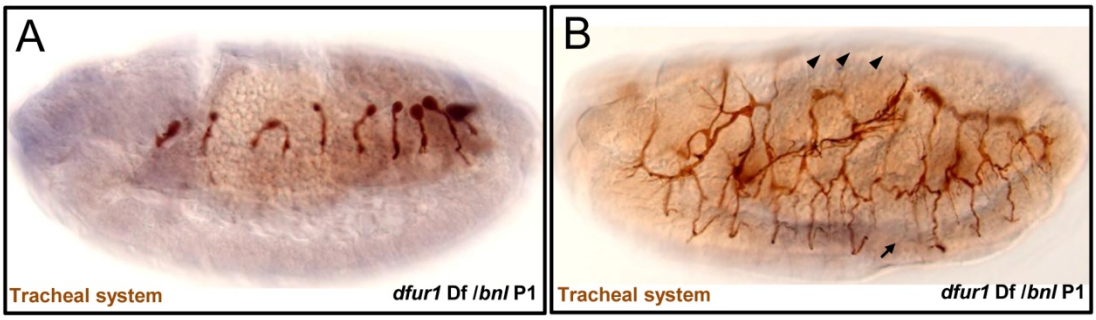

Figure 33: Genetic interaction of *dfur1* and *bnl* in developing tracheal system. Embryos double trans-heterozygous for *dfur1* and *bnl* mutant alleles show severe *bnl* LOF phenotype. Embryonic tracheal system is visualized with the 2A12 antibody. **(A)** In this embryo fusion of the anterior and posterior branches of the dorsal trunk did not occur. **(B)** The embryo has impaired dorsal trunk fusion and missing dorsal (arrowheads) and ganglionic (arrow) branches.

3.4 Proteolytic processing of vertebrate homologues of Bnl

Drosophila Bnl represents the functional homolog of vertebrate FGF10 that is involved in branching morphogenesis of the lung (Min et al., 1998; Introduction 1.2.3). Based on the current results, it is possible that proteolytic processing also contributes to the modulation of FGF10 signaling in vertebrates. *In silico* protein alignment of Bnl and FGF10 homologues from *Xenopus laevis*, *Gallus gallus*, mouse and human was performed to investigate this hypothesis (Materials and methods 2.5.2). This approach revealed a potential furin recognition motif (–R–H–V–R–) located five amino acids upstream of the FGF homology domain in all these proteins (Figure 34A).

In order to assess, whether the identified furin recognition motives are utilized for vertebrate FGF10 processing, a human FGF10 carrying C-terminal 10xMyc-tag was expressed in *Drosophila* Kc cells (Figure 34B) and cell supernatant was subjected to Western blot analysis with the anti-Myc antibody. As shown in Figure 34C, the secreted hFGF10 migrates as two Myc-positive bands of 38 and 34 kDa. However, when co-expressed with the α1-PDX construct, the lower band vanishes from the blot.

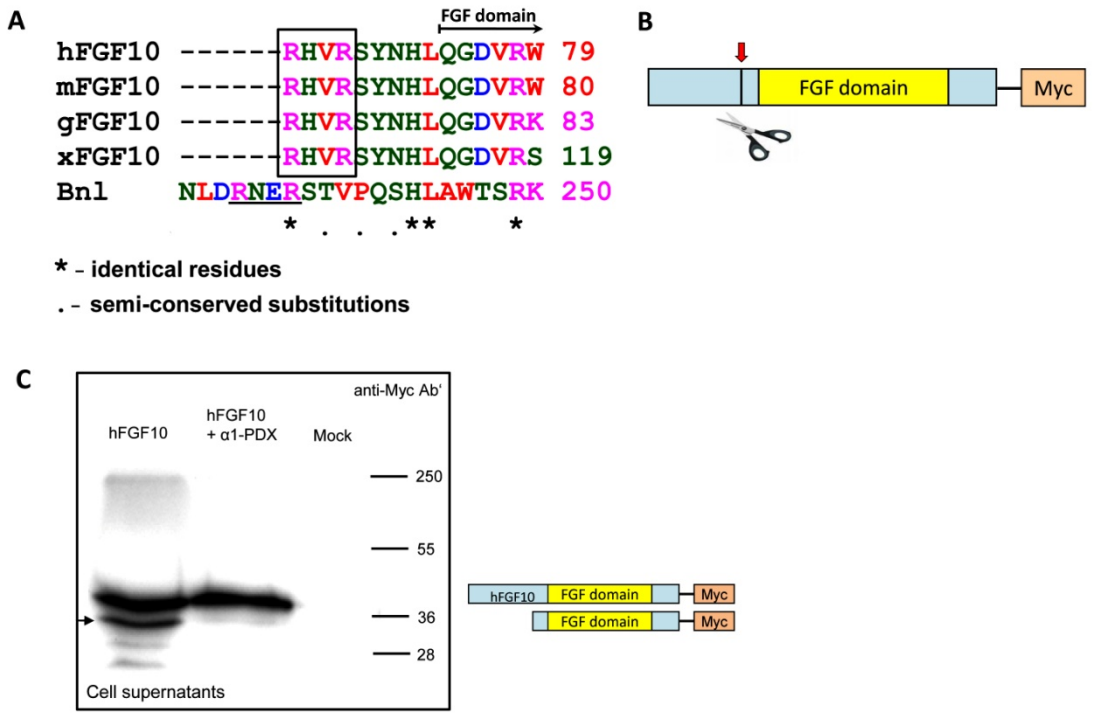

Figure 34: Proteolytic processing of vertebrate FGF10 homologues. (A) Sequence alignment of Bnl and FGF10 homologues from different vertebrate species. Conserved minimal furin recognition motif identified upstream of the FGF domain is shown inside the black frame. Bnl cleavage site FS2 is underlined. Beginning of the FGF domain is shown with an arrow. **(B)** A schematic drawing of the tagged hFGF10 protein. Location of furin recognition motif is indicated with a red arrow. **(C)** Western blot analysis of the FGF10 construct in the presence of α1-PDX inhibitor secreted from *Drosophila* cells. Tagged hFGF10 is detected with the anti-Myc antibody. N-terminally cleaved protein is marked with an arrow. A schematic drawing of the revealed hFGF10 forms are shown on the right.

This result suggests that similar to Bnl, hFGF10 undergoes proteolytic cleavage in its N-terminal region. Moreover, according to the obtained data, this processing relies on the activity of a protease of SPC family, since the addition of the specific inhibitor prevented the cleavage.

Taken together, the experimental data of the present study shows that *Drosophila* FGF homologue Bnl that is required for development of embryonic tracheal system undergoes proteolytic processing in secreting cells. The maturation process includes cleavage of the Bnl proprotein in its N- and C-termini and is carried out by the specific *Drosophila* Furin1 proprotein convertase. It was shown, that the non-cleaved Bnl is readily secreted from the expressing cells and, moreover, is able to specifically interact with the Btl receptor on the cellular surface. However, the unprocessed Bnl forms are unable to induce downstream FGF signaling *in vivo*. Analysis of *dfur1* and *bnl* mutant embryos indicates that Bnl maturation is necessary for the correct formation of the embryonic tracheal system and Dfur1 plays an important role in this process, indicating that the characterized proteolytic processing of Bnl is essential for its biological activation *in vivo*. Moreover, the vertebrate homologue of Bnl, hFGF10, was shown to be proteolytically cleaved by a protease of the SPC family in *Drosophila* cells, suggesting that the proteolytic processing of Bnl homologues is evolutionary conserved.

4 DISCUSSION

The phenomenon of post-translational proteolytic processing of growth factors and other signaling peptides is widespread in eukaryotes. Proteolytic cleavage is known to be a part of maturation process of the β-nerve growth factor (βNGF), members of the transforming growth factor-β (TGF- β) superfamily, platelet derived growth factor (PDGF), vascular endothelial growth factor (VEGF) and others (Bresnahan et al., 1990; Dubois et al., 1995; Siegfried et al., 2003; Stacker et al., 1999). Precursor protein processing usually occurs at dibasic amino acid residues and members of the subtilisin-like proprotein convertase (SPC) family of enzymes were shown to be responsible for this process (Steiner, 1998). For most growth factors and neuropeptides endoproteolytic cleavage represents an activation step and therefore is essential for their biological activity.

This work represents the first report about post-translational processing of *Drosophila* fibroblast growth factor Branchless (Bnl). This protein is involved in development of embryonic and larval tracheal system and represents the functional homologue of human FGF10 (Min et al., 1998). The experiments performed in this study show that Bnl is initially synthesized as a larger precursor protein, which undergoes proteolytic activation in secretory cells. Cleavage removes the extended N- and C-terminal parts of the protein and releases the functional FGF homology domain. In this study, *Drosophila* Furin1 (Dfur1) was identified as a protease required for Bnl processing. *In vivo* analysis indicated that proteolytic cleavage by Dfur1 is required for Bnl protein activation and is essential for its proper function during morphogenesis of embryonic tracheal system. Moreover, analysis of vertebrate homologues of Bnl suggests the conservation of the observed furin-mediated regulation of FGF function in course of evolution.

4.1 Proteolytical processing of *Drosophila* Bnl protein

Drosophila FGF homologue Bnl was discovered almost 15 years ago (Sutherland et al., 1996). Despite the huge evolutional distance between vertebrates and invertebrates, the FGF domain of Bnl demonstrates high homology with human and other vertebrate FGFs (Sutherland et al., 1996). From a functional point of view, Bnl is able to induce cell migration and differentiation via specific interaction with its receptor Btl and is known to function as a

chemoattractant for the cells of *Drosophila* tracheal system (Sutherland et al., 1996; Ribeiro et al., 2002). However, in contrast to all known vertebrate FGFs, which are relatively small in size, the Bnl protein is unusually large (Sutherland et al., 1996; Ornitz and Itoh, 2001). It contains extended N- and C-terminal regions flanking the conserved FGF domain, making the Bnl protein about three times longer than any of the vertebrate FGFs (Sutherland et al., 1996).

Current study provides information about post-translational regulation of the Bnl protein length and biological activity. The performed experiments clearly indicate that Bnl is proteolytically cleaved in its N- and C-termini in cell culture as well as in *Drosophila* embryos. This cleavage occurs intracellularly and all forms of the protein can be secreted from the cells and subsequently detected in conditioned medium. The experiments showed that Bnl processing results in release of the central part of the protein that contains the conserved FGF domain. Since there is no reliable antibody that is able to specifically bind the Bnl FGF domain, detection of the cleaved protein was carried out using N- and C-terminally tagged versions of Bnl. This approach reveals the N- and C-terminal parts of the cleaved growth factor. However, the central domain could only be visualized indirectly with the antibody detecting Bnl fusion tags due to incomplete cleavage of the proprotein (see Figures 13, 15 and 17). Subsequent analysis of *Drosophila* embryo extracts has demonstrated that Bnl cleavage also takes place *in vivo* (Figure 15). Furthermore, the calculated molecular mass of the released central FGF domain of Bnl is about 34-37 kDa, which corresponds to the reported size of vertebrate FGFs.

There are only few reports about post-translational proteolytic processing of FGFs available. It was previously shown that *Xenopus laevis* FGF3 is proteolytically modified by an unknown protease presumably of the proprotein convertase family (Kiefer et al., 1993; Antoine et al., 2000). Similar to Bnl, this protein is processed in its N- and C-termini. Other evidence that the FGFs can be proteolytically processed comes from a study on mouse FGF4 (also known as kFGF) that is processed in its N-terminal region (Kosaka et al., 2009). A single known human FGF, which was shown to undergo proteolytic cleavage, is FGF23 (Fukumoto, 2008). It was recently reported that FGF23 is cleaved in its C-terminal region by a yet unidentified protease of SPC family (Benet-Pages et al., 2004). As described in White et al., 2001, cleavage of FGF23 occurs intracellularly or during its secretion. Thus, according to the available data, proteolytic processing is not common for members of the vertebrate FGF family.

However, the experimental evidence from this study indicates that *Drosophila* FGF Bnl is produced as a precursor that undergoes proteolytic maturation in secreting cells. Moreover, it was described recently that two other *Drosophila* FGFs, Pyr and Ths, which have comparable to Bnl length, undergo intracellular cleavage in *Drosophila* releasing their N-terminal parts containing the FGF domain to extracellular space (Tulin and Stathopoulos, 2010). Altogether, these data suggests that the proteolytic cleavage of large precursors is a common mechanism of FGF modification in *Drosophila*.

4.2 Relevance of anterograde trafficking for Bnl processing and secretion

Vertebrate FGFs differ in their subcellular localization and secretory behavior. Most of them are secreted from producing cells using a hydrophobic signal peptide that serves to target the protein to the classical secretory pathway of the cell. Such proteins are directly synthesized into the ER lumen and further transported to the Golgi apparatus by a anterograde trafficking mechanism. This mechanism includes formation of the coated protein II (COPII) vesicles (reviewed in Fromme et al., 2008). In the Golgi complex the proteins are sorted according to their final destination and purpose and undergo different types of post-translational modification including glycosylation and proteolytic cleavage. Proteins that are assigned for secretion leave the late Golgi compartment as part of secretory vesicles. These vesicles are further transported to the cellular periphery and fuse with the plasma membrane releasing their content to the extracellular space (Reynaud and Simpson, 2002). However, some members of the vertebrate FGF family including FGF1, FGF2, FGF9, FGF16 and FGF20 do not have a classical signal sequence, but are nevertheless secreted from producing cells (Miyake et al., 1998; Ochmachi et al., 2000; Miyakawa et al., 1999; Revest et al., 2000), indicating that these FGFs utilize an alternative secretory pathway independent from the ER and Golgi complex.

As previously described, the Bnl protein carries a predicted 24 amino acid signal sequence in its N-terminus (Sutherland et al., 1996). By inhibiting the formation of COPII vesicles within *Drosophila* Kc cells, it was possible to investigate whether the conventional secretory pathway is employed for Bnl export and effective processing. As represented in Results 3.1.4, the inhibition of cellular anterograde trafficking almost completely abolishes Bnl processing and secretion (Figure 17). This result indicates that Bnl is secreted using the classical secretory rout and thus relates it with conventionally secreted members of FGF family. These data also suggests, that Bnl has to be transported to the Golgi

apparatus to be cleaved. This hypothesis is further confirmed by the subsequent results, showing that Bnl is processed by a furin protease, which preferentially localizes in the Golgi complex (Results 3.2.5, 3.3.7, 3.3.8).

4.3 N-linked glycosylation of the Bnl protein

Western blot analysis showed that the *Drosophila* Bnl protein has dramatically higher molecular weight than was expected from its amino acid sequence. Subsequent experiments indicated that Bnl, similar to the members of vertebrate FGF family, carries N-linked glycosylation (see Introduction 1.2.1, Results 3.1.3).

Sugar modifications fulfill diverse biological functions within the cell. They serve as recognition markers, regulate the turnover of proteins and may contribute to the glycoprotein activity (Helenius and Aebi, 2004; Lederkremer, 2009). Furthermore, they are implicated in correct protein folding and are known to contribute to protein stability (Bellosta et al., 1993; Hanson et al., 2009). Glycosylation is an enzymatic process and was shown to occur in different cellular compartments, including the ER and the Golgi complex (reviewed in Hardingham and Fosang, 1992). There are several known types of protein glycosylation (N- and O-linked glycosylation, phospho-glycosylation and others), but N- and O-linked sugar modifications are the most widespread ones.

Treatment of Bnl with N-glycosidase reduces the apparent molecular weight of the cleaved N-terminal part of the protein, indicating that Bnl is modified at its N-terminal region that is proteolytically removed. Therefore, this modification cannot have a function in the activity of the secreted mature ligand. Based on Western blot analysis of full length Bnl, the glycosylation masks the GFP antibody epitope at the N-terminus of the protein (see Results 3.1.1 and 3.1.3). The high molecular weight products of partial Bnl cleavage could be detected with the anti-GFP antibody only after the treatment with N-deglycosydase (Figure 16). However, this approach could only partially improve N-terminus detection and the secreted full length protein was still invisible with the anti-GFP antibody. This indicates that along with the N-linked glycosylation Bnl carries other types of post-translational modification. Based on *in silico* prediction (Materials and methods 2.5.4), the Bnl protein carries 5 potential N-linked and two O-linked glycosylation sites (Figure 35). The two N- and one O-glycosylation targets are located in the Bnl N-terminal region close to the GFP fusion tag. Therefore, these modifications are likely to be responsible for the impaired binding of the antibody.

Figure 35: *In silico* predicted sites of Bnl N- and O-linked glycosylation. Schematic representation of the tagged Bnl protein with marked predicted glycosylation sites. N-linked glycosylation is shown with red vertical lines; O-glycosylation is marked with green vertical lines.

Furthermore, the unglycosylated (and therefore detectable with the anti-GFP antibody) full length Bnl could only be revealed within the cells and not in conditioned medium (Figure 13). This suggests that Bnl modification may protect the protein from proteolytic processing. A similar effect was demonstrated for the mouse FGF4 (Bellosta et al., 1993). This protein is usually secreted from expressing cells as a N-teminally glycosylated peptide. However, in the absence of glycosylation it appears instable and undergoes proteolytic processing in its N-terminal region (Bellosta et al., 1993). Hence, the unidentified glycosylation masking the GFP antibody epitope of Bnl may serve as a negative regulator of its proteolytic cleavage within the cell.

Moreover, based on the dramatic effect of N-linked glycosylation on Bnl molecular weight, it would be interesting to investigate if the observed modification has an impact on its intracellular sorting, secretion, extracellular stability or biological function. The reported glycosylation could be required for the correct transport of the Bnl protein from the ER to the Golgi complex. Additionally, the described N-glycosylation may serve as a recognition marker for the subsequent proteolysis. In order to test all these hypotheses, the modified amino acids need to be subjected to mutational analysis.

4.4 Characterization of Bnl cleavage sites

Identification of Bnl cleavage sites (see Results 3.2.1–3.2.4 & 3.2.7) showed that Bnl is cleaved in *Drosophila* by a furin proprotein convertase. According to available data, these proteases preferentially localize in the *trans*-Golgi network (Molloy et al., 1994). Moreover, these enzymes are implicated in the majority of proteolytical processing at basic amino acid residues in the eukaryotic secretory pathway (Thomas, 2002).

One of the Bnl N-terminal furin cleavage sites was identified six amino acids upstream of the conserved FGF domain, suggesting that the cleavage does not cause Bnl inactivation but rather represents the mechanism of growth factor

maturation (Results 3.2.3). The identified motif represents a minimal recognition sequence cleaved by a furin proprotein convertase. Subsequent *in silico* analysis revealed the presence of other three potential furin cleavage sites in the Bnl protein: one more site was found in the N-terminus and two in the C-terminus, surrounding the central FGF homology domain (Figure 23). Furin cleavage sites designated with numbers 2 and 3 (FS2 and FS3) are located proximally to the FGF domain and represent minimal furin recognition sequences. The other two furin consensus motives FS1 and FS4 are located distally and contain duplicated minimal sequences (Results 3.2.6).

In order to estimate the relevance of each furin cleavage site for Bnl processing, the recognition motives were sequentially mutated using the site-directed mutagenesis approach (see Results 3.2.7). This experiment revealed that FS1 and FS2 N-terminal furin motives can be utilized independently from each other for Bnl cleavage, since only the mutagenesis of both sites prevented the N-terminal Bnl processing (Figure 24B). In contrast, site-directed mutagenesis of the C-terminal furin motives revealed that the mutation of FS4 alone was able to completely protect the Bnl C-terminus from proteolysis, indicating that FS3 motif is not utilized for the growth factor processing in Kc cells or – less likely – FS3 is only used after the cleavage at the FS4 (Figure 24C).

As an alternative approach, the relevance of the identified cleavage sites for Bnl processing were analyzed on the basis of their evolutional conservation. The results of protein alignment described in the section 3.2.6, indicated that the four furin recognition sites identified in the Bnl protein are conserved in FGF homologues of other *Drosophila* species (Table 1). The alignment revealed a perfect sequence match for the FS1, FS2 and FS4 cleavage motives in all *Drosophila* Bnl homologues. However, the FS3 cleavage site showed a reduced sequence homology in the amino acids irrelevant for the cleavage and the site was not preserved in *Drosophila mojavensis.* This remarkably high degree of sequence identity of the three out of four cleavage sites suggests that the processing of *Drosophila* FGF homologues is essential for *Drosophilidae* development.

The combined results of the mutagenesis and the conservation analysis strongly indicate that Bnl is processed by a furin protease that cleaves the protein at positions FS1, FS2 and FS4. The relevance of the FS3 for the proteolytic procession of Bnl remains unclear, since the performed experiment cannot rule out if this motif is used for the Bnl cleavage *in vivo.* Alternatively, the FS4

cleavage might be a prerequisite for the effective processing at the FS3. Further experiments are required to settle these issues.

4.5 *Drosophila* Furin1 is responsible for Bnl cleavage

Three proprotein convertases (Furin1 (Dfur1), Furin2 (Dfur2) and Amontillado (Amon)) were identified in *Drosophila* (Roebroek et al., 1991; Roebroek et al., 1995; Siekhaus and Fuller, 1999). Dfur1 and Dfur2 demonstrate high homology to the human furin protease and were recently shown to be implicated in proteolytical processing of *Drosophila* TGFβ homologue Decapentaplegic (Dpp). Moreover, the two furins have differential impact on Dpp processing and are involved in modulation of different aspects of its activity (Künnapuu et al., 2009). According to the sequence similarity, *Drosophila* Amon is related to the human prohormone convertase-2 (PC2). This protease was shown to have slightly different substrate specificity than furin and is involved in neuropeptide processing in vertebrates. Amon was shown to be enriched in the embryonic nervous system and was reported to regulate larval hatching behavior (Siekhaus and Fuller, 1999). However, Amon was not detected in the lateral embryonic ectoderm where Bnl is expressed during embryogenesis (Siekhaus and Fuller, 1999). Moreover, Amon was not found in *Drosophila* Kc cells where Bnl cleavage occurs. Thus, it seems to be unlikely, that this protease would contribute to the Bnl processing.

The cell culture based experiments with RNAi-mediated silencing of the expression of either or both *Drosophila furin* (*dfur*) genes indicated, that only Dfur1 proprotein convertase is involved in the Bnl precursor cleavage (Results 3.2.5; Figure 22). This result indicates that the cleavage of Bnl is regulated differently to the described process of Dpp cleavage that requires proteolytic activities of both *Drosophila* furins (Künnapuu et al., 2009). However, it is consistent with the previous study of *dfur1* expression in *Drosophila* embryos (Roebroek et al., 1993) and with present results, showing that *dfur1* transcript is expressed in lateral embryonic ectoderm, close to Bnl secreting cells at the stage 13 of embryogenesis (Sutherland et al., 1996; Results 3.3.6). Thus, according to the experimental evidence and the available data, Bnl is proteolytically processed by Dfur1 proprotein convertase and both proteins overlap in their expression during late stages of *Drosophila* embryogenesis.

Human furin is known to catalyze the processing of various signaling proproteins in *trans*-Golgi network (TGN) (Thomas, 2002), therefore, it is likely that Bnl cleavage also occurs in this compartment. The co-secretion of all Bnl cleavage products to the supernatant may happen due to non-covalent attachment of the cleaved off domains to the central portion of the Bnl protein, as it known for mammalian Notch receptor (Kidd and Lieber, 2002). Alternatively, the processed N- and C-terminal parts may be individually secreted. Although these domains demonstrate no sequence similarity with known proteins (Sutherland et al., 1996), the performed experiments could not exclude that they carry individual biological functions not connected with the FGF signaling in *Drosophila*.

Furthermore, similar to the human furin, Dfur1 also demonstrates dynamic subcellular localization and can be detected in the Golgi as well as on the cellular surface (De Bie et al., 1995). This raises the possibility that the Bnl protein may be cleaved inside the secretory granules. This would explain the appearance of the full length Bnl protein and both cleaved N- and C-terminal domains in conditioned medium (Figure 13).

Taken together, the described experiments strongly indicate that Bnl undergoes proteolytic processing in the late secretory pathway by Dfur1 protease. Further experiments are required to precisely identify the subcellular position of Bnl cleavage and the way of secretion of the cleavage products.

4.6 *In vivo* relevance of Bnl protein processing: a gain-of-function study

In order to investigate whether the proteolytic cleavage affects Bnl biological function, several cell culture and *in vivo* experiments were performed. The receptor-ligand binding assay described in section 3.3.1 showed that the non-cleavable Bnl precursor is efficiently secreted from the cells and is able to specifically interact with the cell surface receptor Btl (Figure 26). This indicates that the extended N- and C-terminal domains of the Bnl precursor do not prevent the formation of a receptor-ligand complex. However, it cannot be excluded that the kinetics and strength of this interaction would differ from that of the processed Bnl protein.

Bnl is known to function as a chemoattractant for the embryonic trachea and is able to provide the directional growth of developing tracheal branches (Sutherland et al., 1996; Wolf and Shuh, 2000; Kadam et al., 2009). Therefore,

Bnl activity can be estimated *in vivo* by misguidance of tracheal branches in response to ectopically expressed Bnl. The results shown in section 3.3.2 indicate that Bnl protein variants, in which the N-terminal or all four furin cleavage sites were mutated, failed to guide growing tracheal branches when expressed in the ectoderm. In contrast, expression of the cleavable Bnl protein at the same location induced the misrouting of the embryonic tracheal branches (Figure 27E). This experiment shows that the proper Bnl processing is critical for its biological activity. However, since Bnl has to travel several cell diameters to reach Btl receptor expressed in the tracheal cells, it is not clear from this experimental design, if cleavage affects the motility of Bnl or it influences its activity as a ligand.

The fact that the N-terminally non-cleavable Bnl variant demonstrates lack of biological activity similar to the completely uncleavable Bnl precursor could be explained in two ways. First, the C-terminal cleavage might be less important for the Bnl activation compared to the N-terminal processing. This hypothesis is consistent with the earlier observation that Bnl C-terminal cleavage in cell culture is generally less efficient than its N-terminal processing. Second, the N-terminal cleavage event may play a permissive role for the subsequent C-terminal processing of Bnl protein *in vivo*. Further experiments are needed to investigate these possibilities.

To directly analyze the ability of the non-cleavable Bnl to activate the receptor, it was directly co-expressed with Btl within the tracheal cells. In this experimental approach, the uncleavable Bnl precursor was observed to induce a dominant negative (DN) effect and introduced a phenotype similar to the *bnl* loss-of-function (LOF) phenotype (Sutherland et al., 1996; Results 3.3.2, Figure 27H). Thus, although the uncleavable Bnl is able to bind the Btl receptor, it cannot induce the receptor activation and provide downstream FGF signaling. Also, the uncleavable precursor occupies the receptor thereby blocking the binding of the endogenous active Bnl ligands and results in a DN effect. The described DN property of the uncleavable Bnl ligand is very similar to that reported for a platelet derived growth factor A (PDGF-A). Its non-cleavable form ARKA^{86} was shown to be effectively secreted from the cells and has been shown to have a dominant negative effect with respect to tumor induction *in vivo* (Siegfried et al., 2003). Moreover, the fact that the ectodermal expression of the uncleavable Bnl variant does not induce the DN phenotype (Figure 27D) indirectly indicates that the N- and C-terminal domains impede the extracellular transport of the Bnl ligand. However, further experimental work is required to confirm this hypothesis.

Furthermore, the ectopic expression experiment using the cleaved central domain alone (Results 3.3.4) revealed that the released Bnl FGF domain is secreted, can move towards tracheal cells and activate the Btl receptor resulting in ectopic tracheal guidance (see Figure 29). This experiment shows that the FGF central domain is the only biologically active part of Bnl.

There are only very few reports about proteolytic regulation of fibroblast growth factor activity. It was shown previously, that the processed FGF3 from *Xenopus laevis* demonstrates several folds higher affinity towards its receptor isoforms FGFR2 (IIIb) and FGFR2 (IIIc) compared to its precursor (Kiefer et al., 1993; Antoine et al., 2000). Furthermore, cleavage products of mouse FGF4 demonstrate 5 times higher affinity towards heparin than the precursor protein. (Bellosta et al., 1993). In contrast, proteolytic cleavage of human FGF23 was recently described to contribute to protein inactivation (Shimada et al., 2001). These observations indicate that proteolytic regulation is not conventional for the members of the FGF family and may cause activation as well as inactivation of the FGF ligands.

Similar to the proteolytically activated vertebrate FGF3 and FGF4, Bnl proteolytic processing induces the release of the functional FGF domain and therefore provides Bnl with the ability to induce receptor activation. The results obtained in this work are in accordance with a model that Bnl cleavage is neither required for its secretion from the cells nor for its binding to the receptor. However, Bnl processing is essential for the induction of its ability to activate the Btl receptor in tracheal cells. The extended N- and C-terminal regions of the Bnl proprotein may cause spatial disturbances that hinder receptor dimerization and thereby prevent downstream signaling cascade. Moreover, since the truncated Bnl FGF domain is fully active, the cleaved N- and C-terminal regions are not required for the Bnl ligand function.

4.7 *In vivo* relevance of Bnl protein processing: a loss-of-function study

Since the promotor region of the Bnl protein is not yet characterized, it is impossible to test if the truncated central FGF domain alone would be sufficient to rescue the mutant *bnl* phenotype and if the uncleavable variant would be inactive. To circumvent this technical problem the cleavage of the endogenous Bnl was inhibited by the tissue-specific expression of the subtilisin-like proprotein convertase (SPC) inhibitor α1-PDX (Benjannet et al., 1997). Interference with the endogenous furin activity in the ectodermal cells that express Bnl results in *bnl*

loss-of-function (LOF) phenotype (Results 3.3.5, Figure 30). Furthermore, the expression of the furin inhibitor in the tracheal cells, where the endogenous Bnl protein is not expressed, had no effect (Figure 30C), showing that the Bnl precursor is cleaved only in the secreting cells. These results further confirm the relevance of Bnl processing for its *in vivo* function.

Nevertheless, it is necessary to take into consideration that the utilized furin inhibitor is active against a broad spectrum of subtilisin-like proteases. Moreover, *Drosophila* Dpp was shown to participate in tracheal morphogenesis and it also requires proteolytic activation by furins (Steneberg et al., 1999; Myat et al., 2005; Künnapuu et al., 2009). Therefore, it is necessary to prove that the observed *bnl* phenotype is only induced by loss of specific Bnl processing by furin. As already discussed, Dfur1 protease is responsible for Bnl proteolytic processing (Results 3.2.5 and Discussion 4.5). Therefore it was investigated, if *dfur1* activity is required for proper tracheal development. According to the experiment described in section 3.3.7, embryos lacking *dfur1* expression show a phenotype similar to *bnl* LOF phenotype (Figure 32). Thus, both the inhibition of furin function in general using the α1-PDX inhibitor and the specific reduction of *dfur1* activity results in the same phenotype. Moreover, the genetic interaction experiment described in section 3.3.8 showed that concurrent 50% reduction of *bnl* and *dfur1* gene dose results in a clear *bnl* loss-of-function phenotype (Figure 33). These data suggest that the *in vivo* activities of *bnl* and *dfur1* genes functionally belong to the same regulation circuit and that the observed tracheal system phenotype in *dfur1* mutants is caused by the inhibition of Bnl proteolytic processing.

Taken together, the combined cell culture and *in vivo* results show that the Bnl protein is proteolytically processed by Dfur1 protease in the secretory pathway of producing cells and that this cleavage is essential for the ligand activation. Moreover, only the released central FGF domain of Bnl is able to activate the Btl receptor *in vivo*, which is a prerequisite for the correct development of *Drosophila* tracheal system.

4.8 Relevance of Bnl processing for vertebrate study

The *in silico* analysis of Bnl homologues from several vertebrate species including human FGF10 revealed the conserved furin recognition site in the N-terminal region of these growth factors (Figure 34A). Subsequent experiments have confirmed that the identified consensus motif of hFGF10 is cleaved in

Drosophila cell culture by a protease of the SPC family of proteolytic enzymes (Results 3.4, Figure 34C). FGF10 is known to function during development of vertebrate lung and, similar to Bnl, provides directional cues for migration of respiratory epithelium. Further experimental work is needed to precisely identify the protease responsible for the FGF10 cleavage and assess whether the observed proteolytic processing occurs in mammalian cells as well. It is also to be explored, if and how the cleavage influences FGF10 biological activity during lung development. From an evolutionary point of view, the proteolytic regulation of protein activity was not preserved for most vertebrate FGFs and was probably compensated by gene duplication and subsequent functional divergence of vertebrate FGF proteins. However, this mechanism was successfully employed for the activation of other signaling molecules in vertebrates (VEGF, PDGF and others) (Stacker et al., 1999; Siegfried et al., 2003). However, the experimental data described in this thesis suggest that the observed proteolytic processing of *Drosophila* FGF Bnl is preserved in course of evolution and may be involved in regulation of FGF10 function during lung development in vertebrates.

4.9 Possible implications of Bnl post-translational regulation in *Drosophila*

According to current data, Bnl undergoes proteolytic processing releasing its central functional domain, which is required and sufficient for Btl receptor activation. Interestingly, *Drosophila* FGF ligands are the only members of the FGF family known up to date that have such long protein sequences. Although it is not clear, whether the activities of the other two *Drosophila* FGFs, Pyr and Ths, are regulated by proteolytic cleavage, the data presented here strongly indicate that Bnl requires proteolytic processing for its activation. This observation suggests that the processing serves as an additional mechanism of FGF activity regulation in *Drosophila*.

Drosophila Bnl demonstrates a highly dynamic expression pattern during embryonic development that relies on complex transcriptional regulation (Merabet et al., 2005). Oriented migration of the tracheal cells requires a precise temporal pattern of Bnl expression. However, *de novo* protein synthesis takes time and is not helpful in case of the urgent need of the ligand. Therefore, the reported Bnl processing may represent a fast reacting mechanism of Bnl activation during tracheal morphogenesis. This would imply that Bnl precursors or partially processed forms have to be stored in the producing cells until the active ligands are needed. In case of demand, the proteins can be immediately activated and

quickly exported from the cells. Moreover, partial processing of the precursors may contribute to protein stability during the storage.

Alternatively, proteolytic processing may serve as an additional control of ligand quality before the secretion. If the newly synthesized Bnl molecule carries non-tolerable amino acid substitutions or folding problems, it will not be proteolytically processed and will be secreted as an inactive precursor. However, this situation implies that the uncleaved Bnl precursor has to demonstrate the impaired extracellular motility and cannot effectively compete with mature Bnl ligands for the receptor binding.

Furthermore, since the Bnl protein contains four potential furin cleavage motives, partial proteolytic processing of these sites by Dfur1 may generate Bnl isoforms of different length with differential biological activities. Some of vertebrate FGF ligands were described to exist as several isoforms with different length and subcellular localizations, which expands the diversity of the available effector molecules (Acland et al., 1990; Kiefer et al., 1994). Currently, little is known about FGF signaling in insects. In contrast to the variety of vertebrate FGFs, there are only three FGF homologues in *Drosophila melanogaster*. They were implicated in a limited number of biological functions, mainly during embryonic development, and were not shown to have structurally or functionally different isoforms (Gryzik et al., 2004; Stathopoulos et al., 2004; Klingseisen et al., 2009; Kadam et al., 2009). Based on the vertebrate studies and on the data from this work, the phenomenon of proteolytic Bnl processing may represent a mechanism for generation of diverse FGF ligands from a single *bnl* gene. According to this assumption, differential proteolytic processing of Bnl furin sites may be regulated by different tissue- or cell-specific post-translational modification and thus provide differential Bnl function at later stages of tracheal development (see Introduction 1.4.2.2). Further study is required to experimentally explore all these hypotheses.

SUMMARY

The present thesis reports about proteolytic processing of a *Drosophila* fibroblast growth factor (FGF) homolog Branchless (Bnl). This secreted protein is essential for the development of embryonic and larval tracheal system. Bnl is shown to directly interact with a receptor tyrosine kinase Breathless (Btl) that is localized on the surface of tracheal cells. Extracellular Bnl functions as a chemoattractant for the growing tracheal branches. It directs migration of the tracheal cells and provides a stereotyped branching pattern for the newly forming respiratory network. Furthermore, Bnl-mediated signaling is required for specific upregulation of branch-dependent genes and formation of terminal branches. Animals deficient for Bnl activity do not develop a normal tracheal system and eventually die during early larval stages. Despite high percent of amino acid homology between Bnl and vertebrate FGFs, there is a remarkable difference in molecular masses of the insect and vertebrate proteins. *Drosophila* Bnl is approximately three times larger than all known vertebrate FGFs.

Experiments of this study show that the Bnl protein is initially synthesized as a larger precursor and is proteolytically cleaved in secreting cells. This processing occurs in the secretory pathway of a cell and liberates the biologically active central FGF homology domain of Bnl whose molecular mass is comparable with that known for vertebrate FGFs. Based on *in silico* analysis and cell culture experiments, *Drosophila* Furin1 was identified as a protease required for Bnl intracellular cleavage. Four furin recognition motives were identified in the Bnl protein. Site-directed mutagenesis of the cleavage sites indicated that only three of them are actually utilized for Bnl processing in cell culture. Furthermore, combination of cell culture based approach and *in vivo* analysis showed that though an uncleavable variant of the Bnl protein is secreted and specifically interacts with the Btl receptor, it is unable to activate downstream signaling cascade and induce directional migration of tracheal cells. Moreover, the uncleavable Bnl functions as a dominant negative ligand when expressed in the target tissue. It was also shown that the Bnl FGF domain alone is sufficient to provide valid FGF signaling *in vivo*. Subsequent genetic experiments revealed the functional connection between *bnl* and *dfur1* genes, indicating that the processing of endogenous Bnl by Dfur1 is essential for proper tracheal development in *Drosophila*.

Furthermore, according to the obtained data, the functional homologue of *Drosophila* Bnl, human FGF10, is proteolytically processed by a furin-related protease in *Drosophila* cells, suggesting that Bnl/FGF10 proteolytic cleavage may represent an evolutionary conserved mechanism of the FGF signaling regulation during morphogenesis of respiratory system.

Taken together, the experimental evidence from this study suggests a novel post-translational mechanism of FGF activity regulation by the furin protease during tracheal system development in *Drosophila melanogaster*. Moreover, it opens the possibility that similar proteolytic regulation of FGF function is employed in respiratory system development of higher organisms.

REFERENCES

Abrahamsen, H. & Stenmark, H. Protein secretion: unconventional exit by exophagy. *Curr. Biol* **20**, R415-418 (2010).

Abramoff, M.D., Magelhaes, P.J., Ram, S.J. "Image Processing with ImageJ". *Biophotonics International* **11**, 36-42 (2004).

Acland, P., Dixon, M., Peters, G. & Dickson, C. Subcellular fate of the int-2 oncoprotein is determined by choice of initiation codon. *Nature* **343**, 662-665 (1990).

Affolter, M. & Caussinus, E. Tracheal branching morphogenesis in *Drosophila*: new insights into cell behaviour and organ architecture. *Development* **135**, 2055-2064 (2008).

Affolter, M., Nellen, D., Nussbaumer, U. & Basler, K. Multiple requirements for the receptor serine/threonine kinase thick veins reveal novel functions of TGF beta homologs during *Drosophila* embryogenesis. *Development* **120**, 3105-3117 (1994).

Alberts, B., Johnson, A., Lewis, J. & Walter, P. Molecular biology of the cell, 4th edition. *GarlandScience,* 1616 (2002).

Altschul, S.F. et al. Gapped BLAST and PSI-BLAST: a new generation of protein database search programs. *Nucleic Acids Res* **25**, 3389-3402 (1997).

Anderson, E.D., VanSlyke, J.K., Thulin, C.D., Jean, F. & Thomas, G. Activation of the furin endoprotease is a multiple-step process: requirements for acidification and internal propeptide cleavage. *EMBO J* **16**, 1508-1518 (1997).

Antoine, M. et al. NH2-Terminal Cleavage of *Xenopus* Fibroblast Growth Factor 3 Is Necessary for Optimal Biological Activity and Receptor Binding. *Cell Growth Differ* **11**, 593-605 (2000).

Asada, M. et al. Characterization of fibroblast growth factor-6 expressed by Chinese hamster ovary cells as a glycosylated mitogen for human vascular endothelial cells. *Growth Factors* **16**, 293-303 (1999).

Auguste, P., Javerzat, S. & Bikfalvi, A. Regulation of vascular development by fibroblast growth factors. *Cell Tissue Res* **314**, 157-166 (2003).

Baer, M.M. et al. The role of apoptosis in shaping the tracheal system in the *Drosophila* embryo. *Mech. Dev* **127**, 28-35 (2010).

Bassi, D.E. et al. Furin inhibition results in absent or decreased invasiveness and tumorigenicity of human cancer cells. *Proc. Natl. Acad. Sci. U.S.A* **98**, 10326-10331 (2001).

Bates, B., Hardin, J., Zhan, X., Drickamer, K. & Goldfarb, M. Biosynthesis of human fibroblast growth factor-5. *Mol. Cell. Biol* **11**, 1840-1845 (1991).

Battersby, A., Csiszár, A., Leptin, M. & Wilson, R. Isolation of proteins that interact with the signal transduction molecule Dof and identification of a functional domain

conserved between Dof and vertebrate BCAP. *J. Mol. Biol* **329**, 479-493 (2003).

Belenkaya, T.Y. et al. *Drosophila* Dpp morphogen movement is independent of dynamin-mediated endocytosis but regulated by the glypican members of heparan sulfate proteoglycans. *Cell* **119**, 231-244 (2004).

Bellaiche, Y., The, I. & Perrimon, N. Tout-velu is a *Drosophila* homologue of the putative tumour suppressor EXT-1 and is needed for Hh diffusion. *Nature* **394**, 85-88 (1998).

Bellosta, P., Talarico, D., Rogers, D. & Basilico, C. Cleavage of K-FGF produces a truncated molecule with increased biological activity and receptor binding affinity. *J. Cell Biol* **121**, 705-713 (1993).

Benet-Pagès, A. et al. FGF23 is processed by proprotein convertases but not by PHEX. *Bone* **35**, 455-462 (2004).

Benjannet, S. et al. α1-Antitrypsin Portland Inhibits Processing of Precursors Mediated by Proprotein Convertases Primarily within the Constitutive Secretory Pathway. *Journal of Biological Chemistry* **272**, 26210-26218 (1997).

Bergwitz, C. et al. Defective O-glycosylation due to a novel homozygous S129P mutation is associated with lack of fibroblast growth factor 23 secretion and tumoral calcinosis. *J. Clin. Endocrinol. Metab* **94**, 4267-4274 (2009).

Bischof, J., Maeda, R.K., Hediger, M., Karch, F. & Basler, K. An optimized transgenesis system for *Drosophila* using germ-line-specific phiC31 integrases. *Proc. Natl. Acad. Sci. U.S.A* **104**, 3312-3317 (2007).

Boddey, J.A. et al. An aspartyl protease directs malaria effector proteins to the host cell. *Nature* **463**, 627-631 (2010).

Boilly, B., Vercoutter-Edouart, A.S., Hondermarck, H., Nurcombe, V. & Le Bourhis, X. FGF signals for cell proliferation and migration through different pathways. *Cytokine Growth Factor Rev* **11**, 295-302 (2000).

Botella, J.A. et al. Deregulation of the Egfr/Ras signaling pathway induces age-related brain degeneration in the *Drosophila* mutant vap. *Mol. Biol. Cell* **14**, 241-250 (2003).

Böttcher, R.T. & Niehrs, C. Fibroblast growth factor signaling during early vertebrate development. *Endocr. Rev* **26**, 63-77 (2005).

Boube, M., Llimargas, M. & Casanova, J. Cross-regulatory interactions among tracheal genes support a co-operative model for the induction of tracheal fates in the *Drosophila* embryo. *Mech. Dev* **91**, 271-278 (2000).

Brand, A.H. & Perrimon, N. Targeted gene expression as a means of altering cell fates and generating dominant phenotypes. *Development* **118**, 401-415 (1993).

Bresnahan, P.A. et al. Human fur gene encodes a yeast KEX2-like endoprotease that cleaves pro-beta-NGF in vivo. *J. Cell Biol* **111**, 2851-2859 (1990).

Brodu, V. & Casanova, J. The RhoGAP crossveinless-c links trachealess and EGFR

signaling to cell shape remodeling in *Drosophila* tracheal invagination. *Genes Dev* **20**, 1817-1828 (2006).

Bush, G. et al. Ligand-induced signaling in the absence of furin processing of Notch1. *Dev. Biol* **229**, 494-502 (2001).

Cabernard, C., Neumann, M. & Affolter, M. Cellular and molecular mechanisms involved in branching morphogenesis of the *Drosophila* tracheal system. *J. Appl. Physiol* **97**, 2347-2353 (2004).

Cela, C. & Llimargas, M. Egfr is essential for maintaining epithelial integrity during tracheal remodelling in *Drosophila*. *Development* **133**, 3115-3125 (2006).

Chanut-Delalande, H. et al. A genetic mosaic analysis with a repressible cell marker screen to identify genes involved in tracheal cell migration during *Drosophila* air sac morphogenesis. *Genetics* **176**, 2177-2187 (2007).

Chen, C.K. et al. The transcription factors KNIRPS and KNIRPS RELATED control cell migration and branch morphogenesis during *Drosophila* tracheal development. *Development* **125**, 4959-4968 (1998).

Chihara, T. & Hayashi, S. Control of tracheal tubulogenesis by Wingless signaling. *Development* **127**, 4433-4442 (2000).

Christofori, G. Split personalities: the agonistic antagonist Sprouty. *Nat. Cell Biol* **5**, 377-379 (2003).

Coulier, F. et al. The FGF6 gene within the FGF multigene family. *Ann. N. Y. Acad. Sci* **638**, 53-61 (1991).

Crump, C.M. et al. PACS-1 binding to adaptors is required for acidic cluster motif-mediated protein traffic. *EMBO J* **20**, 2191-2201 (2001).

Csiszar, A., Vogelsang, E., Beug, H. & Leptin, M. A novel conserved phosphotyrosine motif in the *Drosophila* fibroblast growth factor signaling adaptor Dof with a redundant role in signal transmission. *Mol. Cell. Biol* **30**, 2017-2027 (2010).

Cui, Y. et al. The activity and signaling range of mature BMP-4 is regulated by sequential cleavage at two sites within the prodomain of the precursor. *Genes Dev* **15**, 2797-2802 (2001).

De Bie, I. et al. Processing specificity and biosynthesis of the *Drosophila* melanogaster convertases dfurin1, dfurin1-CRR, dfurin1-X, and dfurin2. *J. Biol. Chem* **270**, 1020-1028 (1995).

de Maximy, A.A. et al. Cloning and expression pattern of a mouse homologue of drosophila sprouty in the mouse embryo. *Mech. Dev* **81**, 213-216 (1999).

Dreyfuss, J.L. et al. Heparan sulfate proteoglycans: structure, protein interactions and cell signaling. *An. Acad. Bras. Cienc* **81**, 409-429 (2009).

Dubois, C.M., Laprise, M.H., Blanchette, F., Gentry, L.E. & Leduc, R. Processing of transforming growth factor beta 1 precursor by human furin convertase. *J. Biol. Chem*

270, 10618-10624 (1995).

Echalier, G. & Ohanessian, A. In vitro culture of Drosophila melanogaster embryonic cells. *In Vitro* **6**, 162-172 (1970).

Emanuelsson, O., Brunak, S., von Heijne, G. & Nielsen, H. Locating proteins in the cell using TargetP, SignalP and related tools. *Nat. Protocols* **2**, 953-971 (2007).

Englund, C., Steneberg, P., Falileeva, L., Xylourgidis, N. & Samakovlis, C. Attractive and repulsive functions of Slit are mediated by different receptors in the *Drosophila* trachea. *Development* **129**, 4941-4951 (2002).

Eriksson, A.E., Cousens, L.S., Weaver, L.H. & Matthews, B.W. Three-dimensional structure of human basic fibroblast growth factor. *Proc. Natl. Acad. Sci. U.S.A* **88**, 3441-3445 (1991).

Eswarakumar, V.P., Lax, I. & Schlessinger, J. Cellular signaling by fibroblast growth factor receptors. *Cytokine Growth Factor Rev* **16**, 139-149 (2005).

Freeman, S.D. et al. Extracellular regulation of developmental cell signaling by XtSulf1. *Developmental Biology* **320**, 436-445 (2008).

Fromme, J.C., Orci, L. & Schekman, R. Coordination of COPII vesicle trafficking by Sec23. *Trends Cell Biol* **18**, 330-336 (2008).

Fukumoto, S. Physiological regulation and disorders of phosphate metabolism-pivotal role of fibroblast growth factor 23. *Intern. Med* **47**, 337-343 (2008).

Gallet, A., Staccini-Lavenant, L. & Thérond, P.P. Cellular Trafficking of the glypican Dally-like is required for full-strength Hedgehog signaling and Wingless transcytosis. *Developmental Cell* **14**, 712-725 (2008).

García-García, M.J. & Anderson, K.V. Essential role of glycosaminoglycans in Fgf signaling during mouse gastrulation. *Cell* **114**, 727-737 (2003).

Gilbert S. F., Developmental biology, 8th edition. *Sinauer Associates Inc.,* 785 p. (2006).

Gisselbrecht, S., Skeath, J.B., Doe, C.Q. & Michelson, A.M. heartless encodes a fibroblast growth factor receptor (DFR1/DFGF-R2) involved in the directional migration of early mesodermal cells in the *Drosophila* embryo. *Genes Dev* **10**, 3003-3017 (1996).

Glazer, L. & Shilo, B.Z. The *Drosophila* FGF-R homolog is expressed in the embryonic tracheal system and appears to be required for directed tracheal cell extension. *Genes Dev* **5**, 697-705 (1991).

Gospodarowicz, D. Purification of a fibroblast growth factor from bovine pituitary. *Journal of Biological Chemistry* **250**, 2515-2520 (1975).

Gryzik, T. & Müller, H.J. FGF8-like1 and FGF8-like2 encode putative ligands of the FGF receptor Htl and are required for mesoderm migration in the *Drosophila* gastrula. *Curr. Biol* **14**, 659-667 (2004).

Guillemin, K. et al. The pruned gene encodes the *Drosophila* serum response factor and regulates cytoplasmic outgrowth during terminal branching of the tracheal system. *Development* **122**, 1353-1362 (1996).

Gupta, R., Jung, E. & Brunak, S. Prediction of N-glycosylation sites in human proteins. *In preparation*, (2004).

Gutiérrez, J. & Brandan, E. A novel mechanism of sequestering fibroblast growth factor 2 by glypican in lipid rafts, allowing skeletal muscle differentiation. *Mol. Cell. Biol* **30**, 1634-1649 (2010).

Hacker, U., Nybakken, K. & Perrimon, N. Heparan sulphate proteoglycans: the sweet side of development. *Nat Rev Mol Cell Biol* **6**, 530-541 (2005).

Hacohen, N., Kramer, S., Sutherland, D., Hiromi, Y. & Krasnow, M.A. sprouty encodes a novel antagonist of FGF signaling that patterns apical branching of the *Drosophila* airways. *Cell* **92**, 253-263 (1998).

Han, C., Yan, D., Belenkaya, T.Y. & Lin, X. *Drosophila* glypicans Dally and Dally-like shape the extracellular Wingless morphogen gradient in the wing disc. *Development* **132**, 667-679 (2005).

Hanson, S.R. et al. The core trisaccharide of an N-linked glycoprotein intrinsically accelerates folding and enhances stability. *Proceedings of the National Academy of Sciences* **106**, 3131-3136 (2009).

Hardingham, T.E. & Fosang, A.J. Proteoglycans: many forms and many functions. *FASEB J* **6**, 861-870 (1992).

Hart, K.C. et al. Transformation and Stat activation by derivatives of FGFR1, FGFR3, and FGFR4. *Oncogene* **19**, 3309-3320 (2000).

Hayflick, J.S., Wolfgang, W.J., Forte, M.A. & Thomas, G. A unique Kex2-like endoprotease from *Drosophila* melanogaster is expressed in the central nervous system during early embryogenesis. *J. Neurosci* **12**, 705-717 (1992).

Helenius, A. & Aebi, M. Roles of N-linked glycans in the endoplasmic reticulum. *Annu. Rev. Biochem.* **73**, 1019-1049 (2004).

Holyoak, T., Kettner, C.A., Petsko, G.A., Fuller, R.S. & Ringe, D. Structural basis for differences in substrate selectivity in Kex2 and furin protein convertases. *Biochemistry* **43**, 2412-2421 (2004).

Hsu, Y.R. et al. Human keratinocyte growth factor recombinantly expressed in Chinese hamster ovary cells: isolation of isoforms and characterization of post-translational modifications. *Protein Expr. Purif* **12**, 189-200 (1998).

Huang, P. & Stern, M.J. FGF signaling in flies and worms: more and more relevant to vertebrate biology. *Cytokine Growth Factor Rev* **16**, 151-158 (2005).

Ikeya, T. & Hayashi, S. Interplay of Notch and FGF signaling restricts cell fate and MAPK activation in the *Drosophila* trachea. *Development* **126**, 4455-4463 (1999).

Imam, F., Sutherland, D., Huang, W. & Krasnow, M.A. stumps, a *Drosophila* Gene Required for Fibroblast Growth Factor (FGF)-directed Migrations of Tracheal and Mesodermal Cells. *Genetics* **152**, 307-318 (1999).

Inoue, H., Nojima, H. & Okayama, H. High efficiency transformation of *Escherichia coli* with plasmids. *Gene* **96**, 23-28 (1990).

Isacson, O., Seo, H., Lin, L., Albeck, D. & Granholm, A.C. Alzheimer's disease and Down's syndrome: roles of APP, trophic factors and ACh. *Trends Neurosci* **25**, 79-84 (2002).

Itoh, N. & Ornitz, D.M. Evolution of the Fgf and Fgfr gene families. *Trends Genet* **20**, 563-569 (2004).

Itoh, N. & Ornitz, D.M. Functional evolutionary history of the mouse Fgf gene family. *Dev. Dyn* **237**, 18-27 (2008).

Jarecki, J., Johnson, E. & Krasnow, M.A. Oxygen regulation of airway branching in *Drosophila* is mediated by *branchless* FGF. *Cell* **99**, 211-220 (1999).

Jarvis, L.A., Toering, S.J., Simon, M.A., Krasnow, M.A. & Smith-Bolton, R.K. Sprouty proteins are in vivo targets of Corkscrew/SHP-2 tyrosine phosphatases. *Development* **133**, 1133-1142 (2006).

Jean, F., Stella, K., Thomas, L., Liu, G., Xiang, Y., Reason, A.J.& Thomas G. alpha1-Antitrypsin Portland, a bioengineered serpin highly selective for furin: application as an antipathogenic agent. *Proc. Natl. Acad. Sci. U.S.A* **95**, 7293-7298 (1998)

Kadam, S., McMahon, A., Tzou, P. & Stathopoulos, A. FGF ligands in *Drosophila* have distinct activities required to support cell migration and differentiation. *Development* **136**, 739-747 (2009).

Kidd, S. & Lieber, T. Furin cleavage is not a requirement for *Drosophila* Notch function. *Mech. Dev* **115**, 41-51 (2002).

Kiefer, P., Mathieu, M., Close, M.J., Peters, G. & Dickson, C. FGF3 from *Xenopus laevis*. *EMBO J* **12**, 4159-4168 (1993).

Kiefer, P., Acland, P., Pappin, D., Peters, G. & Dickson, C. Competition between nuclear localization and secretory signals determines the subcellular fate of a single CUG-initiated form of FGF3. *EMBO J* **13**, 4126-4136 (1994).

Kim, H.J. & Bar-Sagi, D. Modulation of signalling by Sprouty: a developing story. *Nat Rev Mol Cell Biol* **5**, 441-450 (2004).

Klämbt, C. The *Drosophila* gene pointed encodes two ETS-like proteins which are involved in the development of the midline glial cells. *Development* **117**, 163-176 (1993).

Klämbt, C., Glazer, L. & Shilo, B.Z. breathless, a *Drosophila* FGF receptor homolog, is essential for migration of tracheal and specific midline glial cells. *Genes Dev* **6**, 1668-1678 (1992).

Klimpel, K.R., Molloy, S.S., Thomas, G. & Leppla, S.H. Anthrax toxin protective antigen is activated by a cell surface protease with the sequence specificity and catalytic properties of furin. *Proc. Natl. Acad. Sci. U.S.A* **89**, 10277-10281 (1992).

Klingseisen, A., Clark, I.B.N., Gryzik, T. & Müller, H.J. Differential and overlapping functions of two closely related *Drosophila* FGF8-like growth factors in mesoderm development. *Development* **136**, 2393-2402 (2009).

Korc, M. & Friesel, R.E. The role of fibroblast growth factors in tumor growth. *Curr Cancer Drug Targets* **9**, 639-651 (2009).

Kosaka, N., Sakamoto, H., Terada, M. & Ochiya, T. Pleiotropic function of FGF-4: Its role in development and stem cells. *Developmental Dynamics* **238**, 265-276 (2009).

Kouhara, H. et al. A lipid-anchored Grb2-binding protein that links FGF-receptor activation to the Ras/MAPK signaling pathway. *Cell* **89**, 693-702 (1997).

Krysan, D.J., Rockwell, N.C. & Fuller, R.S. Quantitative characterization of furin specificity. Energetics of substrate discrimination using an internally consistent set of hexapeptidyl methylcoumarinamides. *J. Biol. Chem* **274**, 23229-23234 (1999).

Kühnlein, R.P. & Schuh, R. Dual function of the region-specific homeotic gene spalt during *Drosophila* tracheal system development. *Development* **122**, 2215-2223 (1996).

Kühnlein, R.P. et al. spalt encodes an evolutionarily conserved zinc finger protein of novel structure which provides homeotic gene function in the head and tail region of the *Drosophila* embryo. *EMBO J* **13**, 168-179 (1994).

Künnapuu, J., Björkgren, I. & Shimmi, O. The *Drosophila* DPP signal is produced by cleavage of its proprotein at evolutionary diversified furin-recognition sites. *Proc. Natl. Acad. Sci. U.S.A* **106**, 8501-8506 (2009).

Laemmli, U.K. Cleavage of structural proteins during the assembly of the head of bacteriophage T4. *Nature* **227**, 680-685 (1970).

Lederkremer, G.Z. Glycoprotein folding, quality control and ER-associated degradation. *Curr. Opin. Struct. Biol* **19**, 515-523 (2009).

Lee, J.R., Urban, S., Garvey, C.F. & Freeman, M. Regulated intracellular ligand transport and proteolysis control EGF signal activation in *Drosophila*. *Cell* **107**, 161-171 (2001).

Lee, R., Kermani, P., Teng, K.K. & Hempstead, B.L. Regulation of cell survival by secreted proneurotrophins. *Science* **294**, 1945-1948 (2001).

Leibowitz, M.J. & Wickner, R.B. A chromosomal gene required for killer plasmid expression, mating, and spore maturation in *Saccharomyces cerevisiae*. *Proc. Natl. Acad. Sci. U.S.A* **73**, 2061-2065 (1976).

Leptin, M. twist and snail as positive and negative regulators during *Drosophila* mesoderm development. *Genes Dev* **5**, 1568-1576 (1991).

Leptin, M. Gastrulation in *Drosophila*: the logic and the cellular mechanisms. *EMBO J* **18**, 3187-3192 (1999).

Leptin, M. & Affolter, M. *Drosophila* gastrulation: identification of a missing link. *Curr. Biol* **14**, R480-482 (2004).

Lernmark, A. et al. Biosynthesis of insulin and glucagon: a view of the current state of the art. *Ciba Found. Symp* **41**, 7-30 (1976).

Lim, J. et al. The cysteine-rich Sprouty translocation domain targets mitogen-activated protein kinase inhibitory proteins to phosphatidylinositol 4,5-bisphosphate in plasma membranes. *Mol. Cell. Biol.* **22**, 7953-7966 (2002).

Lin, H.Y. et al. Identification of the cytoplasmic regions of fibroblast growth factor (FGF) receptor 1 which play important roles in induction of neurite outgrowth in PC12 cells by FGF-1. *Mol. Cell. Biol* **18**, 3762-3770 (1998).

Lin, X., Buff, E.M., Perrimon, N. & Michelson, A.M. Heparan sulfate proteoglycans are essential for FGF receptor signaling during *Drosophila* embryonic development. *Development* **126**, 3715-3723 (1999).

Lindner, J.R. et al. The *Drosophila* Perlecan gene trol regulates multiple signaling pathways in different developmental contexts. *BMC Dev. Biol* **7**, 121 (2007).

Liu, G. et al. Cytoskeletal protein ABP-280 directs the intracellular trafficking of furin and modulates proprotein processing in the endocytic pathway. *J. Cell Biol* **139**, 1719-1733 (1997).

Llimargas, M. The Notch pathway helps to pattern the tips of the *Drosophila* tracheal branches by selecting cell fates. *Development* **126**, 2355-2364 (1999).

Llimargas, M. Wingless and its signalling pathway have common and separable functions during tracheal development. *Development* **127**, 4407-4417 (2000).

Llimargas, M. & Casanova, J. ventral veinless, a POU domain transcription factor, regulates different transduction pathways required for tracheal branching in *Drosophila*. *Development* **124**, 3273-3281 (1997).

Llimargas, M. & Casanova, J. EGF signalling regulates cell invagination as well as cell migration during formation of tracheal system in *Drosophila*. *Dev. Genes Evol* **209**, 174-179 (1999).

Mackey, A.J., Haystead, T.A.J. & Pearson, W.R. Getting More from Less. *Molecular & Cellular Proteomics* **1**, 139-147 (2002).

Mains, R.E. et al. PACE4: a subtilisin-like endoprotease with unique properties. *Biochem J* **321**, 587-593 (1997).

Mandal, L., Dumstrei, K. & Hartenstein, V. Role of FGFR signaling in the morphogenesis of the *Drosophila* visceral musculature. *Dev. Dyn* **231**, 342-348 (2004).

Martoglio, B. & Dobberstein, B. Signal sequences: more than just greasy peptides.

Trends Cell Biol **8**, 410-415 (1998).

Mbikay, M., Sirois, F., Yao, J., Seidah, N.G. & Chrétien, M. Comparative analysis of expression of the proprotein convertases furin, PACE4, PC1 and PC2 in human lung tumours. *Br. J. Cancer* **75**, 1509-1514 (1997).

Merabet, S., Ebner, A. & Affolter, M. The *Drosophila* Extradenticle and Homothorax selector proteins control *branchless*/FGF expression in mesodermal bridge-cells. *EMBO Rep* **6**, 762-768 (2005).

Michelson, A., Gisselbrecht, S., Buff, E. & Skeath, J. Heartbroken is a specific downstream mediator of FGF receptor signalling in *Drosophila*. *Development* **125**, 4379-4389 (1998).

Mignatti, P., Morimoto, T. & Rifkin, D.B. Basic fibroblast growth factor, a protein devoid of secretory signal sequence, is released by cells via a pathway independent of the endoplasmic reticulum-Golgi complex. *J. Cell. Physiol* **151**, 81-93 (1992).

Min, H. et al. Fgf-10 is required for both limb and lung development and exhibits striking functional similarity to *Drosophila branchless*. *Genes Dev* **12**, 3156-3161 (1998).

Miyakawa, K. & Imamura, T. Secretion of FGF-16 requires an uncleaved bipartite signal sequence. *J. Biol. Chem* **278**, 35718-35724 (2003).

Miyakawa, K. et al. A hydrophobic region locating at the center of fibroblast growth factor-9 is crucial for its secretion. *J. Biol. Chem* **274**, 29352-29357 (1999).

Miyake, A. et al. Structure and expression of a novel member, FGF-16, on the fibroblast growth factor family. *Biochem. Biophys. Res. Commun* **243**, 148-152 (1998).

Mohammadi, M., Olsen, S.K. & Ibrahimi, O.A. Structural basis for fibroblast growth factor receptor activation. *Cytokine Growth Factor Rev* **16**, 107-137 (2005).

Molloy, S.S., Bresnahan, P.A., Leppla, S.H., Klimpel, K.R. & Thomas, G. Human furin is a calcium-dependent serine endoprotease that recognizes the sequence Arg-X-X-Arg and efficiently cleaves anthrax toxin protective antigen. *J. Biol. Chem* **267**, 16396-16402 (1992).

Molloy, S.S., Thomas, L., VanSlyke, J.K., Stenberg, P.E. & Thomas, G. Intracellular trafficking and activation of the furin proprotein convertase: localization to the TGN and recycling from the cell surface. *EMBO J* **13**, 18-33 (1994).

Molloy, S.S., Anderson, E.D., Jean, F. & Thomas, G. Bi-cycling the furin pathway: from TGN localization to pathogen activation and embryogenesis. *Trends Cell Biol* **9**, 28-35 (1999).

Myat, M.M., Lightfoot, H., Wang, P. & Andrew, D.J. A molecular link between FGF and Dpp signaling in branch-specific migration of the *Drosophila* trachea. *Dev. Biol* **281**, 38-52 (2005).

Nickel, W. & Rabouille, C. Mechanisms of regulated unconventional protein secretion.

Nat Rev Mol Cell Biol **10**, 148-155 (2009).

Ohmachi, S. et al. FGF-20, a novel neurotrophic factor, preferentially expressed in the substantia nigra pars compacta of rat brain. *Biochem. Biophys. Res. Commun* **277**, 355-360 (2000).

Ornitz, D.M. FGFs, heparan sulfate and FGFRs: complex interactions essential for development. *BioEssays* **22**, 108-112 (2000).

Ornitz, D.M. & Itoh, N. Fibroblast growth factors. *Genome Biol* **2**, reviews3005.1-reviews3005.12 (2001).

Panganiban, G.E., Rashka, K.E., Neitzel, M.D. & Hoffmann, F.M. Biochemical characterization of the *Drosophila* Dpp protein, a member of the Transforming growth factor beta family of growth factors. *Mol. Cell. Biol* **10**, 2669-2677 (1990).

Park, W.Y., Miranda, B., Lebeche, D., Hashimoto, G. & Cardoso, W.V. FGF-10 is a chemotactic factor for distal epithelial buds during lung development. *Dev. Biol* **201**, 125-134 (1998).

Pellegrini, L. Role of heparan sulfate in fibroblast growth factor signalling: a structural view. *Curr. Opin. Struct. Biol* **11**, 629-634 (2001).

Perkins, L.A., Larsen, I. & Perrimon, N. *corkscrew* encodes a putative protein tyrosine phosphatase that functions to transduce the terminal signal from the receptor tyrosine kinase Torso. *Cell* **70**, 225-236 (1992).

Perkins, L.A., Johnson, M.R., Melnick, M.B. & Perrimon, N. The nonreceptor protein tyrosine phosphatase corkscrew functions in multiple receptor tyrosine kinase pathways in *Drosophila*. *Dev. Biol* **180**, 63-81 (1996).

Perona, J.J. & Craik, C.S. Structural basis of substrate specificity in the serine proteases. *Protein Sci* **4**, 337-360 (1995).

Petit, V., Nussbaumer, U., Dossenbach, C. & Affolter, M. Downstream-of-FGFR is a fibroblast growth factor-specific scaffolding protein and recruits Corkscrew upon receptor activation. *Mol. Cell. Biol* **24**, 3769-3781 (2004).

Plotnikov, A.N., Hubbard, S.R., Schlessinger, J. & Mohammadi, M. Crystal structures of two FGF-FGFR complexes reveal the determinants of ligand-receptor specificity. *Cell* **101**, 413-424 (2000).

Plummer, T.H., Elder, J.H., Alexander, S., Phelan, A.W. & Tarentino, A.L. Demonstration of peptide:N-glycosidase F activity in endo-beta-N-acetylglucosaminidase F preparations. *J. Biol. Chem* **259**, 10700-10704 (1984).

Polanska, U.M., Fernig, D.G. & Kinnunen, T. Extracellular interactome of the FGF receptor-ligand system: complexities and the relative simplicity of the worm. *Dev. Dyn* **238**, 277-293 (2009).

Raabe, T. et al. Biochemical and genetic analysis of the Drk SH2/SH3 adaptor protein of *Drosophila*. *EMBO J* **14**, 2509-2518 (1995).

Raman, K. & Kuberan, B. Differential effects of Heparitinase I and Heparitinase III on endothelial tube formation in vitro. *Biochem. Biophys. Res. Commun* **398**, 191-193 (2010).

Rayburn, L.Y.M. et al. amontillado, the *Drosophila* homolog of the prohormone processing protease PC2, is required during embryogenesis and early larval development. *Genetics* **163**, 227-237 (2003).

Reichman-Fried, M., Dickson, B., Hafen, E. & Shilo, B.Z. Elucidation of the role of *breathless*, a *Drosophila* FGF receptor homolog, in tracheal cell migration. *Genes Dev* **8**, 428-439 (1994).

Revest, J.M., DeMoerlooze, L. & Dickson, C. Fibroblast growth factor 9 secretion is mediated by a non-cleaved amino-terminal signal sequence. *J. Biol. Chem* **275**, 8083-8090 (2000).

Reynaud, E.G. Navigating the secretory pathway: Conference on exocytosis membrane structure and dynamics. *EMBO Reports* **3**, 828-833 (2002).

Rhea, J.M., Wegener, C. & Bender, M. The proprotein convertase encoded by amontillado (amon) is required in *Drosophila* corpora cardiaca endocrine cells producing the glucose regulatory hormone AKH. *PLoS Genet* **6**, e1000967 (2010).

Ribatti, D., Vacca, A., Rusnati, M. & Presta, M. The discovery of basic fibroblast growth factor/fibroblast growth factor-2 and its role in haematological malignancies. *Cytokine Growth Factor Rev* **18**, 327-334 (2007).

Ribeiro, C., Ebner, A. & Affolter, M. In vivo imaging reveals different cellular functions for FGF and Dpp signaling in tracheal branching morphogenesis. *Dev. Cell* **2**, 677-683 (2002).

Ribeiro, C., Neumann, M. & Affolter, M. Genetic control of cell intercalation during tracheal morphogenesis in *Drosophila*. *Curr. Biol* **14**, 2197-2207 (2004).

Rockwell, N.C., Krysan, D.J., Komiyama, T. & Fuller, R.S. Precursor Processing by Kex2/Furin Proteases. *Chemical Reviews* **102**, 4525-4548 (2002).

Roebroek, A.J., Pauli, I.G., Zhang, Y. & van de Ven, W.J. cDNA sequence of a *Drosophila melanogaster* gene, Dfur1, encoding a protein structurally related to the subtilisin-like proprotein processing enzyme furin. *FEBS Lett* **289**, 133-137 (1991).

Roebroek, A.J. et al. Cloning and functional expression of Dfurin2, a subtilisin-like proprotein processing enzyme of *Drosophila melanogaster* with multiple repeats of a cysteine motif. *J. Biol. Chem* **267**, 17208-17215 (1992).

Roebroek, A.J., Creemers, J.W., Pauli, I.G., Bogaert, T. & Van de Ven, W.J. Generation of structural and functional diversity in furin-like proteins in *Drosophila* melanogaster by alternative splicing of the Dfur1 gene. *EMBO J* **12**, 1853-1870 (1993).

Roebroek, A.J., Ayoubi, T.A., Creemers, J.W., Pauli, I.G. & Van de Ven, W.J. The Dfur2 gene of *Drosophila melanogaster*: genetic organization, expression during embryogenesis, and pro-protein processing activity of its translational product

Dfurin2. *DNA Cell Biol* **14**, 223-234 (1995).

Samakovlis, C. et al. Development of the *Drosophila* tracheal system occurs by a series of morphologically distinct but genetically coupled branching events. *Development* **122**, 1395-1407 (1996a).

Samakovlis, C. et al. Genetic control of epithelial tube fusion during *Drosophila* tracheal development. *Development* **122**, 3531-3536 (1996b).

Sambrook, J., Fritsch, E. F., Maniatis, T. Molecular Cloning: a Laboratory Manual, 2^{d} edition. *Cold Spring Harbor Laboratory* (1989).

Sato, M. & Kornberg, T.B. FGF is an essential mitogen and chemoattractant for the air sacs of the *Drosophila* tracheal system. *Dev. Cell* **3**, 195-207 (2002).

Schägger, H. & von Jagow, G. Tricine-sodium dodecyl sulfate-polyacrylamide gel electrophoresis for the separation of proteins in the range from 1 to 100 kDa. *Anal. Biochem* **166**, 368-379 (1987).

Scholz, H., Deatrick, J., Klaes, A. & Klämbt, C. Genetic dissection of *pointed*, a *Drosophila* gene encoding two ETS-related proteins. *Genetics* **135**, 455-468 (1993).

Schumacher, S., Gryzik, T., Tannebaum, S. & Müller, H.J. The RhoGEF Pebble is required for cell shape changes during cell migration triggered by the *Drosophila* FGF receptor Heartless. *Development* **131**, 2631-2640 (2004).

Shimada, T. et al. Mutant FGF-23 responsible for autosomal dominant hypophosphatemic rickets is resistant to proteolytic cleavage and causes hypophosphatemia in vivo. *Endocrinology* **143**, 3179-3182 (2002).

Shishido, E., Ono, N., Kojima, T. & Saigo, K. Requirements of DFR1/Heartless, a mesoderm-specific *Drosophila* FGF-receptor, for the formation of heart, visceral and somatic muscles, and ensheathing of longitudinal axon tracts in CNS. *Development* **124**, 2119-2128 (1997).

Siegfried, G., Khatib, A., Benjannet, S., Chrétien, M. & Seidah, N.G. The Proteolytic Processing of Pro-Platelet-derived Growth Factor-A at RRKR86 by Members of the Proprotein Convertase Family Is Functionally Correlated to Platelet-derived Growth Factor-A-induced Functions and Tumorigenicity. *Cancer Research* **63**, 1458-1463 (2003).

Siekhaus, D.E. & Fuller, R.S. A role for amontillado, the *Drosophila* homolog of the neuropeptide precursor processing protease PC2, in triggering hatching behavior. *J. Neurosci* **19**, 6942-6954 (1999).

Smallhorn, M., Murray, M.J. & Saint, R. The epithelial-mesenchymal transition of the *Drosophila* mesoderm requires the Rho GTP exchange factor Pebble. *Development* **131**, 2641-2651 (2004).

Stacker, S.A. et al. Biosynthesis of Vascular Endothelial Growth Factor-D Involves Proteolytic Processing Which Generates Non-covalent Homodimers. *Journal of Biological Chemistry* **274**, 32127-32136 (1999).

Stathopoulos, A., Tam, B., Ronshaugen, M., Frasch, M. & Levine, M. pyramus and thisbe: FGF genes that pattern the mesoderm of *Drosophila* embryos. *Genes Dev* **18**, 687-699 (2004).

Steiner, D.F. The proprotein convertases. *Curr Opin Chem Biol* **2**, 31-39 (1998).

Steneberg, P., Hemphälä, J. & Samakovlis, C. Dpp and Notch specify the fusion cell fate in the dorsal branches of the *Drosophila* trachea. *Mech. Dev* **87**, 153-163 (1999).

Sugaya, N., Habuchi, H., Nagai, N., Ashikari-Hada, S. & Kimata, K. 6-O-sulfation of heparan sulfate differentially regulates various fibroblast growth factor-dependent signalings in culture. *J. Biol. Chem* **283**, 10366-10376 (2008).

Sutherland, D., Samakovlis, C. & Krasnow, M.A. *branchless* encodes a *Drosophila* FGF homolog that controls tracheal cell migration and the pattern of branching. *Cell* **87**, 1091-1101 (1996).

Tanaka, A. et al. Cloning and characterization of an androgen-induced growth factor essential for the androgen-dependent growth of mouse mammary carcinoma cells. *Proc. Natl. Acad. Sci. U.S.A* **89**, 8928-8932 (1992).

Tanaka-Matakatsu, M., Uemura, T., Oda, H., Takeichi, M. & Hayashi, S. Cadherin-mediated cell adhesion and cell motility in *Drosophila* trachea regulated by the transcription factor escargot. *Development* **122**, 3697-3705 (1996).

Tarentino, A.L. & Plummer, T.H. Substrate specificity of Flavobacterium meningosepticum Endo F2 and endo F3: purity is the name of the game. *Glycobiology* **4**, 771-773 (1994).

Tefft, J.D. et al. Conserved function of mSpry-2, a murine homolog of *Drosophila sprouty*, which negatively modulates respiratory organogenesis. *Curr. Biol* **9**, 219-222 (1999).

Teuchert, M. et al. Sorting of furin at the trans-Golgi network. Interaction of the cytoplasmic tail sorting signals with AP-1 Golgi-specific assembly proteins. *J. Biol. Chem* **274**, 8199-8207 (1999).

Thomas, G. Furin at the cutting edge: From protein traffic to embryogenesis and disease. *Nat Rev Mol Cell Biol* **3**, 753-766 (2002).

Tulin, S. & Stathopoulos, A. Analysis of Thisbe and Pyramus functional domains reveals evidence for cleavage of *Drosophila* FGFs. *BMC Developmental Biology* **10**, 83 (2010).

Turk, B. Targeting proteases: successes, failures and future prospects. *Nat Rev Drug Discov* **5**, 785-799 (2006).

Turner, N. & Grose, R. Fibroblast growth factor signalling: from development to cancer. *Nat Rev Cancer* **10**, 116-129 (2010).

Untergasser, A. et al. Primer3Plus, an enhanced web interface to Primer3. *Nucleic*

Acids Res **35**, W71-74 (2007).

Uv, A., Cantera, R. & Samakovlis, C. *Drosophila* tracheal morphogenesis: intricate cellular solutions to basic plumbing problems. *Trends Cell Biol* **13**, 301-309 (2003).

Vincent, S. et al. DPP controls tracheal cell migration along the dorsoventral body axis of the *Drosophila* embryo. *Development* **124**, 2741-2750 (1997).

Vincent, S., Wilson, R., Coelho, C., Affolter, M. & Leptin, M. The *Drosophila* protein Dof is specifically required for FGF signaling. *Mol. Cell* **2**, 515-525 (1998).

Wallis, D.D. et al. Profibrillin-1 Maturation by Human Dermal Fibroblasts: Proteolytic Processing and Molecular Chaperones. *J Cell Biochem* **90**, 641-652 (2003).

Walsh, C.T., Garneau-Tsodikova, S. & Gatto, G.J. Protein posttranslational modifications: the chemistry of proteome diversifications. *Angew. Chem. Int. Ed. Engl* **44**, 7342-7372 (2005).

Walter, J., Kaether, C., Steiner, H. & Haass, C. The cell biology of Alzheimer's disease: uncovering the secrets of secretases. *Curr. Opin. Neurobiol* **11**, 585-590 (2001).

Wang, Q., Uhlirova, M. & Bohmann, D. Spatial restriction of FGF signaling by a matrix metalloprotease controls branching morphogenesis. *Dev. Cell* **18**, 157-164 (2010).

Wappner, P., Gabay, L. & Shilo, B.Z. Interactions between the EGF receptor and DPP pathways establish distinct cell fates in the tracheal placodes. *Development* **124**, 4707-4716 (1997).

White, K.E. et al. Autosomal-dominant hypophosphatemic rickets (ADHR) mutations stabilize FGF-23. *Kidney Int* **60**, 2079-2086 (2001).

Wilson, R. & Leptin, M. Fibroblast growth factor receptor-dependent morphogenesis of the *Drosophila* mesoderm. *Philos. Trans. R. Soc. Lond., B, Biol. Sci* **355**, 891-895 (2000).

Wilson, R., Battersby, A., Csiszar, A., Vogelsang, E. & Leptin, M. A Functional domain of Dof that is required for Fibroblast growth factor signaling. *Mol. Cell. Biol.* **24**, 2263-2276 (2004).

Wilson, R., Vogelsang, E. & Leptin, M. FGF signalling and the mechanism of mesoderm spreading in *Drosophila* embryos. *Development* **132**, 491-501 (2005).

Wolf, C. & Schuh, R. Single mesodermal cells guide outgrowth of ectodermal tubular structures in *Drosophila*. *Genes Dev* **14**, 2140-2145 (2000).

Woodcock, S.A. & Hughes, D.A. p120 Ras GTPase-activating protein associates with fibroblast growth factor receptors in *Drosophila*. *Biochem. J* **380**, 767-774 (2004).

Yan, D. & Lin, X. *Drosophila* glypican Dally-like acts in FGF-receiving cells to modulate FGF signaling during tracheal morphogenesis. *Dev Biol* **312**, 203-216 (2007).

Yan, D. & Lin, X. Shaping Morphogen Gradients by Proteoglycans. *Cold Spring Harb*

Perspect Biol **1**, (2009).

Zehe, C., Engling, A., Wegehingel, S., Schäfer, T. & Nickel, W. Cell-surface heparan sulfate proteoglycans are essential components of the unconventional export machinery of FGF-2. *Proc. Natl. Acad. Sci. U.S.A* **103**, 15479-15484 (2006).

Zhou, A., Webb, G., Zhu, X. & Steiner, D.F. Proteolytic Processing in the Secretory Pathway. *Journal of Biological Chemistry* **274**, 20745-20748 (1999).

Zhu, X. et al. Three-dimensional structures of acidic and basic fibroblast growth factors. *Science* **251**, 90-93 (1991).

ACKNOWLEDGEMENTS

The present work was carried out in the Research Group of Molecular Cell Dynamics in the Department of Molecular Developmental Biology at the Max-Planck-Institute for Biophysical Chemistry in Göttingen under the supervision of Dr. Gerd Vorbrüggen.

I cordially thank Dr. Gerd Vorbrüggen for his supervision, constant support, encouragement and guidance, for teaching me the basics of fly work and genetics and for fruitful discussions which directed this project.

I am grateful to Prof. Dr. Herbert Jäckle for giving me the opportunity to carry out my work in his department and for his helpful suggestions and support.

I thank members of my doctoral committee, Prof. Dr. Hans-Henning Arnold, Prof. Dr. Reinhard Schuh and Prof. Dr. Norbert Käufer for their time and support.

My special thanks to Tomma Eisbein for her enormous help with experimental work.

I sincerely thank Alf, Ralf, Mathias, Ronald, Ufuk and Toma for technical help and also for helpful comments and fruitful discussions during my seminars.

I am grateful to Gerd, Uli, April, Alexey, Ania and Dima for critical reading of this thesis and for valuable suggestions.

My sincere thanks to the past and present members of the Lab 5, Gerd, Bhavna, Roland, Alexey, Ania and Madhu for the friendly support, technical help and scientific and non-scientific discussions, for the nice time in the lab and creation of pleasant working atmosphere.

I wish to thank all my friends for their support and encouragement.

I would like to express my deep gratitude to my family, Mama, Papa, Babushka and Dima, for their unconditional love, for constant support and belief in me. I cannot imagine where I would be without your love.

And my very special and cordial thanks to Dima for his love, understanding, and endless patience through all my ups and downs, for his constant support through these years. Thanks for everything! ☺

CURRICULUM VITAE

Name	Tatyana Koledachkina
Date of Birth	08.04.1982
Place of Birth	Vyazniky, Russian Federation
Citizenship	russian

Education

1989-1999	High School, Vyazniky, Russian Federation
1999-2004	Diploma in biology, Nizhni Novgorod State University, Faculty of Biology, Nizhni Novgorod, Russian Federation (Supervised by Prof. Dr. Nicolas Matvienko and Dr. Galina Kopilova) Title of Diploma: "Cloning, purification and characterisation of inorganic pyrophosphatases of *Escherichia coli* and *Termus thermophilus*"
2005-2006	International Program in Molecular biology and medicine of the lung (MBML), Justus-Liebig University, Giessen, Germany
2007-till present	PhD thesis in the Group of Molecular Cell Dynamics, Department of Molecular Developmental Biology, Max-Planck-Institute for biophysical Chemistry, Göttingen, Germany (Supervised by Dr. Gerd Vorbrüggen) Title of PhD thesis: Furin-mediated proteolytic activation of *Drosophila* FGF homologue Branchless

Publications

Chanana B., Graf R., **Koledachkina T**., Pflanz R., Vorbrüggen G. AlphaPS2 integrin-mediated muscle attachment in Drosophila requires the ECM protein Thrombospondin. *Mech Dev.* **124** 463-75 (2007).

Denisova O.V., Chernov A.V., **Koledachkina T.Y.**, Matvienko N.I. A tag-based approach for high-throughput analysis of CCWGG methylation. *Anal Biochem.* **369** 154-60 (2007).